ADDIS ABABA UNIVERSITY

ADDIS ABABA INSTITUTE OF TECHNOLOGY

SCHOOL OF CIVIL AND ENVIRONMENTAL ENGINEERING

RELIABILITY OF PROBABILISTIC FINITE ELEMENT METHOD OVER DETERMINISTIC AND TRADITIONAL PROBABILISTIC METHOD IN SLOPE STABILITY ANALYSIS

A Thesis in Geotechnical Engineering

By

Eleyas Wolde Endashaw

April, 2022

Addis Ababa

ADDIS ABABA UNIVERSITY

ADDIS ABABA INSTITUTE OF TECHNOLOGY

SCHOOL OF CIVIL AND ENVIRONMENTAL ENGINEERING

RELIABILITY OF PROBABILISTIC FINITE ELEMENT METHOD OVER DETERMINISTIC AND TRADITIONAL PROBABILISTIC METHOD IN SLOPE STABILITY ANALYSIS

A Thesis in Geotechnical Engineering

By

Eleyas Wolde Endashaw

Advisor

Dr.-Ing. Tensay Gebremedhin

April, 2022

Addis Ababa

A Thesis

Submitted in Partial Fulfillment of the Requirements for the Degree of Master of Science

ADDIS ABABA UNIVERSITY

ADDIS ABABA INSTITUTE OF TECHNOLOGY

SCHOOL OF CIVIL AND ENVIRONMENTAL ENGINEERING

RELIABILITY OF PROBABILISTIC FINITE ELEMENT METHOD OVER DETERMINISTIC AND TRADITIONAL PROBABILISTIC METHOD IN SLOPE STABILITY ANALYSIS

By: Eleyas Wolde Endashaw

The signatories have examined the thesis entitled '**Reliability of Probabilistic Finite Element Method over Deterministic and Traditional Probabilistic Method in Slope Stability Analysis**' presented by **Eleyas Wolde Endashaw**, a candidate for the degree of **Master of Science** and hereby certify that it is worthy of acceptance.

Advisor	Signature	Date
Internal Examiner	Signature	Date
External Examiner	Signature	Date
Chair person	Signature	Date

Reliability Of Probabilistic Finite Element Method Over Deterministic and Traditional Probabilistic Method in Slope Stability Analysis

ADDIS ABABA UNIVERSITY

ADDIS ABABA INSTITUTE OF TECHNOLOGY

SCHOOL OF CIVIL AND ENVIRONMENTAL ENGINEERING

RELIABILITY OF PROBABILISTIC FINITE ELEMENT METHOD OVER DETERMINISTIC AND TRADITIONAL PROBABILISTIC METHOD IN SLOPE STABILITY ANALYSIS

By: Eleyas Wolde Endashaw

The signatories have examined the thesis entitled '**Reliability of Probabilistic Finite Element Method over Deterministic and Traditional Probabilistic Method in Slope Stability Analysis**' presented by **Eleyas Wolde Endashaw**, a candidate for the degree of **Master of Science** and hereby certify that it is worthy of acceptance.

Dr. Tensay Gebremedhin	[signature]	04/07/22
Advisor	Signature	Date
Dr. Tezera Firew	[signature]	04/07/22
Internal Examiner	Signature	Date
Dr. Samuel Tadesse	for [signature]	04/07/22
External Examiner	Signature	Date
Mebruk Mohammed (Dr.-Ing) Dean Civil & Environmental Engineering		
Chair person	Signature	Date

Addis Ababa University Addis Ababa Institute of Technology

i

UNDERTAKING

I attest that research work titled "Reliability of Probabilistic Finite Element Method over Deterministic and Traditional Probabilistic Method of Slope Stability Analysis" is my work. The work has not been presented elsewhere for assessment. Where material has been used from other sources it has been properly acknowledged / referred.

…………………………..

Eleyas Wolde Endashaw

ABSTRACT

Slope Stability is one of the crucial topics in geotechnical engineering to be investigated well because oftentimes slope exists naturally or formed artificially during construction of various civil engineering structures which needs to be at equilibrium. For that matter, there are various methods of analysis. For the last couple of decades, it is observed hard for Engineers to use Probabilistic Slope Stability Analysis due to many reasons. But these days, technological advancements which led to having more rigorous software packages made it be possible to use in the analysis and its merit. The aim of this thesis is to show the use of more reliable method of slope stability analysis for hypothetical back slopes in Addis Ababa where red clay soil is dominant and that is achieved by comparing methods based on a factor of safety, probability of failure, and reliability index.

Limit Equilibrium Method (LEM) and Numerical Method are used for this purpose. Both deterministic and probabilistic analyses are carried on by modeling seven slope geometries with different input parameters from Addis Ababa ring road III project and hypothetical slopes using a two-dimensional Slope Stability analysis software called SlideV6.0. A Global Minimum type of analysis are carried on by using the Slide software. For finite element analysis and probabilistic finite element analysis, RS2 software from Rocscience is used. Uncertainty is accounted for in a better way in probabilistic analysis by defining parameters as a random variable in link with other features.

It is shown by this study that, Probabilistic Finite Element Analysis (PFEA) seeks out the most critical slip surface than that of the finite element method. In addition, even if the factor of safety found from the deterministic analysis is greater than one still a probability of failure is observed. Moreover, it is attested that the factor of safety is not the only measure for slope stability, but other measures exist while using probabilistic analysis.

Key words: Slope, Probabilistic analysis, FEM, PFEA, Slope Stability

ACKNOWLEDGMENTS

Above all, all Glory and Honor to the Almighty and then, I take the opportunity to acknowledge persons and institutions who have contributed a lot to my research. My sincere gratitude goes to my advisor Dr.-Ing Tensay Gebremedhin for his guidance with full of patience, comments, and his invaluable role in collecting all necessary data and equipment. And then, I am extremely grateful to KAAD and Alumni members in Bon and Addis Ababa. It was once not viable to make it without their scholarship offer.

I would like to express thanks also to the Ethiopian Roads Authority Research Center (ERARC) for allowing me to use the raw data they have collected for this research and am thankful to the Ethiopian Railway Center of Excellence and all staff members for letting me use the computer lab of the center. Moreover, my heartfelt gratitude to my professors and all staff under the chair of Geotechnical Engineering at Addis Ababa University.

Finally, I highly appreciate my beloved family, ministry of Science and Higher Education, Community of St. John Addis Ababa, and all good friends who have contributed much to this research in different ways.

TABLE OF CONTENETS

LIST OF TABLES

LIST OF FIGURES

LIST ABBREVIATIONS

AASHTO – American Association of State Highway and Transportation Officials

COV – Coefficient of Variation

EGS - Ethiopian Geological Survey

ERA – Ethiopian Road Authority

FEM – Finite Element Method

FOSM – First Order Second Moment

FS – Factor of Safety

GM – Global Minimum

LAS – Local Average Subdivision

LEM - Limit Equilibrium Method

MCS – Monte-Carlo Simulation

PFEA – Probabilistic Finite Element Analysis

PLC – Private Limited Company

PSSA – Probabilistic Slope Stability Analysis

RHS – Right Hand Side

RI- Reliability Index

RS – Rock and Soil

RS2 – A 2D Finite Element Software from Rocscience

SS – Sliding Surface

SSRF - Shear Strength Reduction Factor

USGS - United States Geological Survey

CHAPTER 1 INTRODUCTION

1.1 Background

Slope stability analysis is one of the main areas of interest to geotechnical engineers in analyzing and designing different geotechnical structures like retaining structures, tunnels, shoring systems, reinforced earth structures, and so on. Analysis of the safety level of slopes is very important for proper geotechnical risk management and assessment. There are classical or conventional and advanced ways of slope stability analysis used for both natural and man-made slope stability analysis. But the conventional methods made many assumptions and have limitations in simulating the real soil conditions. However, the advanced methods of analyses are found to be more realistic in considering the variability of the soil properties to assess the reliability and risk associated with the projects since the soil is an inherently heterogeneous, non-single-phase material that has natural variability and uncertainty in its properties.

To simulate the uncertainty of soil properties in recent years, probabilistic approaches are more and more widely used for the safety assessment of slopes as mentioned by El-Ramly et.al., (2002) and are more reliable in providing an acceptable design criterion. The degree of safety can be determined through probabilistic slope stability analyses with the consideration of uncertainties and variability in material properties, as well as in environmental factors, like the fluctuation of the groundwater table due to seasonal variation. It is noted by various researchers, Oguz et.al., (2017), that a slope with a deterministic safety factor (FS) that we gate from the conventional methods larger than 1.00 may have a probability of failure greater than 0%.

Moreover, an advanced and rigorous probabilistic approach for modeling the influence of statistically described soil properties on design outcomes in geotechnical engineering have emerged during the early ‘90s (Fenton & Vanmarcke, 1990) and (Griffiths & Fenton, 1993). Among these, finite element based probabilistic analysis and Random Finite Element Method (RFEM) can be mentioned. The latter one encompasses both random field theory and the finite element method. The method was applied to several areas of geotechnical engineering including slope stability analysis according to Griffiths et.al., (2000), (2004). The Local Average Subdivision method (LAS) proposed by Fenton and Vanmarcke (Fenton G. A., 1990) is used for generating the random fields. According to Allahverdizadeh et.al., (2015), in traditional probabilistic analyses, spatial variability is neglected by implicitly assuming perfect correlation, which does not necessarily result in a conservative estimate of the probability of failure.

This research is aimed to show the reliability of Probabilistic Finite Element Method (PFEM) in slope stability analysis over deterministic and other traditional (conventional) probabilistic analysis by using various slopes in Ethiopia in link with various stakeholders like Ethiopian Roads Authority (ERA) and Geological Survey of Ethiopia (GSE).

Hence, to achieve the stated goal, data is gathered for the selected specific site and appropriate software programs are chosen. In order to investigate the instability, both Limit Equilibrium Method (LEM) and Finite Element Method (FEM) are used. For the limit equilibrium method (deterministic and probabilistic analyses), Slide software from Rocscience is used and for finite element and probabilistic finite element method of analysis, RS2 software is used also from Rocscience.

From the analysis followed, it is found that the probabilistic finite element method seeks out the most critical slip surface relative to other methods of slope stability analysis. In addition, even in LEM, still probabilistic analysis gives a lesser safety factor than that of deterministic analysis when a probabilistic analysis is computed in overall slope type. And also, from the deterministic analysis, a higher factor of safety that seems safe is observed, but not, since the probability of failure exceeded zero.

1.2 Statement of the Problem

Conventional limit equilibrium methods are under use for the assessment of slope stability in routine practice in parts of the world as well as in our country Ethiopia and the soil profiles are often assumed to be uniform and homogenous which is not true in reality. In addition to this, the conventional slope stability analyses are often performed with in deterministic analysis framework were single estimates or characteristic values for soil parameters are used.

To consider the spatial variability and uncertainty of soil properties most of the time a higher value of factor of safety is adopted in deterministic methods as stated by Chok et.al., (2015). As a result, the conventional approach may not be reliable to estimate the potential failure of slope.

But with all these limitations, we are using the conventional and deterministic analysis approach in our country. As it was mentioned in previous section, we adopt a higher factor of safety which is uneconomical to avoid risk, and as it has already been researched by many for instance Oguz et.al., (2017) even if a high factor of safety is adopted, there may be a probability of failure. In many parts of our country, we see many man-made and natural slope failures and some of them are disastrous for life and infrastructures. Method of analysis can be one of the ways to minimize risk and failure.

1.3 Objective of the Study

1.3.1 General objective

The general objective of this research is to investigate the reliability of static Probabilistic Finite Element Method (PFEM) of analysis over that of deterministic LEM and traditional probabilistic LEM in slope stability analysis in terms of Factor of Safety (FS), Probability of failure (P_f), Reliability index (RI) and Critical failure surfaces in different hypothetical slopes in Ethiopia.

1.3.2 Specific objectives

- Investigate the effect of defining material properties as a random variable in probabilistic slope stability analyses.
- Investigate the effect of analysis type on safety factor values and stability condition of slopes.
- Investigate the effect of assuming a slip surface in advance on the value of safety factor.

1.4 Scope of the Study

Slope stability analysis is a vast area of research in geotechnical engineering. In this research, only a few LEM of analyses are considered and from the probabilistic analysis method, the Monte Carlo and Latin hypercube are used.

Besides, the study is limited to Static slope stability analysis, in other words, the dynamic slope stability analysis is not included in the scope.

1.5 Significance of the study

The Ethiopian Geological Survey (GSE) and Ethiopian Roads Authority (ERA) are reporting many slope failures in a different part of the country. For instance, around Dessie, Wondo Genet, Blue Nile Gorge, Jimma basin, Goffa, Sawla, Jinka and Wolaita area are few among many. As a country, we are investing much money for roads and other infrastructures but due to slope stability problems their functionality does not last long. A well-proven analysis method in addition to other aspects like understanding the possible causes of failure, has a significant contribution to minimize failures which also impact the economy positively.

1.6 Organization of the Thesis

This thesis is organized in 5 chapters and appendices, each presenting condensed information entitled with. A summary is given for each below.

Chapter 1: This chapter presents a general introduction to the thesis, from what the research idea is initiated, it states the aim of the thesis, all the ways how the research is done, its scope, and limitations.

Chapter 2: In this chapter, numerous pieces of literature are reviewed about the topic including related works done by former scholars. The key points in slope stability analysis and the different types of slope stability analyses are discussed in this chapter and especially probabilistic analysis.

Chapter 3: Depicts materials and methods utilized in this research. It presents the general background of the study area and its various formations including characterization of the land slide. It states how data is gathered and describes briefly the background of software programs used. This chapter gives the general procedure and process of how the analysis is carried on step by step for each methodology mentioned in chapter one.

Chapter 4: The results from the analysis carried on are interpreted briefly in this chapter. Outputs are summarized and discussed by using plots from the software used which elaborate the findings. Comparison between analyses is also made in this chapter.

Chapter 5: This is the last chapter containing major findings and recommendations. The conclusions made from the values obtained from LEM of analysis and the Numerical method of analysis are indicated. Finally, data logs, output data, material boundary, model geometry coordinates, and all necessary information used in the software are presented from Appendix A-D.

CHAPTER 2 LITERATURE REVIEW

2.1 Definition and Background

A slope is defined as a surface of which one end or side is at a higher level than another; a rising or falling surface. It is an inclined soil mass without support (Salunkhe, Bartakke, Chvan, & Kothavale, 2017). The slope of the earth classified as Natural, the one that is formed by natural factors and exists in nature and Manmade that is formed by human actions which include the sides of cuttings, the slopes of embankments constructed for roads, railway lines, canals, etc. and the slopes of earth dams constructed for storing water (Murthy, 2002).

According to Salunkhe et al., (2017), these natural and manmade slopes may be grouped under finite and infinite slopes depending on the extent of inclination. when a slope has a limited length of inclination it can group under finite slope and when a slope represents the boundary surface of a semi-infinite soil mass or ideally the inclination is extended to unlimited length and the soil properties for all identical depths below the surface are constant the slope is termed as an infinite slope. The slope is used to canal banks, road cuts, landfills open-pit mining, excavations, the earthen dam, railway formation, highway embankment, levees, etc.

Something involving a downward and outward movement of the whole mass of soil that involves in the failure we call it a slide. gravitational forces and force due to seepage water, erosion, sudden lowering of water near to a slope, external loading, geological feature, earthquake forces are the main triggering forces for slope failure within the soil (Figure 2.1). They may also fail due to adjacent excavation or undercutting of its foot, or due to gradual disintegration of the structure of the soil due to weathering (Salunkhe, Bartakke, Chvan, & Kothavale, 2017).

The movement of the slope is either by expansion and contraction of soil due to the variation in temperature called soil-creep or sudden movement of large soil mass refers to mass slides or flow slides which occur when the soil starts to flow outward and downward from its natural position (Teferra A. and Leikun M., 1999).

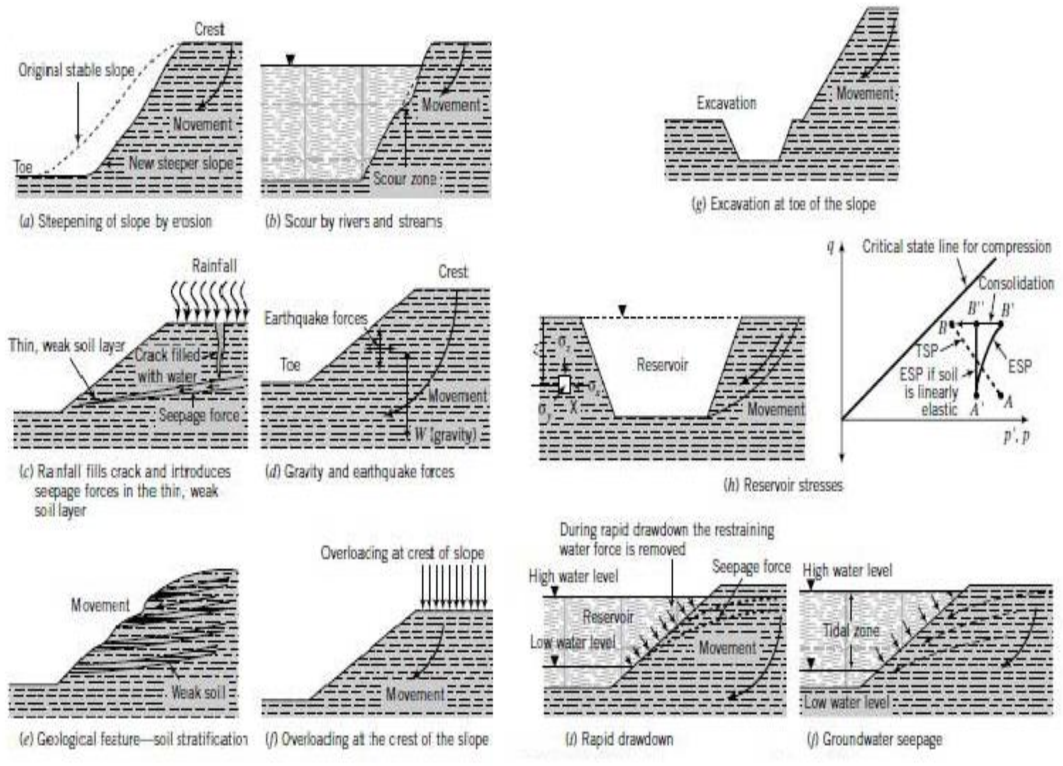

Figure 2.1 Causes of slope failure (Civil Seek, 2018)

One of the oldest, controversial, and arguably the most researched and the least understood topic of geotechnical engineering is the stability of slopes. In their book titled Soil Strength and Slope Stability Duncan et al., (2014) said that "Evaluating the stability of slopes in the soil is an important, interesting, and challenging aspect of civil engineering". Among various works in this field in terms of different approaches (theoretical, experimental, analytical, statistical, and numerical), Terzaghi's (1950) work entitled "Mechanism of Landslides" is well known. Researchers are looking for an advanced approach today since the solution of slope stability problems requires the understanding of analytical methods and their application, the awareness of known methods and their drawbacks becomes a crucial topic.

2.2 Shear Strength for Slope Stability

Effective or total stress parameters can be used to assess the stability of a slope. For cohesionless soils forming the slope material, the effective stress analysis is best suitable since drainage occurs quickly after loading (or unloading) of the slope disregarding exceptional circumstances. For the case of clay-type soils, with low pore pressures, permeability and hence there is time-dependent stability of the slope (ETİZ, 2019) an effective stress approach with drained shear strength parameters can be applicable if the pore-water pressures can be estimated fairly close. If it is not possible to estimate or determine the pore water pressure, the total stress type of analysis may have to be employed. In practice, it is common to use the total stress analysis for short-term stability problems and the effective stress principle is used to assess the long-term stability, assuming that all excess pore pressure generated during loading will be fully dissipated (Abramson, Thomas S. Lee, Sharma, & Glenn, 2001).

2.3 Slope Stability Analysis

The reason for slope stability analysis is to assess the safe design of manmade or natural slopes and the equilibrium conditions. The slope is the resistance of inclined surface at some angle to failure by sliding or collapsing which may cause loss of life and asset. It is, therefore essential to check the stability of proposed slopes.

The stability of a slope can be checked in terms of factor of safety; for analysis either factor of safety for shearing strength i.e., the ratio of shear strength (shearing resistance) to the shear stress (mobilized shear strength) along sliding surface or factor of safety for cohesion i.e., the ratio of available cohesion intercept and the mobilized cohesion intercept might be used (Murthy, 2002). And also, there is a factor of safety for friction which is the ratio of available frictional strength to mobilized frictional strength.

During the analysis of slope, there should be a distinction between finite and infinite slopes (in this paper only analysis of finite slope is reviewed). Thanks to the advancement of modern methods of soil testing and stability analysis, a safe and economical design of slope are admissible (Salunkhe, Bartakke, Chvan, & Kothavale, 2017).

Slope stability analysis is broadly classified as:

A. Static Slope Stability Analysis

B. Dynamic Slope Stability Analysis

A. Static Analysis

i. Limit equilibrium method:

- Swedish slip circle method of analysis
- The ordinary method of slices
- Simplified bishop's method of analysis
- Janbu's method of analysis
- Spencer's method of analysis
- Sarma method of analysis
- Taylor's stability number
- Probabilistic analysis based on LEM

ii. Numerical method:

- Finite difference method
- Finite Discrete method
- Finite Element method
- The probabilistic FE method

iii. Numerical method of modeling:

- Continuum modeling
- Discontinuum modeling
- Hybrid/coupled modeling

2.3.1 Limit Equilibrium Analysis

The limit equilibrium method is a conventional slope stability assessment approach, which considers force or moment equilibria of the soil mass remaining above a probably assumed failure surface (ETİZ, 2019). The basic assumption of the limit equilibrium method is that Coulomb's failure criterion is satisfied. Culmann (1875) assumed the failure surface as a plane shown in Figure 2.2 for the analysis of slopes which is mainly of interest because it serves as a test of the validity of the assumption of plane failure along the assumed failure surface. It starts from the known or assumed values of forces acting on the free body diagram taken from the slope and then the shear resistance is calculated, this calculated value is compared with the available shear strength (Murthy, 2002).

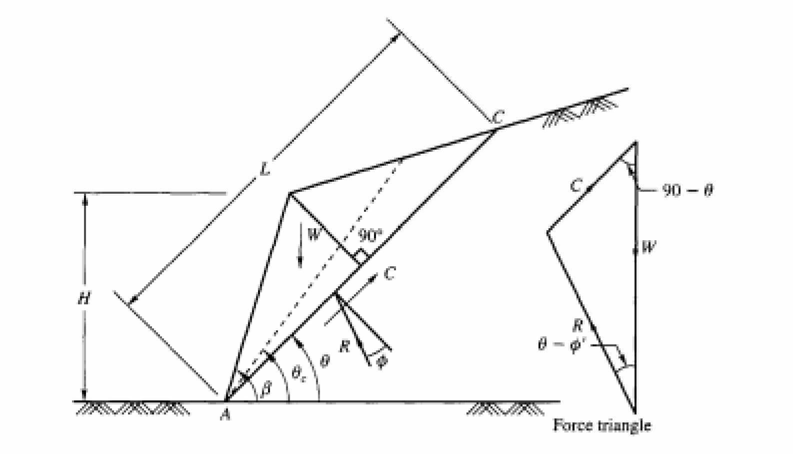

Figure 2.2 Stability of slopes by Culmann method (Murthy, 2002)

There is a circular failure surface as the investigation shows. When soil slips along a circular surface, such a slide may be termed as a rotational slide. Such failures can be classified as slope failure, toe failure, and base failure as shown in Figure 2.3.

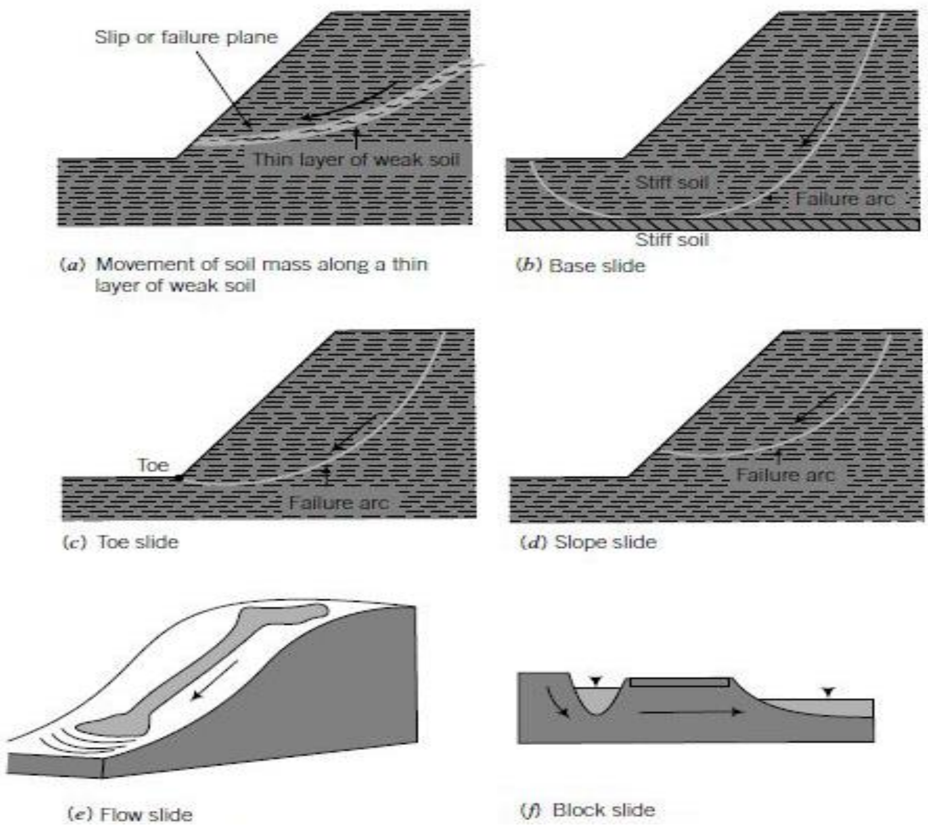

Figure 2.3 Common types of slope failures (Civil Seek, 2018)

In the LEM method, the soil mass above the slip surface is assumed to be rigid at the time of failure, the available shear strength is assumed to be mobilized at the same rate at all points of the slip surface. This implies that FS is constant throughout the failure surface. In LEM factor of safety can be calculated in the limit force and moment equilibriums (ETİZ, 2019). Some of the LEMs are briefly discussed in the next section.

2.3.1.1 Swedish Slip Surface Method

It is also known as the circular arc method or φ=0 method of analysis (Teferra A. and Leikun M., 1999). In 1922 the Geotechnical Commission was appointed by the Swedish State Railways to investigate solutions following a costly slope failure. The analysis followed for this project has laid a base for the development of the limit equilibrium analysis method. The method has become known as the Swedish Slip Circle Method. In this method, a cylindrical shape that looks a circle in cross-section is assumed.

This method assumes zero resultant interslice force, a circular slipping surface, and the equilibrium of overall moment is satisfied but the equilibrium of individual slice moment, equilibrium of both vertical and horizontal forces is not satisfied.

2.3.1.2 Ordinary Method of Slices

It is known as the "Ordinary Method of Slices" or Fellenius 'method developed by Fellenius in 1936. In any method of slices, the soil mass above the failure surface is subdivided into vertical slices, and the stability is calculated for each slice. Fellenius' Method simplifies the equation by assuming that the forces acting on the sides of each slice cancel each other (Fellenius, 1936).

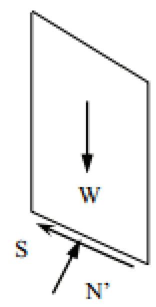

Figure 2.4 Forces on ordinary method slice (Aryal, 2006)

Where, S = shear force acting at the base of a slice (kN), N'= effective base normal force acting on SS (kN)

The ordinary method of slices doesn't satisfy the force equilibrium of both the entire slide mass and individual slices and doesn't satisfy the equilibrium of moment of individual slice but overall moment equilibrium. It assumes a circular slipping surface.

2.3.1.3 Simplified Bishop's Method

This method accounts for the interslice normal forces, which increase the accuracy of calculating the factor of safety (FS). The method of slices, therefore developed is known as the "Simplified Bishop's Method" (Bishop A.W., 1955). However, Bishop's Method still cannot satisfy all the conditions of static equilibrium for example equilibrium of horizontal forces, equilibrium of moment for an individual slice. All interslice forces are assumed to be zero, which reduces the number of unknowns by (n-1). Remaining (4n-1) unknowns, overdetermined solution as horizontal force equilibrium not satisfied for a slice (ETİZ, 2019).

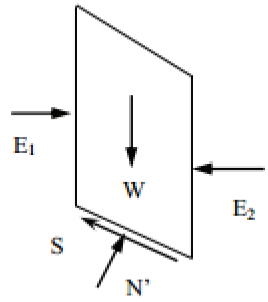

Figure 2.5 Forces on Simplified Bishop's slice (Aryal, 2006)

Where, S = shear force acting at the base of a slice (kN), N'= effective base normal force acting on SS (kN), W weight of each slice or total sliding mass (kN), E = interslice normal force (kN).

2.3.1.4 Morgenstern – Price Method

It is known as the "Morgenstern-Price Method". Morgenstern and Price developed this alternative method for analyzing slides with a non-circular failure path (Morgenstern & Price, 1965). This method satisfies all equilibrium of forces and moments. unlike the method of analysis discussed earlier, it is possible to assume any shape of the sliding surface. The morgenstern-price method sets an arbitrary mathematical function to describe the direction of the interslice forces.

$$\lambda f(x) = \frac{x}{E} \tag{2.1}$$

Where λ is a constant scale factor of the assumed function to be evaluated when solving for the FS and f(x) = interslice force function that varies continuously along the slip surface.

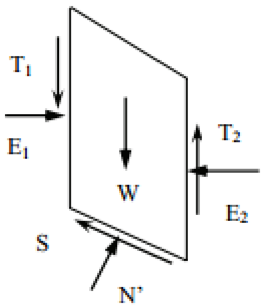

Figure 2.6 Forces on Morgenstern-Price slice (Aryal, 2006)

In general, Morgenstern-Price Method considers both interslice forces, assumes an interslice force function, f(x), allows selection for interslice force function, computes FS for both force and moment equilibrium (Aryal, 2006).

2.3.1.5 Spencer's Method

This method is a complete equilibrium method known as Spencer's Method, which satisfies the equilibrium of both force and moment. As a result, the FS calculated by this method should be more precise. In spencer's method, it is possible to assume a non-circular slip surface which is useful because many slope failures do not have exactly circular failure surfaces (Spencer, 1967).

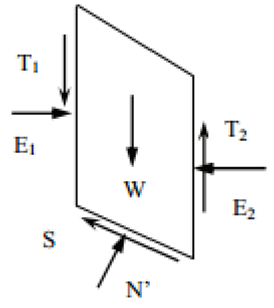

Figure 2.7 Forces on Spencer's slice (Aryal, 2006)

2.3.1.6 Janbu's Method

Janbu has developed three different methods of slope stability analysis namely, "Janbu's Simplified Method" (Janbu, 1954a), Janbu's generalized method, and Janbu's direct method. a non-circular failure surface is possible in Janbu's simplified method which considers the interslice forces with an assumption of interslice/ tangential forces are equal to zero, but includes a correction factor to compensate for the interslice forces.

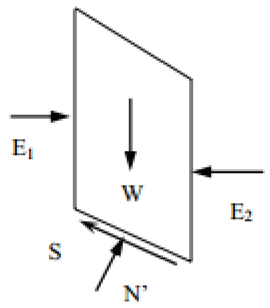

Figure 2.8 Forces on Janbu's simplified slice (Aryal, 2006)

However, in Janbu's generalized method both interslice forces and assume a line of thrust to determine a relationship for interslice forces. satisfies both force and moment equilibriums, handles complex geometry and failure surfaces, is an advanced method among LE methods.

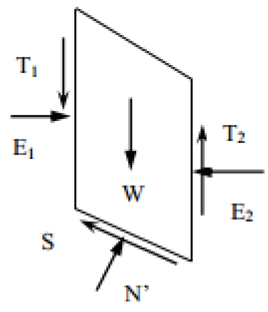

Figure 2.9 Forces on Janbu's generalized slice (Aryal, 2006)

Finally, Janbu's direct method is based on a series of charts as a powerful tool to carry out slope stability analysis. Besides, surcharge load, groundwater, and tension crack loading conditions are possibly integrated during analysis (Aryal, 2006).

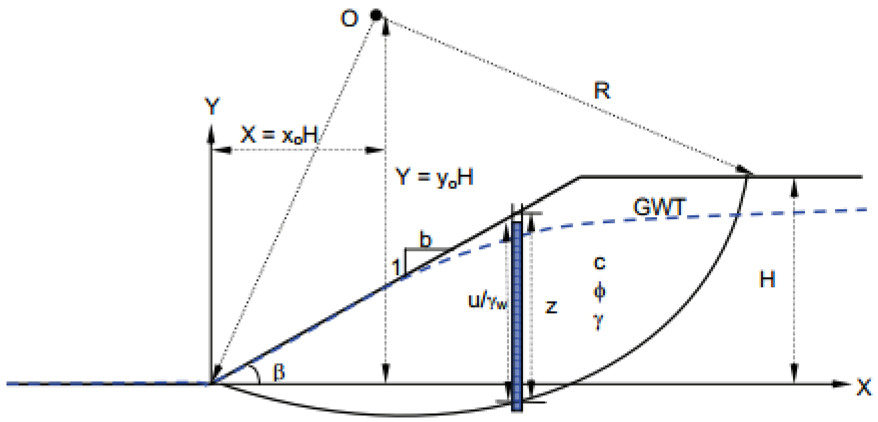

Figure 2.10 Slope geometry illustrating Janbu's direct method (Aryal, 2006)

2.3.1.7 Sarma's Method

In 1973, Sarma came up with a method for general blocks or a non-vertical slice. considers both interslice normal and shear forces, satisfies both moment and force equilibrium, and relates the interslice forces by a quasi-shear strength equation.

$$T = ch + Etan\varphi \qquad (2.2)$$

Where, c, φ are shear strength parameters, and 'h' is height.

Overall, limit equilibrium method:

- gives different results in different methods because all methods make different assumptions.
- uses an upper bound solution
- the sliding block is assumed to be rigid
- distribution of FS is taken as constant throughout the failure zone
- distribution of stress is taken as constant throughout the failure zone
- it doesn't give the displacement of the sliding block

2.3.1.8 Probabilistic Slope Stability Analysis

The variability of soil property and uncertainty is not considered in conventional deterministic slope stability analysis explicitly but relies on conservative parameters and designs to deal with uncertain conditions. However, Probabilistic analyses allow uncertainty to be quantified and incorporated rationally into the design process. Besides, it can be applied in LEM and FEM of analysis. Probabilistic slope stability analysis (PSSA) was first introduced into slope engineering in the 1970s (El-Ramly, Morgenstern, & Cruden, 2002).

According to El-Ramly et al., (2002), there are four reasons for practicing engineers facing difficulties in using PSSA:

- less comfortability dealing with probabilities due to limited understanding of statistics and probability.
- due to the common misconception that probabilistic analyses require significantly more data, time, and effort than deterministic analyses.
- Due to misconception that PSSA replaces deterministic but rather they are supplementary to each other.
- limited studies regarding benefits and illustration of PSSA and
- acceptable probabilities of unsatisfactory performance (or failure probability) are ill-defined, and the absence of a link between a probabilistic assessment and a conventional deterministic assessment.

In the technical sense, variability can be defined as an observable manifestation of heterogeneity of one or more physical parameters and/or processes. It is an inherent property to a natural material. The uncertainty reflects the decision (or necessity) to recognize and address the observed variability in one or more soil properties of interest (Phoon & Kulhawy, 1999). It arises from the difficulty in measuring properties.

Geotechnical uncertainties may be aleatory uncertainty (inherent variability) or epistemic uncertainty (measurement error, statistical estimation error, and model error). The main source of uncertainty in soil is from spatial variability of soil properties. Soil is variable in composition and properties from place to place even in a homogenous soil layer. This variability is due to factors like composition, deposition condition, stress history, and physical and mechanical decomposition process. Figure 2.11 compares the spatial variability of two artificial sets of data. The upper plot is highly erratic and the data are almost uncorrelated, whereas the lower plot is characterized by high spatial continuity. The pattern of soil variability is characterized by the autocorrelation distance or scale of fluctuation. A large autocorrelation length implies soil homogeneity and a short autocorrelation length shows erratic variability.

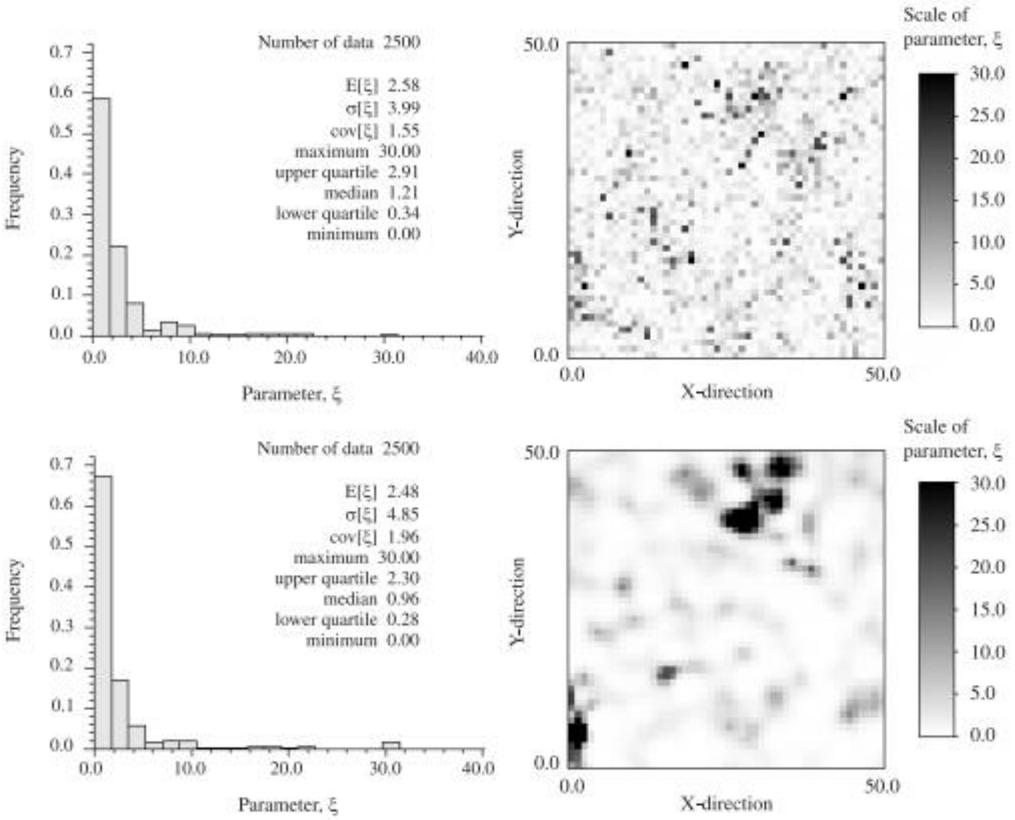

Figure 2.11 Very erratic spatial structure (upper right) and a highly continuous structure (lower right), both with similar histograms (El-Ramly, Morgenstern, & Cruden, 2002)

The other measure of uncertainty is in spatial averaging. Rather than soil properties at discrete locations, the performance of a structure is often controlled by the average soil properties within a zone of influence. Slope failure is more likely to occur when the average shear strength along the failure surface is insufficient rather than due to the presence of some local weak pockets. The uncertainty of the average shear strength along the slip surface, not the point strength, is therefore a more accurate measure of uncertainty (El-Ramly, Morgenstern, & Cruden, 2002).

As stated by Griffiths et al., (2015) slope stability analysis has received more attention in the case of probabilistic geotechnical analysis, it seems likely that a very significant bibliography is now available like Matsuo and Kuroda (1974), Alonso (1976), Tang et al. (1976) and Vanmarcke (1977).

According to El-Ramly et al., (2005) probabilistic procedures for slope stability analysis vary in assumptions, limitations, capability to handle complex problems, and mathematical complexity and they can be grouped in two categories: approximate methods (the FOSM method, the point estimate method) and Monte Carlo simulation. However, now a days another sampling method called Latin Hypercube is emerged. Approximate methods make assumptions that often limit their application to specific classes of problems and do not provide any information about the shape of the probability density function, so the failure probability can only be obtained by assuming a parametric probability distribution of the factor of safety (typically normal or log-normal). Estimates of low probabilities, required for safe structures, are sensitive to the assumed distribution. Some of the probabilistic slope stability Analysis methods are discussed briefly in the fore coming sections.

2.3.1.8.1 First Order Second Moment (FOSM) Method

It is called FOSM because it uses the first order of the Taylor approximation terms about the second moments (mean and variance). This method is an approximate approach that uses the first order approximation of the mean, standard deviation, and variance of the performance function (the distribution of the factor of safety) which depends on the first order Taylor's Series expansion and neglect the higher order terms (AKBAŞ, 2015). In slope stability works, this function is the factor of safety which is calculated by the method of slices. FOSM calculates the reliability index (β) from the mean value (μ_{FS}) and standard deviation (σ_{FOS}) of a factor of safety.

$$\beta = \frac{\mu_{FS} - 1}{\sigma_{FS}} \tag{2.3}$$

The advantage of this method is that it can show the relative contributions of each random variable to the performance function. This can be useful since the designers can focus on the most affecting variable. This is not provided in many of the other methods. On the other hand, the demerit of the method is to deal with the partial derivative of the performance function, especially if it has a complicated form (AKBAŞ, 2015).

2.3.1.8.2 Point Estimate Method

It is known as Rosenblueth's method. It's an approximate and easy to use and straightforward method where the designers are not required to know much of a probability theory. The method approximates the moments of the performance function that contains random variables. As it is first and second moments of a function are mean and variance, respectively and the square root of the variance is the standard deviation. initially, it is seen as an over approximate approach. However, its satisfactory accuracy is shown by Baecher & Christian (2005) in several numerical case studies. The correlation between variables is possible in addition to its simplicity. But this method is better for problems with few variables to save computation time (AKBAŞ, 2015).

2.3.1.8.3 First Order Reliability Method (FORM)

In FOSM and point estimate method, first, for the estimation of performance function, only the mean and variance of the random variables and their linear combination are used, and second, in knowing the form of distribution of performance function the probability of failure of performance function can be obtained from reliability index information. To overcome these two assumptions FORM developed.

The first order reliability method (FORM) is a process that can be used to determine the probability of a failure given the distribution data and limit state function. The method is based on the Hasofer-Lind reliability index (β_{HL}) (Hasofer and Lind 1964), which can be described as the distance, in standard deviation units, between the most probable set of values and the most probable set of values that causes a failure. Calculation of this value is an iterative process, finding the minimum value of a matrix calculation subject to the constraint that the values result in a system failure. The reliability index can be determined and then the probability of failure, P_f, (Griffiths, Fenton, & Denavit, 2007). the distance in standard deviation units between the most probable set of random variables (the means), and the most probable set of random variables that causes a failure is called the reliability index, and an iterative process is used for its determination.

$$\beta_{HL} = \min_{g \to 0} \sqrt{\left(\frac{x_i - \mu_i}{\sigma_i}\right)^T + [R]^{-1} \left(\frac{x_i - \mu_i}{\sigma_i}\right)^T} \tag{2.4}$$

Where, $\left(\frac{x_i - \mu_i}{\sigma_i}\right)^T$ is the vector of random variable values reduced to standard normal space, $[R]$ is the correlation matrix of the values of the variables.

2.3.1.8.4 Monte Carlo simulation Method

The Monte Carlo method is a powerful slope stability analysis developed in 1949 by John von Neumann and Stanislaw Ulam ((Eckhardt, 1987), (Fishman, 1995)). Monte Carlo

Simulation (MCS) is based on a random sampling procedure (sometimes called pseudo-random numbers (Zhang, Ji, & Xu, 2020) in which input variables affecting the performance function (distribution of FS) is randomly selected from a region of interest and results on the performance function is evaluated. Monte Carlo simulation is a powerful tool for slope stability risk analysis.

In this method, an iterative process using deterministic methods of slope stability analysis is applied. Monte Carlo simulation is a popular method of slope stability risk analysis much used by engineers because of its simplicity and no need for comprehensive mathematical and statistical knowledge (Sharma, 2016). The first step of a Monte Carlo simulation is to identify a deterministic model where multiple input variables are used to estimate a single value outcome. Step two requires that all variables or parameters be identified. Next, the probability distribution for each independent variable is established for the simulation model, (i.e., normal, beta, lognormal, etc.). Next, a random trial process is initiated to establish a probability distribution function for the deterministic situation being modeled.

Generalized steps can be defined as follows: (AKBAŞ, 2015)

A. Fixing geometry of the slope to be analyzed and the most likely (mean) values of the required soil parameters.
B. Choosing the shear strength soil model (Mohr-Coulomb, Hoek-Brown, etc.)
C. Determination of the randomly treated input parameters (i.e., unit weight, cohesion, internal friction angle, pore water pressure coefficient, etc.)
D. For each random variable, choosing the relevant COV from the literature unless information on the variability of site-specific soil is sufficient.
E. Choosing the statistical distribution (normal, lognormal, etc.) of the random parameter.
F. Choosing several required analyses (N) and sampling methods.
G. Choosing the shape of a slip surface (circular, non-circular, etc.) if necessary.
H. Carrying the slope stability analysis N-times.

This procedure will result in a statistically distributed N-times factor of safeties, probability of failure, critical probabilistic failure surface, and reliability index (AKBAŞ, 2015).

The limitation of this method is that generated number may not cover the necessary region of interest depending on the values parameters defined, seed, and the number of realizations. In addition to that, depending on the probability of failure of the performance function, necessary random number realization can be too much.

2.3.2 Numerical Method

2.3.2.1 Finite element Method

In the finite element method (FEM) the limitations of the limit equilibrium method are solved. In FEM, the soil continuum is divided into discrete units called "finite elements". The finite elements are interconnected at nodal points and the prescribed boundaries of the mass continuum. In typical geotechnical applications, the displacement method of formulation of the FEM is utilized to calculate displacements, stresses, and strains at the nodal points.

In LEM statics of force and moment equilibrium are considered but in FEM stress-strain relationship is used like constitutive law. Stress redistributions can be computed since it is based on the stress-strain relationship. Besides, compatibility between structural members and soil media can be done without much problem due to its meshing process. The principal uses of the finite element method as stated by Duncan (1996) for design are:

- it provides estimates of displacements and construction pore water pressures.
- it provides a displacement pattern that may show potential and possibly complex failure mechanisms. Once a potential failure mechanism is recognized, the factor of safety against a shear failure developing by that mode can be computed using conventional limit equilibrium procedures.
- it provides estimates of mobilized stresses and forces.
- the finite element method may be particularly useful in judging what strengths should be used when materials have very dissimilar stress-strain and strength properties, i.e., where strain compatibility is an issue.
- the FEM can help identify local regions where "overstress" may occur and cause cracking in brittle and strain softening materials. An essential input to the stability

analyses for reinforced slopes is the force in the reinforcement. The FEM can provide useful guidance for establishing the force that will be used.

The shear strength reduction factor (SSRF) method is employed in FEM to analyze slope which provides a very quick and reasonable estimate of stability. This method is based on the reduction of cohesion (c) and friction angle (tanφ) of the soil.

$$\mathrm{SSRF} = FS = \frac{C}{C_{reduced}} = \frac{\tan\varphi}{\tan\varphi_{reduced}} \tag{2.5}$$

The parameters are reduced in steps until the soil mass fails. Different computer programs which are based on the finite element method, use the stress reduction method in the analysis of slope. One of the main advantages of the Shear Strength Reduction Technique (SSRF) is that the safety factor emerges naturally from the analysis without assuming any particular form of failure mechanism in advance.

The shear strength reduction factor ‘F’ increases incrementally until the global failure of the slope reaches, implies, under a physically real convergence criterion, finite element calculation diverges. The lowest factor of safety of slope lies between the shear strength reduction factor F at which the iteration limit is reached and the immediately previous one. The procedure described at this moment can predict the factor of safety within one loop and can be easily implemented in a computing code (Nakamura, 2008). However, FEM is time consuming and complex because no assumptions are made to simplify the problem and further processing is required because FEM does not provide a value for the overall factor of safety of the computed stresses.

2.3.2.2 Probabilistic Finite Element Method

Probabilistic Finite Element Method (PFEM) determine the effect of uncertainty or variability of input parameters on the results of the finite element analysis by defining input parameters as random variables. The PFEM combines elastic-plastic finite element analysis with random field theory in slope stability analysis (Allahverdizadeh, ASCE, Griffiths, Fenton, & ASCE, 2015).

The PFEM is used in link with Monte Carlo simulations with many different realizations of the soil properties onto a finite element mesh in which the stability analysis is repeated until the probabilities relating to output quantities of interest become statistically reproducible. In the case of slope stability analysis, the probability of failure is defined by dividing the number of realizations in which the slope failed by the total number of realizations as stated by Griffiths et al., (2007). Because of avoiding of assumption of shape and location of failure surface PFEM is more realistic and powerful probabilistic slope stability analysis.

The unique feature of this method is the ability to seek out the weakest and most critical path and it doesn't stick with a certain shape of failure surface while accounting for spatial variability of soil (Griffiths & Fenton, 2004). It incorporates the main advantage of FEM in this regard.

2.4 Summary of Related Studies

Oguz et al., (2017)**,** investigated the effects of the Coefficient of Variation (COV) and the Cross-Correlation of Shear Strength Parameters. COV is defined as the ratio between standard deviation and mean. In their study, they considered uncertainty of soil properties by different levels of coefficient of variation. They used the limit equilibrium method for slope stability analyses with a normal statistical distribution of geotechnical material properties. The results showed that the Probability of failure (P_f) and the critical failure surface are significantly influenced by the COV level, cross correlation of shear strength parameters, and the traditional FS level of the slopes. Moreover, the inverse relation between FS and P_f is demonstrated to be nonlinear and the COV level has a significant effect on this relationship.

It is shown that large values of COV, i.e., significant variation in material properties, can cause large values of P_f for slopes with FS greater than unity and P_f decreases with increasing COV for FS less than unity, and deterministic FS alone will not be sufficient to indicate this danger in slope stability. As cohesion increases the friction angle decreases, this is termed as a negative cross correlation which is considered in their study.

There are suggested values of COV by different researchers in the literatures. But care should be given in using these values since it is not clearly presented how these values are recorded. Duncan and others provided a summary of COV values for various property or in situ test results, only properties related to this study are presented in Table 2.1 (Duncan, Member, & ASCE, 2000).

Table 2.1 Values of Coefficient of Variation (V) for Geotechnical Properties and In Situ Tests (Duncan et al., 2000)

Property or in situ test result	COV (%)	Reference
Unit weight (γ)	3–7%	Harr (1984), Kulhawy (1992)
Buoyant unit we (γ_b)	0–10%	Lacasse and Nadim (1997), Duncan (2000)
Effective stress friction angle (φ')	2–13%	Harr (1984), Kulhawy (1992)
Undrained shear strength (S_u)	13–40%	Harr (1984), Kulhawy (1992), Lacasse and Nadim (1997), Duncan (2000)

Phoon and Kulhawy conducted the effect of COV on the analysis of slope stability and they reported a summary of values for different soil types and different soil properties which can be used as a guideline during limitation on the availability of sufficient data (Phoon & Kulhway, 1999).

Table 2.2 Approximate guidelines for design soil property variability (Phoon & Kulhway, 1999)

Design property	Test	Soil type	Point COV(%)	Spatial avarage (%)
S_u (UC)	Direct (lab)	Clay	20–55	10–40
S_u (UU)	Direct (lab)	Clay	10–35	7–25
S_u (CIUC)	Direct (lab)	Clay	20–45	10–30
S_u (field)	VST	Clay	15–50	15–50
φ’	Direct (lab)	Clay, sand	7–20	6–20
φ’ (TC)	q_T	Sand	10–15	10

Where,

S_u, undrained shear strength; S_u (field), corrected S_u from vane shear test(VST); φ’, effective stress friction angle; φ’cv, constant-volume φ; TC, triaxial compression; UC, unconfined compression test.

Nikolaos Alamanis in recent years summarized the value of mean and COV for different types of soil properties. Here only some of the soil properties are presented, for further inquiry, the reader can refer (Alamanis, 2017).

Table 2.3 Average values μ and coefficient of variation COV for the active angle of internal friction (Alamanis, 2017)

Researcher	Year	Mean μ	COV
Harr	1987		2% - 13%
Kalhawy	1992		2% - 13%
Phoon and his colleagues	1995	20 - 40 (deg)	5% - 15%
Lacasse and his colleagues	1997		2% - 5%
Suchomel	2010	21 (deg)	8%
Phoon and his colleagues	1999	21-40 (deg)	5% - 15%
Duncan	2000		2% - 13%
Jeremic and his colleagues	2007		2% - 5%
Griffiths and his colleagues	2002	35 (deg)	5% - 50%
El Ramley and his colleagues	2002	35 (deg)	5.60%
Schweiger	2005	35 (deg)	0

Table 2.4 Average values of μ and coefficient of variation COV for active cohesion (Alamanis, 2017)

Researcher	Year	Mean μ	COV
Griffiths and his colleagues	2002	24KN/m2	30%
Suchomel	2010	10KN/ m2	21%
Harr	1987		20%
Cherubini	1997		20%-30%
Li and his colleagues	1987		40%

Table 2.5 Average values μ and coefficient of variation COV for the unit weight (Alamanis, 2017)

Researcher	Year	Mean μ(kN/m3)	COV
Harr	1987	1%-10%	
Phoon and his colleagues	1995	13-20	<10%
Smith and his colleagues	2004	20	0%
Duncan	2000	14-20	<10%
Wang and his colleagues	2010	20	6%
Hicks and his colleagues	2002	20	0%
Griffiths and his colleagues	2002	20	0%
Schweiger	2005	20	0%

El-Ramly et al., (2002), have investigated the impact of uncertainty on the reliability of slope design and performance assessment. According to their study, conventional slope practice based on the factor of safety cannot explicitly address uncertainty, thus compromising the adequacy of projections. Probabilistic techniques are rational means to quantify and incorporate uncertainty into slope analysis and design. They have used Microsoft® Excel 97 and @Risk as a tool based monte carlo simulation. An important conclusion of thier study is that probabilistic analyses can be applied in practice without an extensive effort beyond that needed in a conventional analysis. They believe that combining conventional deterministic slope analysis and probabilistic analysis will be beneficial to slope engineering practice and will enhance the decisionmaking process.

Nejan Huvaj and Emir Ahmet Oğuz (2018)**,** investigated a well-documented landslide case study to demonstrate the importance of probabilistic approach in slope stability. They investigated the effects of considering variability in material properties and compared deterministic and probabilistic slope stability analyses results. Deterministic limit equilibrium, probabilistic limit equilibrium, and probabilistic finite element analyses are conducted for Lodalen landslide in Oslo, Norway and they compared results with each other. They have investigated factor of safety, the probability of failure and the most critical failure surface with and without statistical cross-correlation of soil's shear strength parameters. They comeup with the conclusion that the critical failure surface in a slope can be different indeterministic LEM, probabilistic LEM, and probabilistic FEM analyses. It would be best to identify the most critical failure surface by making use of all available methods, including probabilistic approaches.

R.K Sharma (2016)**,** have worked on probabbilistic analysis and reach to a conclusion that traditional slope stability analysis is limited to the use of single valued parameters to analyze a slope's characteristics. Thus, traditional analysis methods yield single valued estimates for factor of safety of a slope's stability. Yet, the inherent variability of the soil characteristics which affect slope stability shows that the stability of a slope is a probabilistic rather than a deterministic situation. In other words, the stability of a slope is a random process which is dependent on the relative distribution of controlling soil parameters. For a natural slope, the stability deciding parameters vary considerably throughout the extent of slope. In his study, the variability of soil properties and their effect on stability of a natural slope studied by incorporating the probabilistic analysis using Monte Carlo simulation and deterministic analysis using Geo-Studio and PLAXIS. The results obtained from probabilistic approach can be used to determine the probability of failure corresponding to a particular of factor of safety and an allowable risk criterion can be used to establish a consistent target for the design process.

CHAPTER 3 MATERIALS AND METHODS

3.1 Introduction

The Ethiopian Geological Survey and Ethiopian Roads Authority have made some effort even though there is no comprehensive record of landslides and their consequence is made in detail in Ethiopia. Despite all challenges many scholars have reported on slope instability problems in different parts of the country like Dessie, Abay gorge, Jimma basin, Goffa, Gilgel Gibe-II, and Sodo-Shone areas, shale hill slopes, Tarmaber and surrounding area, wollo, wondogenet, and Tekeze hydro power project as shown in Figure 3.1.

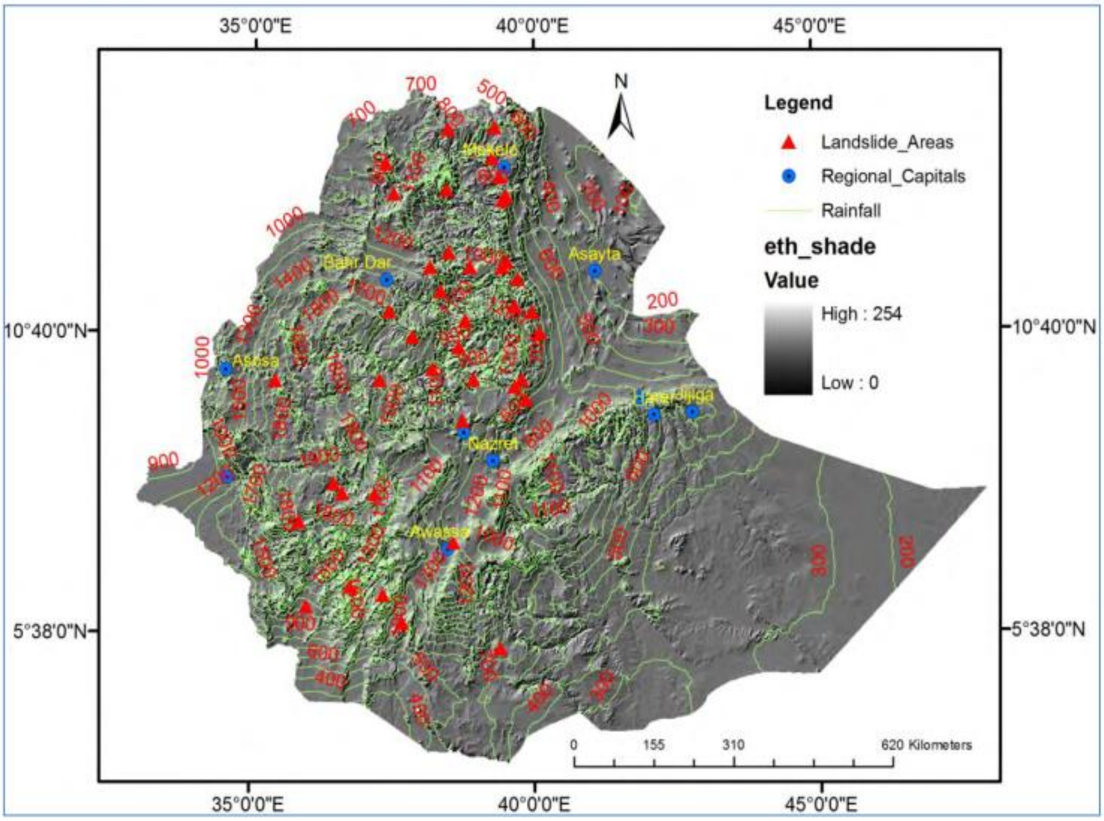

Figure 3.1 Location of landslide affected areas in the highlands of Ethiopia, Modified after the works of the various researchers (Woldearegay, 2013)

3.2 Study Area

The chosen study areas are found in the capital city of Ethiopia, Addis Ababa where red clay soil is dominantly exists. A typical red clay locations were selected among the sub cities of Addis Ababa namely, Kolfe Keranio, Arada, and Gulele sub cities. The specific locations were Addisu Gebeya, Kolfe, Asko and Arada.

Figure 3.2 Site Location (Google Earth)

3.3 Regional Geology

Addis Ababa is positioned on the western edge of the main Ethiopian Rift Valley. Normal faults down thrust towards the rift characterize the Mio-Pliocene boundary, which shows Mio-Pliocene volcanic. The massive fault marks the upper (outside) edge of the margin immediately north of the Addis Ababa-Ambo Road, it runs roughly east-west. The lower limit runs northeast to southwest, parallel to the major fissure systems in the area from Nazareth to Awash Station, the rift-floor (Akalu, 2017).

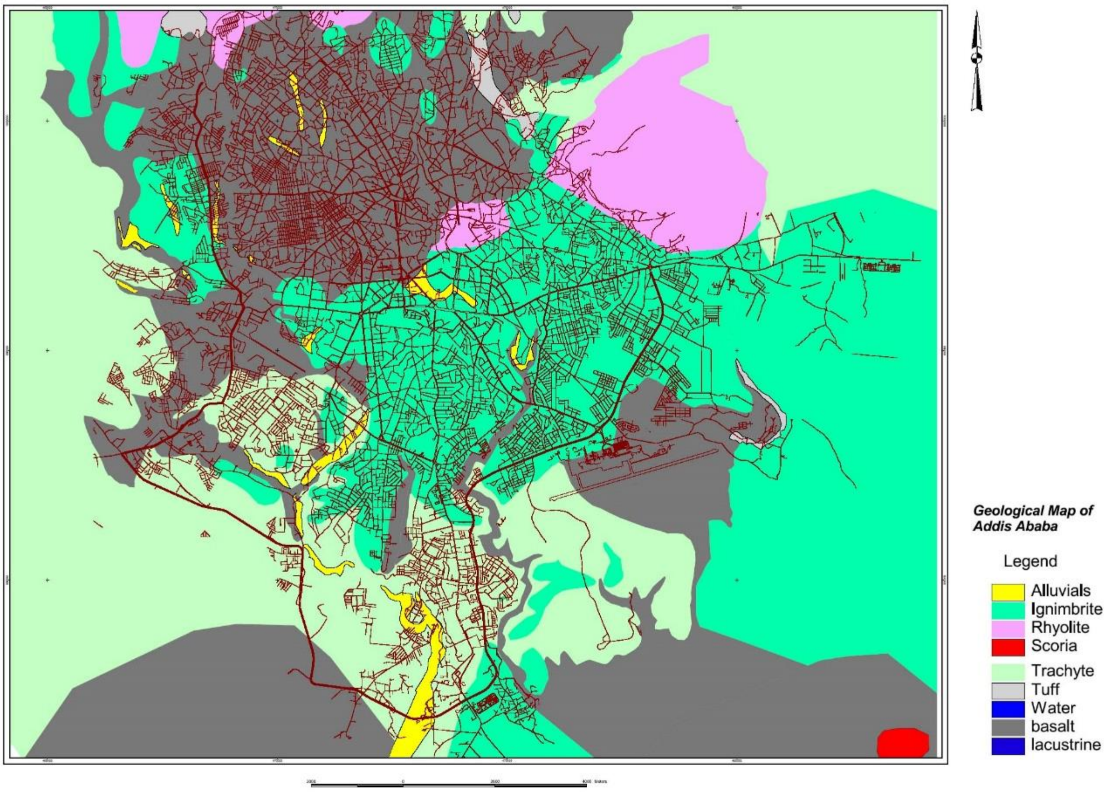

Figure 3.3 Geological map of Addis Ababa City (Geology of Ethiopia, 1998)

Trachy-basalts (around general wingate school), Ignimbrites, and Basalts are the principal occurrences with in western areas of Addis Ababa, as per geological map of Addis Ababa. Addis Ababa basalt, primarily alkaline and olivene basalt, and Addis Ababa ignimbrite cover parts of Gulele, Addis Ketema, and Arada. Wechecha's core volcanics, Entoto's pyroclastic trachytic lava flows cover the majority of Kolfe Keraniyo's subcity (Akalu, 2017).

As proposed by many researchers, Miocene-Pleistocene volcanic sequence from bottommost to topmost is Addis Ababa Basalts, Bofa Basalts, Alaji Basalts, Entoto Silicics, and Nazareth Group.

Addis Ababa basalt is porphyritic in texture which dominantly cover the central part the city. Bafo basalts found in the southeastern region of Addis Ababa characterized by big vesicles that are filled by calcite. It has a restricted location outcrop from southwards of Akaki river basin. Alaji basalts has various textures from porphyritic to aphanitic covers the north and northeastern part of the city. Entoto Silicic found at the bottom of entoto hills composed of rhyolites and trachytes. The Nazareth group is composed of three units identified as lower welded tuff, aphanitic basalt and upper welded tuff which covers south of Filwoha fault and extended towards Nazareth (Haile Sellasie, 1989).

3.4 Seismicity of the region

According to the seismic hazard map of Ethiopia, parts of Addis Ababa city like bole and kaliti town lies in zone three. Our country Ethiopia adopted an earthquake code of design standards for buildings based on the seismic zone map by Pierre Gouin. Consequently, Ethiopia is broadly subdivided into four seismic zones depending upon more than 500 historic earthquake records covering the year between 1400-1974. The seismic hazard within each zone has been assumed to be constant through local variations are expected.

The seismic hazard map of Ethiopia as provided in the Ethiopian Building Code Standard is based on a 100-year return period or approximately 50% of being exceeded in 50 years. Each seismic zone 1 to 4 is assigned a constant bedrock acceleration ratio α_0 of 0.03, 0.05, 0.07, or 0.1, respectively, however, Zone 0 is considered seismic free. In this map, the study site belongs to Zone 1 with α_0 = 0.03.

Based on the new code ES EN 1998-1:2015 the seismic hazard map is divided into five zones based on bedrock acceleration with a reference return period of 475 years with a 10% probability of exceedance in 50 years. The study area was found in the same zone according to the new code.

Table 3.1 Bed rock acceleration ratio (ES EN 1998-1:2015 Design of Structures for earthquake resisistance , 2015)

Zone	5	4	3	2	1	0
$\alpha_0 = a_g/g$	0.2	0.15	0.1	0.07	0.04	0

3.5 Topography

When we come to the overall topography of Addis Ababa, the city is surrounded by volcano formed mountains like Wechecha mountain at the west, Furi mountain at the southwest, Entoto mountain at the north, and Yerer mountain at southeast side. Light brown and yellowish-brown soils are common in the north, northeast and northwest part due leaching occurred in steep slope. However, soils in the southern, southeastern, central and western parts are dark grey soils in color.

3.6 Climate

In Ethiopia, the climate varies mostly with altitude, and it goes from the hot and arid climate of the lowlands to the cool climate of the plateau. In general, there are five climatic zones, "Kur" (Alpine), above 3000 meters above sea level; "Dega" (Temperate), 2300 meters to around 3000 meters; "Weina Dega" (Subtropical), 1500 meters to around 2300 meters; "Kolla" (Tropical), 800 meters to about 1500 meters; and "Bereha" (Desert), less than 800 meters. The majority of Addis Ababa is classified as Weina Dega (subtropical) (Akalu, 2017).

3.7 Temperature

Addis Ababa, the capital, is located at 2,300 meters (7,500 feet) above sea level, with altitudes ranging from 2,100 to 2,700 meters (7,000 to 9,000 feet) in different sections of the city, and enjoys a warm temperature. From November to February, when lows drop below 10 °C (50 °F), nights are cool, even cold, while days are pleasant, with highs around 23/25 °C (73/77 °F), except in July, August, and September, when highs drop to approximately 20/21 °C (68/70 °F) during the rainy season. As is customary in Ethiopia, the months of March and May are the warmest of the year, albeit by a few degrees.

Table 3. 2 Average Temperature (Climate- Ethiopia, n.d.)

Addis Ababa - Average temperatures (1991-2020)						
Month	**Min (°C)**	**Max (°C)**	**Mean (°C)**	**Min (°F)**	**Max (°F)**	**Mean (°F)**
January	9	24	16.3	48	75	61.4
February	10	25	17.5	50	77	63.5
March	12	25	18.6	54	77	65.5
April	13	25	18.8	55	77	65.8
May	13	25	18.6	55	76	65.5
June	12	23	17.5	54	73	63.4
July	12	21	16.4	54	69	61.6
August	12	20	16.2	54	69	61.2
September	12	21	16.5	53	71	61.7
October	10	23	16.6	51	73	61.8
November	9	23	16.1	49	73	61
December	8	23	15.5	47	73	59.9
Year	11	23.1	17	51.9	73.5	62.5

3.8 Rainfall

Rainfall averages 1,160 mm (46 in) per year, with a peak from June to September, which is the only particularly rainy period. From November to February, there is minimal rain and only a few showers; from March to May, afternoon showers become more common, occurring 7/10 days per month, and practically every day in July and August.

Table 3. 3 Average Precipitation (Climate- Ethiopia, n.d.)

Addis Ababa - Average precipitation			
Month	**Millimeters**	**Inches**	**Days**
January	13	0.5	3
February	30	1.2	5
March	60	2.4	7
April	80	3.1	10
May	85	3.3	10
June	140	5.5	20
July	280	11	27
August	290	11.4	26
September	150	5.9	18
October	25	1	4
November	7	0.3	1
December	7	0.3	1
Year	1165	45.9	132

3.9 Data Collection

The data used for this research have been taken from two previous research works carried on in Addis Ababa red clay soil. Among these researches the first one was aimed to investigate the effect of remolding on mechanical behavior of Addis Ababa red clay soil (Lukas, 2010) and the second one was aimed to investigate the engineering characteristics of red clay soil in western Addis Ababa (Akalu, 2017). The former study was carried on sites located at Addisu Gebeya and Kolfe and two samples were used for each, the shear strength parameters determined from triaxial test (CU) and for the later research, samples were taken from Asko and Arada area, direct shear test was used to determine the shear strength parameters. Some soil parameters which are unable to get from these researches, literature recommended values are used with caution by considering the soil profile, each layer material description and soil log.

3.10 Software used for Analysis

By using the advantage of computer technology advancement nowadays software programs are widely used in the advanced Engineering world. There are different types of geotechnical software programs used to analyze the stability of any natural and manmade slopes. Slide from Rocscience is one of the various software packages used to analyze slope stability problems and used for this research. It is a 2D slope stability analysis program for assessing the safety factor or likelihood(probability) of failure. It is possible to assume both circular and non-circular failure surfaces in soil or rock slopes. Outstandingly, Slide is so user friendlily to utilize, and yet complex models can be created and analyzed rapidly and effectively. Modeling of external loading, groundwater, and support can be done in different ways in the Slide (Rocscience web help, 2021).

Slide analyzes the stability of slip surfaces utilizing vertical slice limit equilibrium methods (e.g., Bishop, Janbu, Spencer, etc.). Every single slip surface can be analyzed or search methods can be connected to find the critical slip surface for a given slope. It is possible in Slide to carry out deterministic (safety factor) or probabilistic (probability of failure) investigations.

Program modules in the Slide are three namely, model, compute and interpret module. filling and editing the model boundaries, loads, material properties, groundwater conditions, slip surface definition, and saving the input file is done in the model module and it is a pre-processing program. The second one is a compute engine or program module that runs from the Slide Model program. Finally, data visualization and interpretation of the Slide analysis results is performed by Slide interpret program as post-processing. This includes slope stability results as well as finite element groundwater results if you have performed a groundwater seepage analysis (Rocscience web help, 2021).

One of the unique features of this software is that there is a way to carry out a probabilistic analysis and this is a good insight to know that factor of safety is not the only criteria for failure as explained in the literature review section. In a conventional slope stability analysis, it is expected that the values of all model input parameters are precisely known. For a given slip surface, a single value of the safety factor is calculated. This sort of investigation can be termed a deterministic analysis. In reality, the values of many input parameters for a given slope instability are not very well-identified, that’s why the probabilistic method to the analysis of slope stability can be suitable for better risk minimization.

In a probabilistic slope stability analysis, assigning statistical distributions to model input parameters, like material properties, support properties, loads, water table location, etc. are possible by the user. In doing so the degree of uncertainty in the value of the parameters is accounted for in a better way. Based on the user-defined statistical distributions and by entering the appropriate parameters for the distribution (standard deviation, minimum and maximum values, correlation coefficient) input data samples are randomly generated. A given slip surface may then have numerous diverse values of safety factors calculated. This allows the distribution of safety factors, from which a probability of failure for the slope can be calculated (Rocscience web help, 2021).

Based on the selected statistical distribution, sampling method, and several samples(N) defined N values of random variables are generated. By loading a new set of random variable samples, and re-running the analysis Probabilistic Analysis is carried out that is repeated N times as shown in Figure 3.4 where N is the number of Samples defined in a project setting.

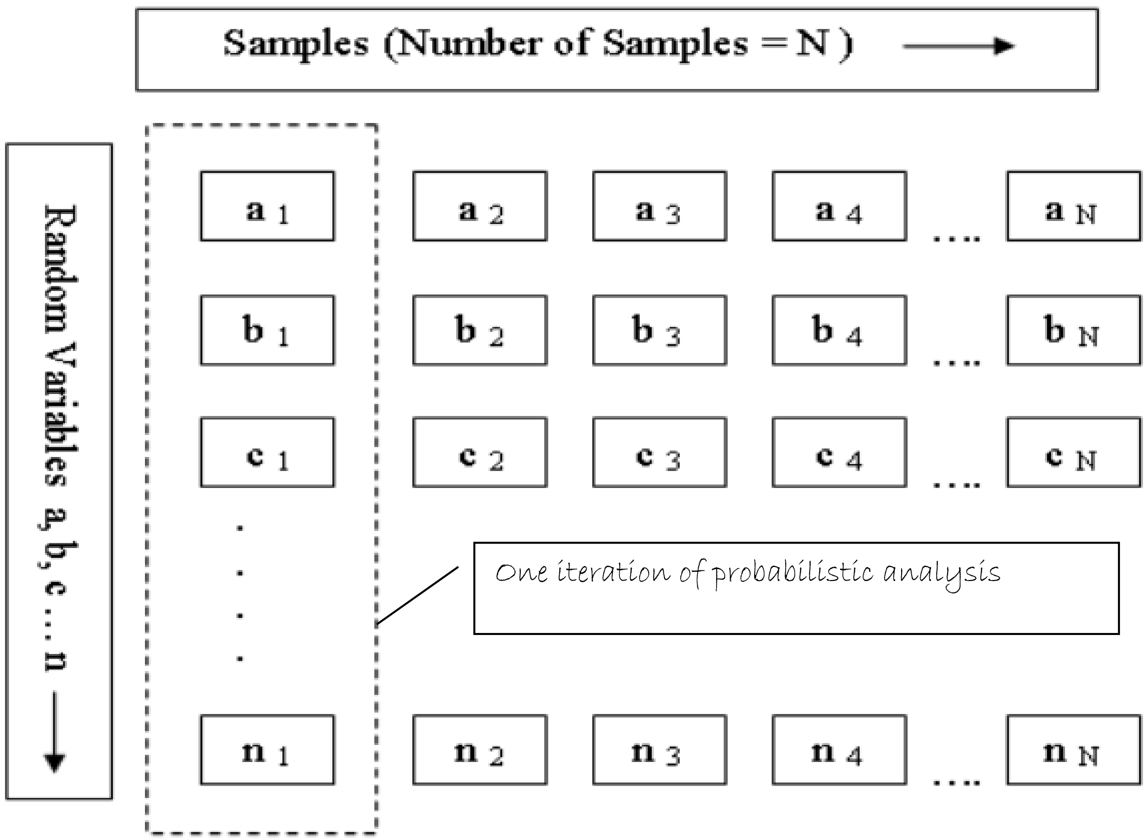

Figure 3.4 Random Variable Samples used in Probabilistic Analysis (Rocscience web help, 2021)

There are two sampling methods in Slide namely Monte Carlo and Latin Hypercube sampling which determines statistical inpoout distributions for the random variables. The Monte Carlo sampling technique uses accidental numbers to sample from the input data probability distributions. It is applied to a wide variety of problems involving random behavior, in geotechnical engineering (Rocscience web help, 2021). Latin Hypercube sampling method is based upon "stratified" sampling with random selection within each stratum. This results in a smoother sampling of the probability distributions.

In probabilistic slope stability analysis critical probabilistic slip surface can be shown which will not be always the same as the critical deterministic slip surface (i.e., the slip surface with the lowest safety factor when all input parameters are equal to their mean value). In general, the critical probabilistic surface and the critical deterministic Surface (i.e., the deterministic global minimum slip surface) can be different surfaces.

In addition to the factor of safety, probability of failure and reliability index are used as a measure of safety in probabilistic analysis. By definition probability of failure is the ratio of the number of failed surfaces to a total number of slip surface in the analysis and the Reliability Index characterizes the number of standard deviations which separate the mean Factor of Safety from the critical Factor of Safety (= 1) (Rocscience web help, 2021).

The second software used for this research is RS2 from Rocscience. RS2 is a powerful 2D finite element package used for various engineering projects like excavation design, slope stability, groundwater seepage, probabilistic analysis, consolidation, and dynamic analysis in soil and rock applications (Rocscience, 2021).

RS2 has a similar graphical user interface with that of Slide except for some and the major feature which makes RS2 different from the Slide is that it is finite element-based software. Unlike that of Slide, there is no predetermined failure surface in RS2 but rather it works under the principle of strength reduction factor. It is possible to use different soil models like Mohr-Coulomb and Generalized Hoek-Brown and other constitutive models. Besides, it is also possible to work on probabilistic analysis on finite element mesh which integrates the advantage of defining parameters as random variables than deterministic ones.

3.11 Analysis Methods

By using those two software packages discussed in brief, two types of analysis are carried out. These are deterministic and probabilistic analyses as summarized below.

- ❖ Slide V6.0 from Rocscience – Limit equilibrium method
  - ✓ Deterministic analysis
  - ✓ Probabilistic analysis
- ❖ RS2 V11.0 – Constitutive equations
  - ✓ Finite element analysis
  - ✓ Probabilistic finite element analysis

3.12 Input parameters

The following parameters are defined for both software programs to be used wherever necessary. These data are taken from previous research works on the same location as mentioned the research works in data collection section. But, Modulus of elasticity, poison's ratio, and porosity values are taken from different kind of literature (Bowles, 1997) and summarized useful parameters of the university of Stanford (Stanford University, 2014) cause during soil investigation, these parameters are not considered.

- Kolfe 1
  - Cohesion (C') = 23.4 kN/m^2
  - Internal friction angle (ϕ') = 16.7^o
  - Unit weight (γ_{sat}) = 18 kN/m^3
  - Elastic modulus = 100 000 kPa
  - Poison's ratio = 0.4
  - Porosity = 0.5
- Kolfe 2
  - Cohesion (C') = 19.2 kN/m^2
  - Internal friction angle (ϕ') = 23^o
  - Unit weight (γ_{sat}) = 18 kN/m^3
  - Elastic modulus = 50 000 kPa
  - Poison's ratio = 0.4
  - Porosity = 0.5
- Kolfe 3
  - Cohesion (C) = 102.1 kN/m^2
  - Internal friction angle (ϕ') = 0^o
  - Unit weight (γ_{sat}) = 22 kN/m^3
  - Elastic modulus = 100 000 kPa
  - Poison's ratio = 0.4
  - Porosity = 0.5
- Addisu gebeya 1
  - Cohesion (C') = 20 kN/m^2
  - Internal friction angle (ϕ') = 15.5^o
  - Unit weight (γ_{sat}) = 20kN/m^3

  - Elastic modulus = 50 000 kPa
  - Poison’s ratio = 0.4
  - Porosity = 0.5
- Addisu gebeya 2
  - Cohesion (C’) = 15.3 kN/m^2
  - Internal friction angle (ϕ’) = 21.3^o
  - Unit weight (γ_{sat}) = 19.5 kN/m^3
  - Elastic modulus = 50000 kPa
  - Poison’s ratio = 0.4
  - Porosity = 0.5
- Arada
  - Cohesion (C’) = 71kN/m^2
  - Internal friction angle (ϕ’) = 6^o
  - Unit weight (γ_{sat}) = 20 kN/m^3
  - Elastic modulus = 50 000 kPa
  - Poison’s ratio = 0.4
  - Porosity = 0.5
- Asko
  - Cohesion (C’) = 19 kN/m^2
  - Internal friction angle (ϕ’) = 23^o
  - Unit weight (γ_{sat}) = 19 kN/m^3
  - Elastic modulus = 50 000 kPa
  - Poison’s ratio = 0.4
  - Porosity = 0.5

3.13 Modeling

3.13.1 Slide V6.0

The hypothetical soil geometry is modeled. It is a homogenous soil stratum. Ground water table is assumed by considering the ground water depth variation in Addis Ababa as shown in the Slide V6.0 model in Figure 3.5-3.7. A total of six geometries were modeled with varying dimensions in the horizontal direction and vertical direction. For the assignment of external loading, the worst combination of truck design load is taken including the design lane load and its position is defined as per AASHTO design requirement.

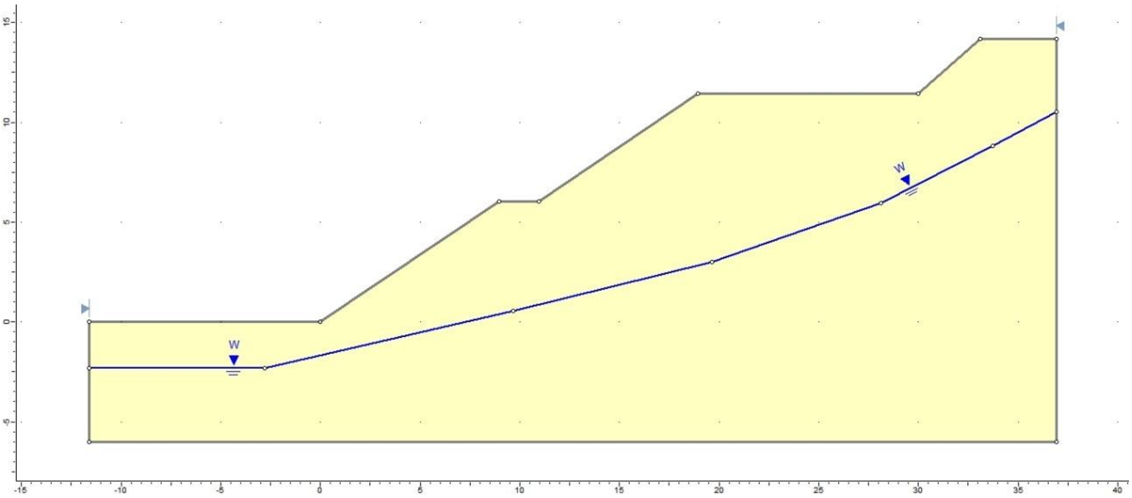

Figure 3.5 Soil geometr y Addisu gebeya 1, slide V6.0

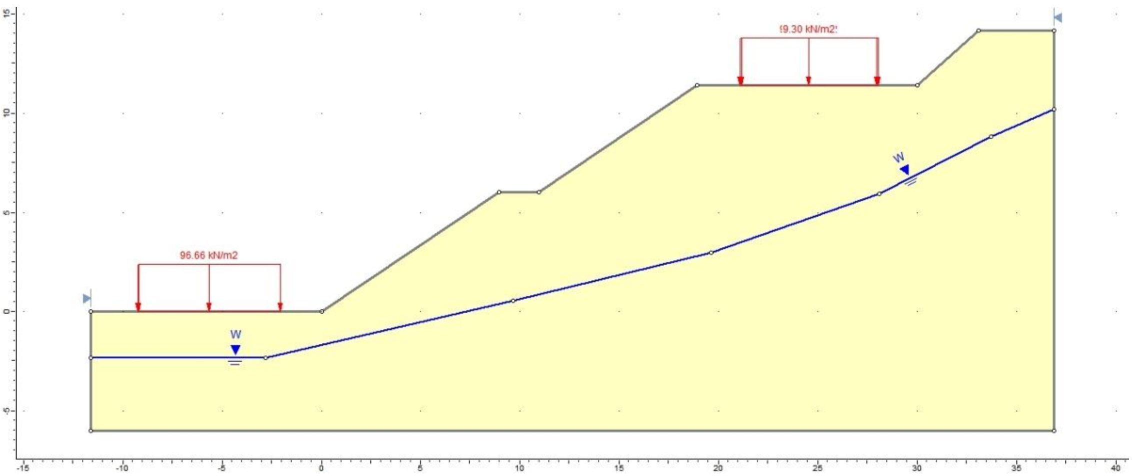

Figure 3.6 Soil geometry Addisu gebeya 2, slide V6.0

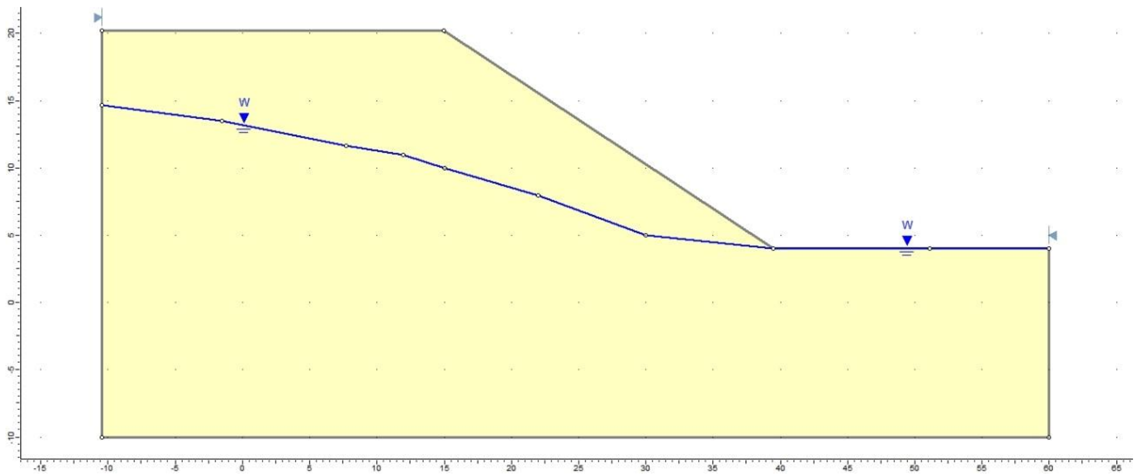

Figure 3.7 Soil geometry Kolfe 2, slide V6.0

Both deterministic and probabilistic analyses are carried out by using the advantage of Slide to run both at the same time. While working on the model important project settings are fixed. Among the various methods of analysis Bishop's Simplified, GLE/Morgenstern-Price, Janbu simplified and Spencer methods are selected by considering the satisfaction of equilibrium of forces and moments. The groundwater analysis is set to water surface implies that water surface is used to define the pore pressure conditions for each soil type.

For the probabilistic analysis, the sampling method is set to Latin hypercube which uses random numbers to sample from the input data probability distributions with 1000 samples which converges as shown in the Figure 3.8 and sensitivity is checked. The method is based upon "stratified" sampling with random selection within each stratum. The analysis method is global minimum type of analysis.

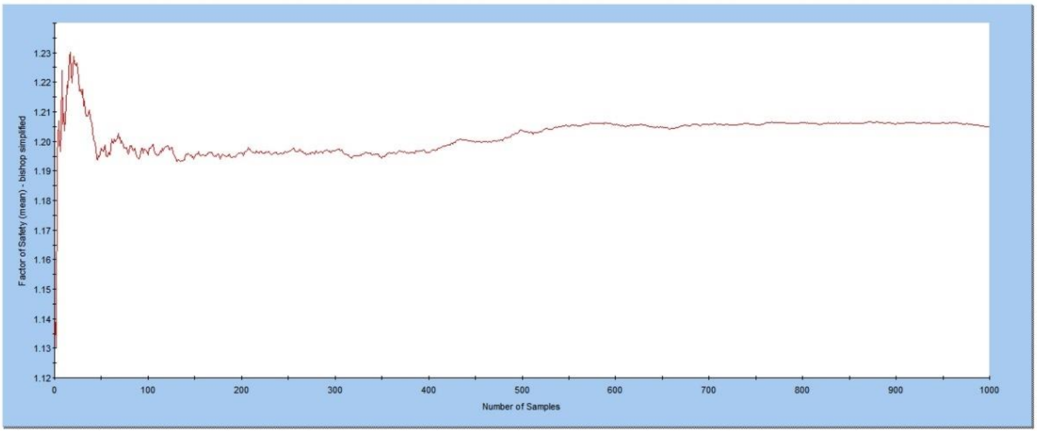

Figure 3.8 Convergence plot Addisu gebeya 2

The failure surface is assumed to be circular with an auto refine critical search method by which different slip surfaces are generated each time when analysis runs.

There are different strength type models available in Slide for modeling the shear strength of the various materials. For this research Mohr-Coulomb, sterngth type is selected (Equation 3.1).

$$\tau = c' + \sigma_n \tan\varphi' \tag{3.1}$$

As mentioned erlier, the groundwater method is set as water surface for pore pressure calculation by using Equation 3.2.

$$u = \gamma_w \, h H_u \tag{3.2}$$

Where, $u =$ pore pressure, γ_w = unit weight of water, h= the vertical distance from the base of a slice to a Water Surface and H_u= the Hu coefficient for the soil type (either user-defined or Auto). For this case, it is defined as auto H_u= $cos^2\,\alpha$ to be calculated from the water surface where α is water surface inclination as shown in Figure 3.9.

Since the analysis is carried out in undrained conditions excess pore water pressure is expected apart from the initial pore pressure calculated previously. For this excess pore pressure calculation due to a sudden increase in pore pressure within a soil due to rapidly applied loading conditions (undrained loading) a "B-bar" method is used from Skempton 1954. It says that the change in pore pressure is assumed to be directly proportional to the change in vertical stress.

$$\nabla u = \bar{B} \nabla \sigma_v \quad (3.3)$$

Where, ∇u is change in excess pore pressure, $\bar{B}$ is the overall pressure coefficient (Skempton), $\nabla \sigma_v$ is the change in vertical stress that may be due to the weight of added layers of material, external loads, seismic loads, or a combination of these factors. Hence, the final pore pressure which is used in the stability computation is equal to the Initial Pore Pressure + Excess Pore Pressure.

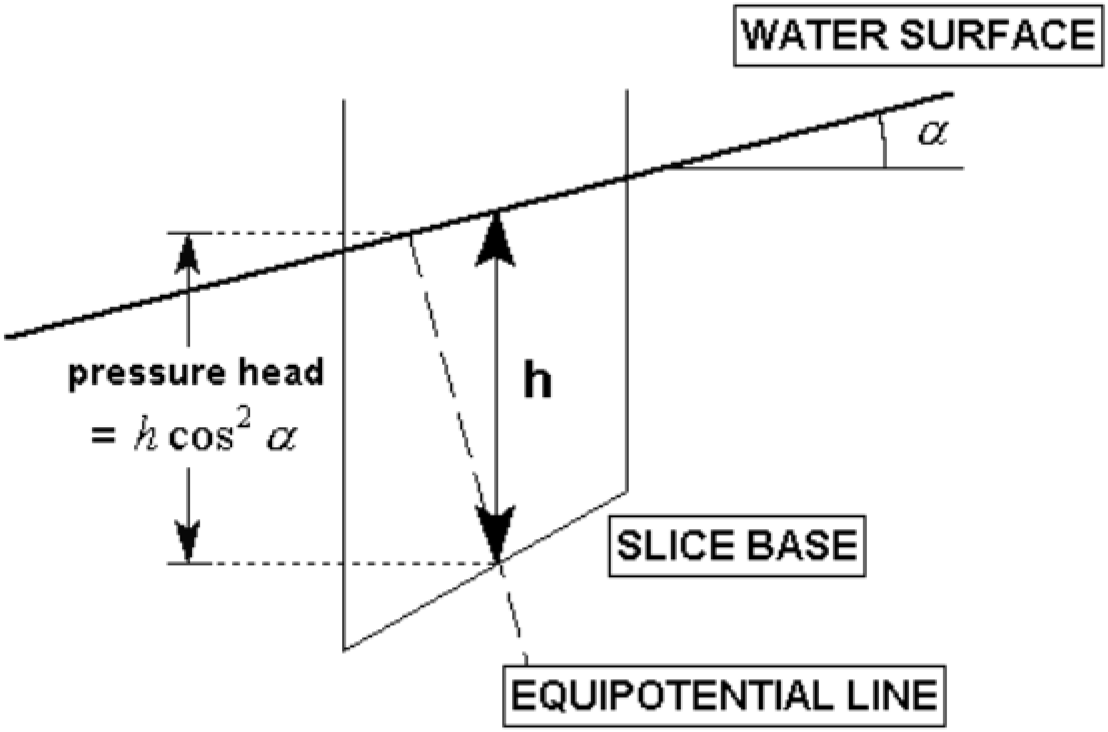

Figure 3.9 Automatic Calculation of Hu coefficient (Rocscience web help, 2021)

In a conventional or traditional slope stability analysis, it is assumed that the values of all model input parameters are precisely known. For a given slip surface, a single value of the safety factor is calculated. This type of analysis can be referred as a deterministic analysis. For the probabilistic analysis, it needs to define some additional input data over the deterministic one. Since it is difficult to be precise in knowing soil properties, probabilistic method of analysis is better in compromising this uncertainty of soil parameters. For that matter, parameters are defined as a random variable and by assigning statistical distribution together with the statistical parameters of the distribution (mean, standard deviation, minimum and maximum values). By defining a "probability density function" for the random variable random input data samples are generated. Then a given slip surface has different safety factors from that probability of failure is calculated.

The values found from soil investigation are taken as mean values and the standard deviation is calculated from the coefficient of variation value from literature as described elsewhere in the literature section by using the following equation. Maximum and minimum values are determined automatically.

$$\mathrm{COV(V)} = \frac{\sigma}{\bar{X}} \tag{3.4}$$

Where, σ is standard deviation, $\bar{X}$ is mean and V is coefficient of variation. a summary is listed in Table3.3.

Table 3.4 Defined COV from different kinds of literature

S.NO.	Material	COV (%)	Source
1	Cohesion	25	Cherubini 1997
	Unit weight	6	Wang and his colleagues 2010
	Friction angle	8	Harr, Kalhawy, and Duncan

Finally, a factor of safety is calculated as follows:

$$FS = \frac{\tau_{ff}}{\tau} \tag{3.5}$$

where τ_{ff} is the maximum shear stress that the soil can sustain at the value of normal stress of σ_n, τ is the actual shear stress applied to the soil.

In addition to factor of safety and probability of failure, the reliability index is the other measure of slope instability in probabilistic analysis which is calculated by using the Equation (3.6) for normal and lognormal distribution (3.7).

$$\beta = \frac{\mu - 1}{\sigma} \tag{3.6}$$

Where, β is normal reliability index, μ is mean factor of safety and σ is the standard deviation of a factor of safety.

$$\beta_{ln} = \frac{\ln\left[\frac{\mu}{\sqrt{1+V^2}}\right]}{\sqrt{\ln(1+V^2)}} \tag{3.7}$$

Where, β_{ln} is lognormal reliability index, μ is the mean factor of safety and V is the coefficient of variation.

3.13.2 RS2 V11.0

The same soil profile is modeled by using FEM-based RS2 software. By using this software two types of analyses are carried out. The first one is the FEM method of slope stability analysis and the second one is probabilistic slope stability analysis. All input parameters are the same as those parameters defined in Slide however, additional parameters are required for the analysis carried on in later software. These are elastic modulus, poison’s ratio, and porosity.

For the finite element analysis, the following necessary steps are followed:

- ✓ Delineation and discretization of the domain
- ✓ Writing element stiffness matrix
- ✓ Assembling the element stiffness matrix to get global stiffness matrix
- ✓ Applying appropriate boundary condition
- ✓ Solving the equations
- ✓ Post processing

The delineated and discretized model is shown in Figure 3.10:

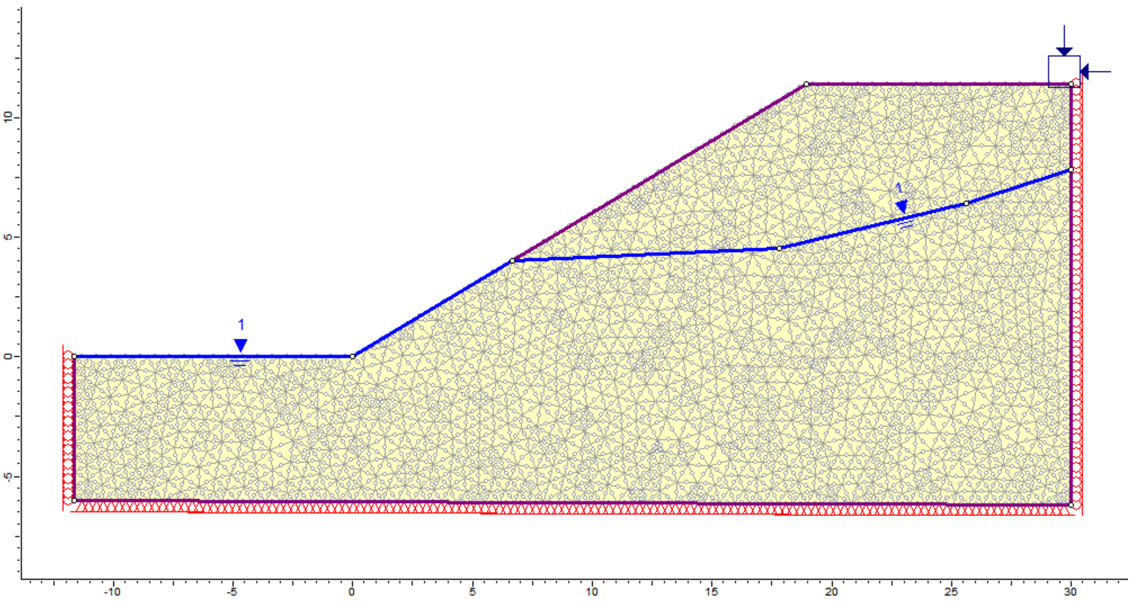

Figure 3.10 Discretized and meshed model by RS2 Asko

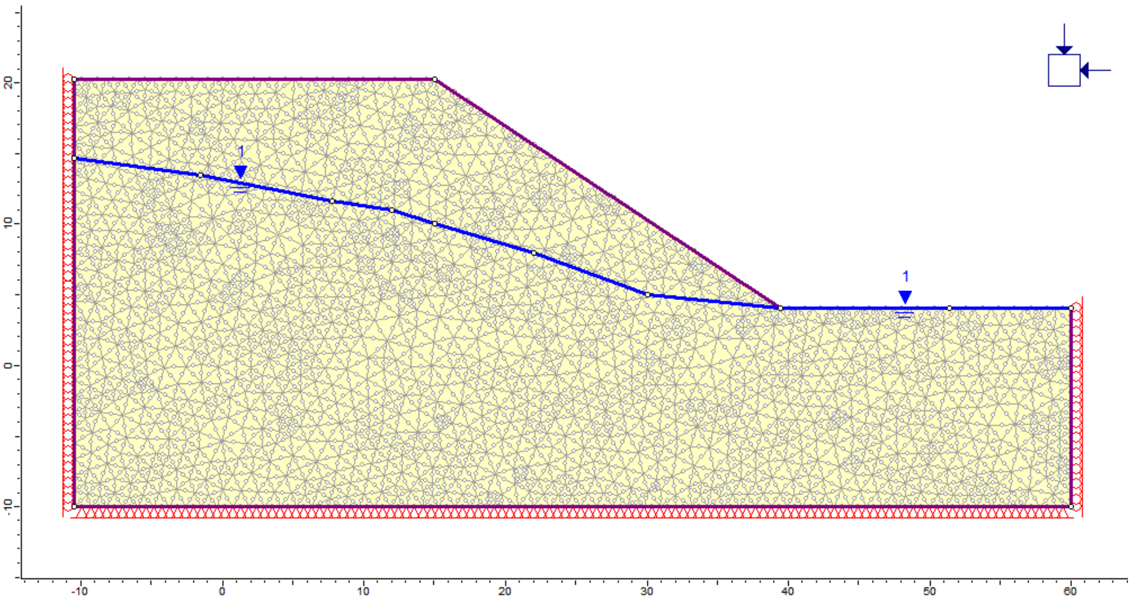

Figure 3. 11 Discretized and meshed model by RS2 Kolfe 1

Quadratic triangular element with three nodes at corner and three at the middle 6 nodes with two degrees of freedom for each node is defined. The quality of the mesh is checked all good. For the whole model, the number of elements becomes 4929 with 19730 degrees of freedom.

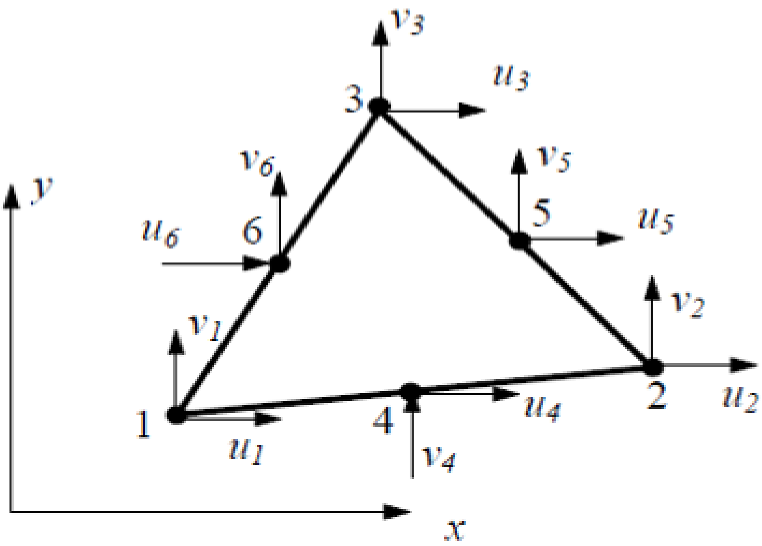

Figure 3.12 Quadratic Triangular element

The analysis type is assumed to be a plain strain in which failures are of infinite length in the out-of-plane direction, and therefore the strain in the out-of-plane direction is zero.

In RS2 the following are computed in a plain strain case.

- ✓ the major and minor in-plane principal stresses ($\sigma_1$and σ_3)
- ✓ the out-of-plane principal stress (σ_Z)
- ✓ in-plane displacements and strains

where, $\sigma_1$and $\sigma_3$are computed by using the following equations.

$$\sigma_1 = \frac{\sigma_z + \sigma_x}{2} + \sqrt{\left[\frac{\sigma_z - \sigma_x}{2}\right]^2 + \tau_{zx}{}^2} \tag{3.8}$$

$$\sigma_3 = \frac{\sigma_z + \sigma_x}{2} - \sqrt{\left[\frac{\sigma_z - \sigma_x}{2}\right]^2 + \tau_{zx}{}^2} \tag{3.9}$$

The other important step is the material definition section. The elastic material properties of Young's Modulus and Poisson's Ratio are assumed to be isotropic implies there is no variation of these properties in every direction. When we come to the material strength parameter, we need to consider the failure (strength) criteria and the material type (elastic or plastic). There are different types of strength criteria in RS2. One of these is the

Elastic/Plastic mode of failure includes Mohr-Coulomb, Hoek-Brown, Drucker-Prager, Generalized Hoek-Brown, and Discrete function strength criteria. For this research case, Mohr-Coulomb strength type is used for soil.

The material type by itself is defined as plastic with equal residual and peak strength parameters which means the material is elastic-plastic. In the elastoplastic constitutive model yield surface and potential functions are used for the derivation of constitutive equations of the materials. In general, in the formation of elastoplasticity yield criterion function, flow rule, Hooke's law, Additivity postulate, and hardening rule are involved as stated below respectively.

$$F_m(\sigma_{ij}, \kappa) = 0 \tag{3.10}$$

Where σ_{ij} is stress tensor, κ material state parameter, and m tell a number of yield surface.

$$Q_m(\sigma_{ij}) = Constant, \qquad \dot{\varepsilon}_{ij}^{p} = \sum_{m} \dot{\lambda}_m \frac{\partial Q_m}{\partial \sigma_{ij}} \tag{3.11}$$

it is assumed that the plastic strain increments ($\dot{\boldsymbol{\varepsilon}}_{\boldsymbol{ij}}^{\boldsymbol{p}}$) are coaxial with the gradient of plastic potential function Q.

$$\dot{\sigma}_{ij} = D^{e}{}_{ijkl}\dot{\varepsilon}^{e}{}_{kl} \tag{3.12}$$

$$\dot{\varepsilon}_{kl} = \dot{\varepsilon}^{e}{}_{kl} + \dot{\varepsilon}^{p}{}_{kl} \tag{3.13}$$

$$\dot{k} = f(\varepsilon^{p}{}_{kl}) \tag{3.14}$$

Where $\varepsilon^{p}{}_{kl}$ plastic strain increment, $\varepsilon^{e}{}_{kl}$ is elastic strain increment and $\dot{\lambda}_m$ plastic multiplier and equation 3.11 is called flow rule.

Hooke's law (3.12) relates the increment of stress to the increment of elastic strains using the elastic constitutive equations. The additivity postulate (3.13) simply sums up the increment of elastic and plastic strain to form the increment of strain. The hardening (3.14) controls the behavior of material after initial yielding. The expansion/shrinkage of the yield loci is controlled by hardening/softening rules. One of the elastoplastic model Mohr-Coulomb failure criteria in our case in terms of principal stress is given by:

$$F_s = \frac{1}{2}(\sigma_1 - \sigma_3) + \frac{1}{2}(\sigma_1 + \sigma_3)\sin\varphi - c\cos\varphi = 0 \qquad (3.15)$$

The analysis is carried out by the principle of shear strength reduction factor as depicted by the equation (3.16) as reduction of strength until a failure happens.

$$\frac{\tau}{SRF} = \frac{c - \sigma_n \tan\varphi}{SRF} \qquad (3.16)$$

After the application of SRF, c and φ becomes:

$$c_{SRF} = \frac{c}{SRF} \quad and \quad \varphi_{SRF} = \operatorname{atan}\left(\frac{\tan\varphi}{SRF}\right) \qquad (3.17)$$

Finally, for the probabilistic analysis, the materials are defined as a random variable with appropriate statistical distribution function by using the Latin hypercube method, the same procedure followed as discussed for Slide software.

CHAPTER 4 RESULTS AND DISCUSSIONS

This chapter presents the major findings and discussion on results in a brief way based on the analysis type carried on. As mentioned in the methodology section two major types of analyses were used and these are the Limit Equilibrium Method (LEM) and Finite Element Method (FEM) of analysis. However, the focus is on probabilistic analysis by using the Rocscience software package for both limit equilibrium and finite element method of analysis.

4.1 Limit Equilibrium Analysis

By using Slide, factor of safety is computed by both deterministic and probabilistic analysis. In LEM, it is possible to get a better result depending on how we search for the minimum slip surface. The researcher has tried all the different ways of searching mechanisms and the best one is selected (i.e., Auto refine search). With this search method, a probabilistic based LEM factor of safety is computed by using global minimum analysis and overall slope analysis, and nearly the same results were found, the results are summarized in Table 4.1 for global minimum analysis.

The global minimum analysis result is shown in Figure 4.1. Since it is a probabilistic analysis, the expected output values are a deterministic factor of safety, mean factor of safety, probability of failure, and reliability index for the normal and lognormal distribution. Pictures showing the minimum slip surfaces are listed in Appendix D.

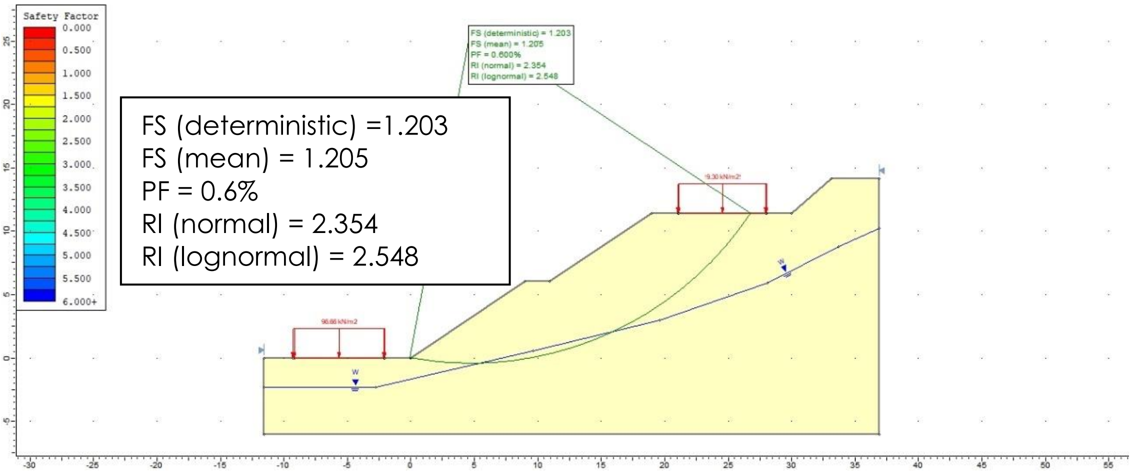

Figure 4.1 Global minimum analysis showing global minimum slip surface for Bishop, Addisu gebeya 2

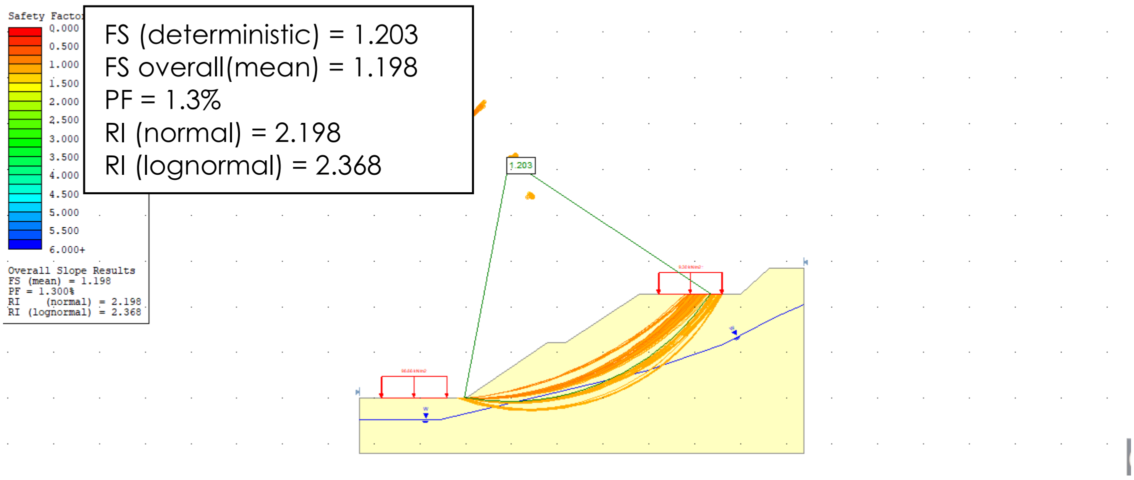

Figure 4.2 Global minimum analysis showing all slip surfaces for Bishop, Addisu gebeya 2

Table 4.1 Factor of safeties, global minimum analysis type

Method of Analysis	Deterministic Analysis	Probabilistic Analysis			
Kolfe 1					
	FS	FS	Reliability index normal	Reliability index lognormal	Probability of failure (%)
Bishop simplified	1.194	1.197	1.580	1.679	5.400
GLE/Morgenstern-Price	1.192	1.195	1.850	1.678	5.300
Janbu Simplified	1.082	1.085	0.726	0.704	22.90
Spencer	1.195	1.196	1.588	1.688	5.100

Kolfe 2					
Bishop simplified	1.355	1.359	3.148	3.619	0.200
GLE/Morgenstern-Price	1.354	1.357	3.134	3.601	0.200
Janbu Simplified	1.212	1.216	2.054	2.222	2.400
Spencer	1.354	1.357	3.131	3.598	0.200
Kolfe 3					
Bishop simplified	2.872	2.883	2.544	4.065	0.300
GLE/Morgenstern-Price	2.880	2.895	2.552	4.085	0.300
Janbu Simplified	2.785	2.796	2.501	3.942	0.300
Spencer	2.882	2.889	2.548	4.072	0.300
Addisu gebeya 1					
Bishop simplified	1.341	1.347	2.064	2.333	2.300
GLE/Morgenstern-Price	1.339	1.344	2.050	2.315	2.400
Janbu Simplified	1.210	1.216	1.381	1.462	9.300
Spencer	1.339	1.345	2.049	2.314	2.400
Addisu gebeya 2					
Bishop simplified	1.203	1.205	2.354	2.548	0.600
GLE/Morgenstern-Price	1.196	1.201	2.322	2.509	0.600
Janbu Simplified	1.050	1.052	0.706	0.690	22.400
Spencer	1.195	1.201	2.338	2.526	0.600
Arada					
Bishop simplified	2.265	2.272	3.164	4.587	0.000
GLE/Morgenstern-Price	2.264	2.271	3.166	4.588	0.000
Janbu Simplified	2.164	2.169	2.946	4.176	0.000
Spencer	2.265	2.271	3.169	4.593	0.000
Asko					
Bishop simplified	1.411	1.414	2.766	3.229	0.300
GLE/Morgenstern-Price	1.409	1.413	2.771	3.234	0.300
Janbu Simplified	1.301	1.304	2.207	2.466	1.200
Spencer	1.411	1.414	2.777	3.242	0.200

Table 4.1 shows that the factor of safety of deterministic and probabilistic analysis are nearly equal. This is something expected to happen if the analysis is correct. However, after the concept of probabilistic analysis, a factor of safety is not the only measuring criteria for failure but also other additional measuring ways called reliability index and probability of failure values to be used.

The value of the reliability index is of two types (i.e., normal and lognormal) but the best fit for this slope data is normal as indicated in appendix A for all analysis methods. For a safe design of slope, the reliability index value should be at least 3 or above. Nevertheless, that is attained for some slopes in this case (reliability index value, Table 4.1).

Finally, the probability of failure is the other measure of slope stability. From the last column of Table 4.1, in all cases the failure probability is more than nil in percent except for the case of Arada. If we take the deterministic factor of safety value of Bishop's Simplified method of analysis of Arada and Janbu simplified method of Addisu gebeya 2, it is 1.194 and 1.05 respectively. some one can say that this slope is safe since these values are greater than 1 if 1 is taken as a reference for the general case. However, even if FS>1 the probability of failure is 5.4% and 22.4% respectively. This implies that there may a probability to fail for a given slope even if FS is greater than one. One thing to bear in mind is that there is no value of failure which is termed as less (small) or that's okay even if its value is unity or less.

The Janbu simplified method gives a lesser value of factor of safety relative to the others. However, the probability value is greater than the rest methods. This assures the inverse proportionality between the probability of failure and the safety factor. *Output results of GM slope analysis are presented in Appendix A.*

4.2 Finite Element Analysis

The second major type of analysis used for this research is the finite element method of analysis. It is a more rigorous and advanced type than that of LEM. By using the RS2 program both the pure finite element method of analysis and probabilistic finite element analysis are computed. The results are presented separately in the next section.

4.2.1 FEM by using RS2

One of the limitations of the limit equilibrium method is assuming the shape of the slip surface prior to failure. Due to the SSR technique in the finite element method, no-slip surface is assumed before failure occurs. As depicted in Figure 4.3, the critical strength reduction factor which is the same as a factor of safety of the slope becomes 1.17 for

Addisu gebeya 2 and decreased for others also. this indicates that more critical and weak surfaces are possible to find in FEM than LEM. *Refer appendix B for output results of FEM analysis.*

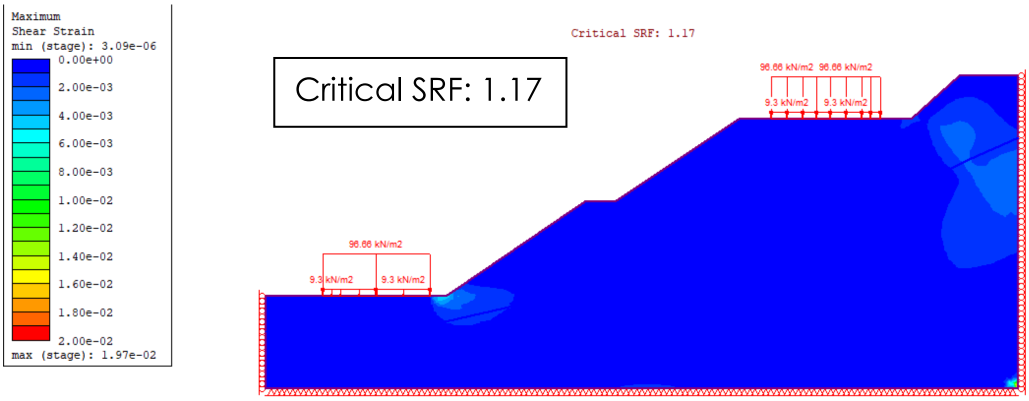

Figure 4.3 Critical SRF showing contour of the maximum shear strain, Kolfe 1

Table 4.2 Summary of factor of safety result from RS2

Site	Deterministic Analysis FS
Kolfe 1	1.07
Kolfe 2	1.18
Kolfe 3	2.60
Addisu gebeya 1	1.34
Addisu gebeya 2	1.17
Arada	2.14
Asko	1.00

With a rigorous method, it is possible to simulate the deformed shape of elements and the way how material moves during failure. Knowing the value of displacement value is advantageous for minimization of risks due to the failing slope. The critical displacement value (for SRF value of 1.17, the displacement is 0.023 m from its former position) is shown in Figure 4.5. It illustrates the deformed shape, displacement value, and boundaries of the model.

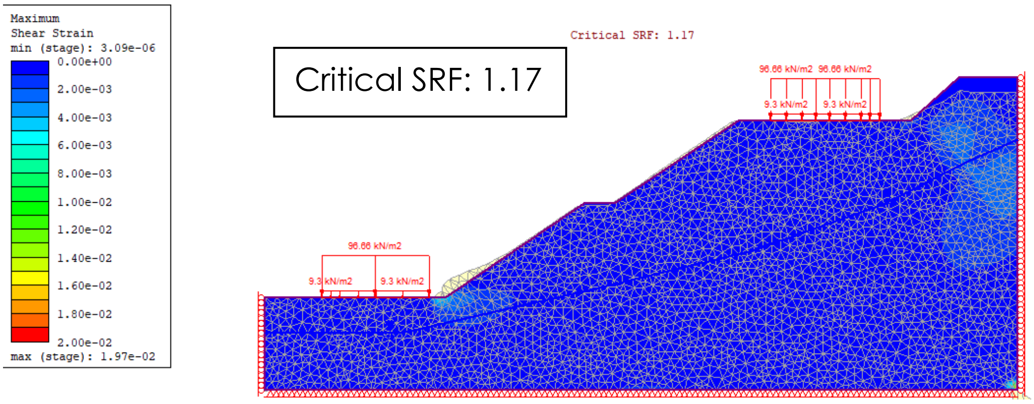

Figure 4.4 Deformed shape and Boundaries, Addisu gebeya 2

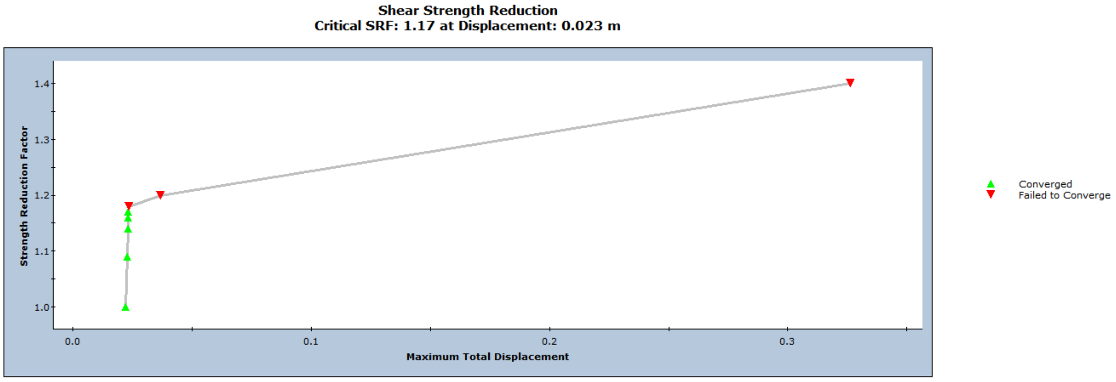

Figure 4.5 Maximum total displacements at critical SRF, Addisu gebeya 2

4.2.2 Probabilistic FEM Analysis by Using RS2

Even though FEM is better in showing the most critical slip surface, the parameters used are defined as definitive or fixed variable. Nevertheless, the uncertainty of values can be considered by defining parameters as a random variable. By doing so, a lesser factor of safety is found i.e., from 1.17 to 0.97.

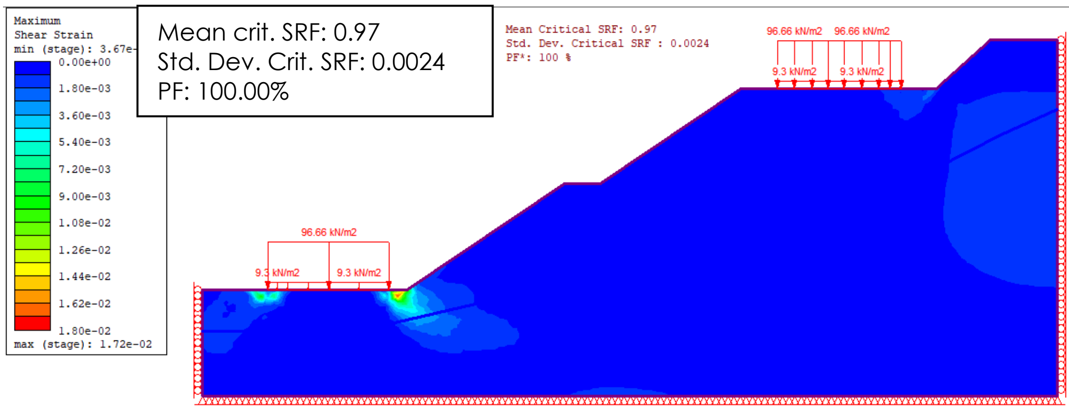

Figure 4.6 Mean critical SRF, showing the contour of Maximum shear plastic strain

As shown in Figure 4.6, the probability of failure is higher than LEM. The mean critical SRF is the average critical strength reduction factor from the entire constituent files of the probabilistic analysis and the standard deviation of the critical strength reduction factors from the entire constituent files of the probabilistic analysis. The safety factor from probabilistic and FEM are much close, this is due to fewer number of parameters defined as random variables in which the shear strength is dependent for the reason that lack of high-speed computer for computation. A better result is expected by defining more parameters as a random variable. *Refer appendix C for output results of PFEM analysis.*

As depicted in Figure 4.7, the deformed shape and boundary deformation sever at the toe.

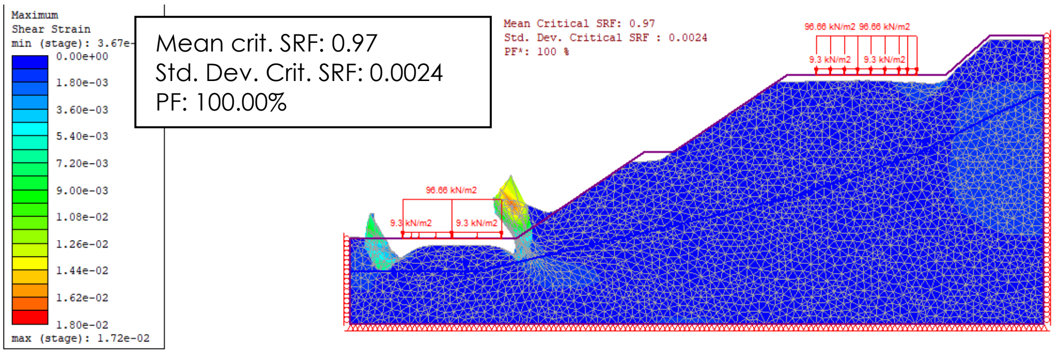

Figure 4.7 Deformed shape and boundaries, Addisu gebeya 2

For comparison purposes, results from all analysis methods discussed in the previous sections are compiled in Table 4.3.

Table 4.3 Summary of findings

Method of Analysis	Site	Deterministic (Average)	Probabilistic (Average)			
		FS	FS	RI (Average normal)	RI (Average lognormal)	P_f (Average)
LEM (GM)	Kolfe 1	1.166	1.168	1.436	1.437	9.68
	Kolfe 2	1.318	1.322	2.866	3.260	0.75
	Kolfe 3	2.854	2.866	2.536	4.041	0.30
	Addisu gebeya 1	1.341	1.342	2.063	2.333	2.3
	Addisu gebeya 2	1.161	1.165	1.930	2.060	6.05
	Arada	2.400	2.245	3.111	4.486	0.00
	Asko	1.383	1.386	2.615	3.040	0.50
FEM	Kolfe 1	1.070	-	-	-	-
	Kolfe 2	1.180	-	-	-	-
	Kolfe 3	2.600	-	-	-	-
	Addisu gebeya 1	1.340	-	-	-	-
	Addisu gebeya 2	1.170	-	-	-	-
	Arada	2.140	-	-	-	-
	Asko	1.000	-	-	-	-
PFEM	Addisu gebeya 2	1.17	0.97	-	-	100.00

CHAPTER 5 CONCLUSIONS AND RECOMMENDATIONS

As it is stated in the first chapter, main objective of this study was showing the reliability of probabilistic slope stability analysis over deterministic slope stability analysis. An effort is made to meet the stated objective and the main objective is achieved by acknowledging all the limitations of the study. The main emphasis is given for probabilistic analysis and good results are found in both LEM and FEM-based analysis. Even though FEM is well-suited method of analysis that avoids many assumptions and works by the principle of seeking out the weakest surface, probabilistic analysis is more appreciated for its account for soil uncertainties which is the limitation of FEM.

5.1 Conclusions

The following major conclusions are drawn from this research:

- ✓ a factor of safety greater than unity cannot guarantee the analysis to be termed as safe because a probability of failure greater than zero is shown for FS greater than 1.
- ✓ FEM lies on safe side than that of both deterministic and probabilistic LEM of analysis and finally,
- ✓ A finite element-based probabilistic analysis is more reliable than that of deterministic FEM and the traditional (conventional) probabilistic method of slope stability analysis.

5.2 Recommendation

Despite the promising results found, there are few points to be taken as a recommendation for further investigation on the same or related topic. The number of samples used for finite element probabilistic analysis is 70 and all parameters are not defined as random variables due to a lack of high-performance computer if more random variables are defined.

References

AASHTO. (2012). *AASHTO LRFD BRIDGE DESIGN SPECIFICATIONS.* Washington, DC, US.

Abramson, L. W., Thomas S. Lee, S. L., Sharma, S., & Glenn, M. B. (2001). *Slope Stability and Stabilization Methods (2nd ed.).* John Wiley and Sons, Inc.

ACI Commitee 318. (2014). *Building Code Requirements for Structural Concrete (ACI 318-14) AND Commentary on Building Code Requirements for Structural Concrete (ACI 318R-14).* American Concrete Institure.

Akalu, M. (2017). *Engineering Characteristics of Red Soil: A Case from Western Addis Ababa Ethiopia.* Addis Ababa.

AKBAŞ, B. (2015). *Probabilistic analysis using limit equilibrium, Finite element and random finite element.* Middle East Technical University.

Alamanis, N. (2017). Uncertainties and optimization in geotechnical engineering. *American Scientific Research Journal for Engineering, Technology, and Sciences (ASRJETS) Volume 38*, 92-111.

Allahverdizadeh, p., ASCE, S. M., Griffiths, D. V., Fenton, G. A., & ASCE, M. (2015). The random finite element method (RFEM) in probabilistic slope stability analysis with consideration of spatial variability of soil properties. (pp. 1946-1955). San Antonio, Texas: ASCE. doi:https://doi.org/10.1061/9780784479087.178

Aruna, M. (2008). Shear Behavior of Concrete Beams Reinforced with High Performance Steel Shear Reinforcement.

Aryal, K. P. (2006). *Slope stability evaluations by limit equilibrium and finite element methods.* Trondheim, Norway: Norwegian University of Science and Technology.

ASCE-ACI Committee 445. (1998, December). Recent Approaches to Shear Design of Structural Concrete. *American Society of Civil Engineers*.

Baecher , G. B., & Christian , J. T. (2005). *Reliability and statistics in geotechnical engineering.* Chichester, West Sussex, England: " John Wiley & Sons Inc.

Bentz, C. E., Vecchio, F. J., & Collins, M. P. (2006). Simplified Modified Compression Field Theory for Calculating Shear Strength of Reinforced Concrete Elements. *ACI Structural Journal*(July-August).

Bishop A.W. (1955). The Uses of the Slip Circle in the Stability Analysis of Slopes. *Geotechnique*, 7-17.

Bowles, J. E. (1997). *Fundation analysis and design.* The McGraw-Hill Companies,Inc.

Chok, Y. H., Jaksa, M. B., Griffiths, D. V., Fenton, G. A., & Kaggwa, W. S. (2015). probablistic analiysis of spatial variable c-phii slope. *Australian Geomechanics journal*, 17-27.

Civil Seek. (2018, July 18). *Slope Failure; its Types, Causes, Technical Terms.* Retrieved February 11, 2021, from civil seek: https://civilseek.com/slope-failure/

Climate- Ethiopia. (n.d.). Retrieved from Climate to Travel .

Collins, M. P., Bentz, E. C., Sherwood, E. G., & Xie, L. (2007). AN ADEQUATE THEORY FOR THE SHEAR STRENGTH OF REINFORCED CONCRETE STRUCTURES.

Davidson, A. (1983). *Reconnaissance Geology and Geochemistry of Parts of Ilubabor Kefa,Bull. No2. Ottawa.* Ethiopia.

Derbie, M. (2019). *A comparative study of deterministic and probabilistic approaches of slope stability analysis,A Thesis in Geotechnical Engineering.* Addis Ababa: Addis Ababa University.

Duncan, J. M. (1996). State of the art: Limit equilibrium and finite-element analysis of slopes. *Journal of Geotechnical Engineering, 122*(7), 577-596. doi:https://doi.org/10.1061/(ASCE)0733-9410(1996)122:7(577)

Duncan, J. M., Member, H., & ASCE. (2000). Factors of safety and reliability in geotechnical engineering. *Journal of geotechnical and geoenvironmental engineering, 126*(4), 307-316.

Eckhardt, R. (1987). Stan Ulam, John von Neumann, and the Monte Carlo method. *Los Alamos Science,Special Issue*, 131-137.

El-Ramly, H., Morgenstern, N. R., & Cruden, D. M. (2002). Probabilistic slope stability analysis for practice. *Canadian Geotechnical Journal, 39*(3), 665-683. doi:DOI: 10.1139/t02-034

El-Ramly, H., Morgenstern, N. R., & Cruden, D. M. (2002). Probabilistic slope stability analysis for practice. *Canadian Geotechnical Journal, 39*(3), 665-683. doi:DOI: 10.1139/t02-034

El-Ramly, H., Morgenstern, N. R., & Cruden, D. M. (2005). Probabilistic slope stability analysis for practice. *Geotechnique, 55*(1), 77-84. doi:https://doi.org/10.1139/t02-034

(2015). *ES EN 1998-1:2015 Design of Structures for earthquake resisistance* .

ETİZ, M. C. (2019). *Comparison of Limit Equilibrium Method and 2-D, 3-D Finite Element Slope Stability Models: A case study on the slope in Akapinar district, in Ankara.* Ankara: middle east technical university.

European Standard. (1992). *Eurocode 2: Design of Concrete Structures.* European Commitee for Standardization.

Fellenius, W. (1936). Calculation of stability of earth dams. Transactions 2nd international congress on large dams. *International Commission on Large Dams.* Washington D.C.

Fenton, G. A. (1990). Simulation of random fields via local average Subdivision. *J Geotech Geoenviron*, 1733-1749.

Fenton, G. A., & Vanmarcke, E. H. (1990). Simulation of random fields via local average subdivision. *journal of engineering mechanics, 116*(8), 1733-1749. doi:https://doi.org/10.1061/(ASCE)0733-9399(1990)116:8(1733)

Fishman, G. (1995). Monte Carlo: Concepts, algorithms, and applications.

Frank, J. V. (2000, January - February). Analysis of shear-critical reinforced concrete beams. *ACI Structural Journal, 97*.

Geology of Ethiopia. (1998). Retrieved from https://sites.google.com/site/linkstogeologyofethiopia/map/geological-map-of-addis-ababa

Ghoneim, M., & EL-Mihilmy, M. (2008). *Design of Reinforced Concrete Structures* (2nd edition ed.). Egypt: Cairo University.

Griffiths , D. V., & Fenton, G. A. (2004). Probabilistic slope stability analysis by finite elements. *Journal of Geotechnical and Geoenvironmental Engineering, 130*(5), 507–518. doi:https://doi.org/10.1061/(ASCE)1090-0241(2004)130:5(507)

Griffiths , D. V., & Fenton, G. A. (2004). Probabilistic slope stability analysis by finite elements. *Journal of Geotechnical and Geoenvironmental Engineering, 130*(5), 507–518. doi:https://doi.org/10.1061/(ASCE)1090-0241(2004)130:5(507)

Griffiths, D. V., Fenton, G. A., & Denavit, M. D. (2007). Traditional and advanced probabilistic slope stability analysis. doi:https://doi.org/10.1061/40914(233)19

Griffiths, D. V., & Fenton, G. A. (1993). Seepage beneath water retaining structures founded on spatially random soil. *Geotechnique, 43*(4), 577–587. doi:https://doi.org/10.1680/geot.1993.43.4.577

Griffiths, D. V., & Fenton, G. A. (2000). Influence of soil strength spatial variability on the stability of an undrained clay slope by finite elements. *Proceeding of GeoDenver 2000* (pp. 184–193). Denver, Colorado, United States: ASCE. doi:https://doi.org/10.1061/40512(289)14

Griffiths, D., Huang, J., & Fenton, G. (2015). Probabilistic slope stability analysis using RFEM with non-stationary random fields., (pp. 704-709). doi:doi:10.3233/978-1-61499-580-7-704

Haile Sellasie, g. a. (1989). The Addis Ababa-Nazareth Volcanics A Miocene-Pleistocene Volcanic Succession in Ethiopian Rift. *Ethiopian Journal of Science*.

Janbu, N. (1954a). *Stability analysis of slopes with dimensionless parameters, Thesis for the doctor of science in the field of civil engineering.* Harvard University Soil Mechanics Series.

Le, T. M., Sanchez, M., Gallipoli, D., & Wheeler, S. (2014). Probabilistic modelling of auto-correlation characteristics of heterogeneous slopes. *Geomechanics and Geoengineering, 10*(2), 95-108.

Lukas, M. (2010). *A STUDY ON THE EFFECT OF REMOLDING ON THE MECHANICAL BEHAVIOR OF ADDIS ABABA RED CLAY SOIL*. Addis Ababa.

Morgenstern, N. R., & Price, V. E. (1965). The analysis of the stability of general slip surface. *Geotechnique, 15*(1), 79-93. doi:https://doi.org/10.1680/geot.1965.15.1.79

Murthy, V. s. (2002). *Principles and practices soil mechanics and foundation engineering.* New York: Taylor & Francis Inc.

Nakamura, A. (2008). Embankment basal stability analysis using shear strength reduction finite element method. *10th International, Symposium, On landslides and Engineered slopes* (pp. 851-856). Boca Raton: CRC Press,.

Nilson, A. H., Darwin, D., & Dolan, W. C. (2010). *Design of Concrete Structures* (14th edition ed.). New York, US: Mc Graw Hill Companies.

Oguz, E. A., Yalcin, Y., & Huvaj, a. N. (2017). Probabilistic slope stability analyses: Effects of the coefficient of variation and the cross-correlation of shear strength parameters. *Geotechnical Frontiers 2017 GSP 278* (pp. 363-371). ASCE.

Oğuz, N. H. (2018). Probabilistic Slope Stability Analysis. *Sakarya University Journal of Science*, 1458-1465.

Peter, M. (1985). Truss Models in Detailing.

Phoon, k. k., & Kulhawy, F. H. (1999). Evaluation of geotechnical property variability. *Canadian Geotechnical Journal, 36*(4), 625-639. doi:https://doi.org/10.1139/t99-039

Phoon, K. K., & Kulhway, F. H. (1999). Characterization of geotechnical variability. *Canadian Geotechnical Journal, 36*(4), 612–624. doi:https://doi.org/10.1139/t99-038

Rocscience. (2021). *products*. Retrieved from Rocscience: https://www.rocscience.com/software/rs2

Rocscience web help. (2021). *Slide program overview*. Retrieved from C:\Program Files (x86)\Rocscience\Slide 6.0\WebHelp\Slide.htm

Salunkhe, D. P., Bartakke, R. N., Chvan, G., & Kothavale, P. R. (2017). An Overview on Methods for Slope Stability Analysis. *International Journal of Engineering Research & Technology (IJERT), 6*(3), 528-535.

SG Consulting Engineers PLC. (2016). *Detailed Geotechnical Investigation Report on the Landslide Problem along Jimma-Mizan Road.*

Sharma, R. K. (2016). Reliability analysis of slope stability using monte carlo simulation and comparison with deterministic analysis. *International Conference on Computational Methods(ICCM).*

Spencer, E. (1967). A method of analysis of the stability of embankments assuming parallel inter-slice forces. *Geotechnique, 17*(1), 11-26. doi:https://doi.org/10.1680/geot.1967.17.1.11

Stanford University. (2014, April). Some Useful Numbers.

Teferra A. and Leikun M. (1999). *Soil Mechanics.* Addis Ababa: Adiss Ababa University.

Terzaghi, k. (1950). Mechanism of landslides. Application of geology to engineering practice. New York: Geological Society of America.

Transportation Reasearch Board Executive Commitee . (2005). Simplified Shear Design of Structural Concrete Members. *NCHRP, NCHRP REPORT 549*.

Weight, K. J., & Macgregor, J. G. (2012). *Reinforced Concrete Mechanics & Design* (6th edition ed.). New Jersey, US: Pearson Education.

Woldearegay, K. (2013). Review of the occurrences and influencing factors of landslides in the highlands of Ethiopia: With implications for infrastructural development. *Momona Ethiopian Journal of Science (MEJS) v5*, 3-31.

Zakaria, M., Ueda, T., Wu, Z., & Meng, L. (2009). Experimental Investigation on Shear Cracking Behavior in Reinforced Concrete Beams with Shear Reinforcement.

Zhang, Y., Ji, E., & Xu, W. (2020). In *Probabilistic slope stability analysis for embankment dams* (pp. 1-19). Nanjing, China.

APPENDIX A

Slide Analysis Information

SLIDE - An Interactive Slope Stability Program

Project Summary

- File Name: Addisu gebeya 2.slim
- Slide Modeler Version: 6.02
- Project Title: SLIDE - An Interactive Slope Stability Program
- Date Created: 3/24/2022, 11:40:57 AM

General Settings

- Units of Measurement: Metric Units
- Time Units: days
- Permeability Units: meters/second
- Failure Direction: Right to Left
- Data Output: Standard
- Maximum Material Properties: 20
- Maximum Support Properties: 20

Analysis Options

Analysis Methods Used

- Bishop simplified
- GLE/Morgenstern-Price with interslice force function: Half Sine
- Janbu simplified
- Janbu corrected
- Spencer

- Number of slices: 25
- Tolerance: 0.005
- Maximum number of iterations: 50
- Check malpha < 0.2: Yes
- Initial trial value of FS: 1
- Steffensen Iteration: Yes

Groundwater Analysis

- Groundwater Method: Water Surfaces
- Pore Fluid Unit Weight: 9.81 kN/m3

- Advanced Groundwater Method: Excess Pore Pressure

Random Numbers

- Pseudo-random Seed: 10116
- Random Number Generation Method: Park and Miller v.3

Surface Options

- Surface Type: Circular
- Search Method: Auto Refine Search
- Divisions along slope: 10
- Circles per division: 10
- Number of iterations: 10
- Divisions to use in next iteration: 50%
- Composite Surfaces: Disabled
- Minimum Elevation: Not Defined
- Minimum Depth: Not Defined

Loading

- 4 Distributed Loads present

Distributed Load 1

- Distribution: Constant
- Magnitude [kPa]: 96.66
- Orientation: Normal to boundary
- Creates Excess Pore Pressure: No

Distributed Load 2

- Distribution: Constant
- Magnitude [kPa]: 9.3
- Orientation: Normal to boundary
- Creates Excess Pore Pressure: No

Distributed Load 3

- Distribution: Constant
- Magnitude [kPa]: 9.3
- Orientation: Normal to boundary
- Creates Excess Pore Pressure: No

Distributed Load 4

- Distribution: Constant
- Magnitude [kPa]: 96.66
- Orientation: Normal to boundary
- Creates Excess Pore Pressure: No

Material Properties

Property	Red Clay-Addisu Gebeya 2
Color	
Strength Type	Mohr-Coulomb
Unit Weight [kN/m3]	19.5
Cohesion [kPa]	15.3
Friction Angle [deg]	21.3
Water Surface	Water Table
Hu Value	Automatically Calculated
Material Weight Causes Excess Pore Pressure	
B_bar value	0.18

Probabilistic Analysis Input

General Settings

- Sensitivity Analysis: On
- Probabilistic Analysis: On
- Sampling Method: Latin-Hypercube
- Number of Samples: 1000
- Analysis Type: Global Minimum

Variables

Material	Property	Distribution	Mean	Min	Max	Standard Deviation
Red Clay-Addisu Gebeya 2	Cohesion	Normal	15.3	3.825	26.775	3.825
Red Clay-Addisu Gebeya 2	Phi	Normal	21.3	16.188	26.412	1.704
Red Clay-Addisu Gebeya 2	Unit Weight	Normal	19.5	15.99	23.01	1.17

Correlation Coefficients

Material	Correlation
Red Clay-Addisu Gebeya 2	-0.5

Global Minimums

Method: bishop simplified

- FS: 1.202620
- Center: 4.727, 26.038
- Radius: 26.483
- Left Slip Surface Endpoint: -0.108, 0.000
- Right Slip Surface Endpoint: 26.809, 11.418
- Resisting Moment=43736.8 kN-m
- Driving Moment=36368 kN-m
- Total Slice Area=132.185 m2

Method: janbu simplified

- FS: 1.050110
- Center: 7.258, 18.655
- Radius: 20.723
- Left Slip Surface Endpoint: -1.766, 0.000
- Right Slip Surface Endpoint: 26.677, 11.418
- Resisting Horizontal Force=1618.01 kN
- Driving Horizontal Force=1540.8 kN
- Total Slice Area=178.123 m2

Method: janbu corrected

- FS: 1.130140
- Center: 7.349, 18.603
- Radius: 20.620
- Left Slip Surface Endpoint: -1.545, 0.000
- Right Slip Surface Endpoint: 26.677, 11.418
- Resisting Horizontal Force=1732.89 kN
- Driving Horizontal Force=1533.34 kN
- Total Slice Area=177.086 m2

Method: spencer

- FS: 1.195030
- Center: 4.891, 26.323
- Radius: 26.836
- Left Slip Surface Endpoint: -0.329, 0.000
- Right Slip Surface Endpoint: 27.207, 11.418

- Resisting Moment=45602.8 kN-m
- Driving Moment=38160.2 kN-m
- Resisting Horizontal Force=1486.66 kN
- Driving Horizontal Force=1244.03 kN
- Total Slice Area=137.318 m2

Method: gle/morgenstern-price

- FS: 1.196050
- Center: 4.727, 26.038
- Radius: 26.483
- Left Slip Surface Endpoint: -0.108, 0.000
- Right Slip Surface Endpoint: 26.809, 11.418
- Resisting Moment=43497.9 kN-m
- Driving Moment=36368 kN-m
- Resisting Horizontal Force=1431.67 kN
- Driving Horizontal Force=1197 kN
- Total Slice Area=132.185 m2

Valid / Invalid Surfaces

Method: bishop simplified

- Number of Valid Surfaces: 2393
- Number of Invalid Surfaces: 2

Error Codes:

  - Error Code -112 reported for 2 surfaces

Method: janbu simplified

- Number of Valid Surfaces: 2362
- Number of Invalid Surfaces: 33

Error Codes:

  - Error Code -108 reported for 33 surfaces

Method: janbu corrected

- Number of Valid Surfaces: 2362
- Number of Invalid Surfaces: 33

Error Codes:

- Error Code -108 reported for 33 surfaces

Method: spencer

- Number of Valid Surfaces: 2233
- Number of Invalid Surfaces: 162

Error Codes:

- Error Code -108 reported for 89 surfaces
- Error Code -111 reported for 70 surfaces
- Error Code -112 reported for 3 surfaces

Method: gle/morgenstern-price

- Number of Valid Surfaces: 2280
- Number of Invalid Surfaces: 115

Error Codes:

- Error Code -108 reported for 44 surfaces
- Error Code -111 reported for 69 surfaces
- Error Code -112 reported for 2 surfaces

Error Codes

The following errors were encountered during the computation:

- -108 = Total driving moment or total driving force < 0.1. This is to limit the calculation of extremely high safety factors if the driving force is very small (0.1 is an arbitrary number).
- -111 = safety factor equation did not converge
- -112 = The coefficient M-Alpha = cos(alpha)(1+tan(alpha)tan(phi)/F) < 0.2 for the final iteration of the safety factor calculation. This screens out some slip surfaces which may not be valid in the context of the analysis, in particular, deep seated slip surfaces with many high negative base angle slices in the passive zone

Slice Data

- **Global Minimum Query (bishop simplified) - Safety Factor: 1.20262**

Slice Numbe r	Width [m]	Weight [kN]	Base Material	Base Cohesion [kPa]	Base Friction Angle [degrees]	Shear Stress [kPa]	Shear Strength [kPa]	Base Normal Stress [kPa]	Pore Pressure [kPa]	Effective Normal Stress [kPa]
1	1.0767	8.02413	Red Clay-Addisu Gebeya 2	15.3	21.3	15.9904	19.2303	10.0807	0	10.0807
2	1.0767	26.4375	Red Clay-Addisu Gebeya 2	15.3	21.3	21.5376	25.9015	27.1914	0	27.1914
3	1.0767	43.9872	Red Clay-Addisu Gebeya 2	15.3	21.3	26.6686	32.0722	43.0184	0	43.0184
4	1.0767	60.6078	Red Clay-Addisu Gebeya 2	15.3	21.3	31.3812	37.7397	57.5547	0	57.5547
5	1.0767	76.3061	Red Clay-Addisu Gebeya 2	15.3	21.3	35.6937	42.9259	70.8568	0	70.8568
6	1.0767	91.0843	Red Clay-Addisu Gebeya 2	15.3	21.3	39.3665	47.343	82.9796	0.793523	82.186
7	1.0767	104.94	Red Clay-Addisu Gebeya 2	15.3	21.3	42.3892	50.9781	93.9919	2.48185	91.5101
8	1.0767	117.867	Red Clay-Addisu Gebeya 2	15.3	21.3	45.1885	54.3446	103.902	3.75773	100.144
9	1.0767	127.259	Red Clay-Addisu Gebeya 2	15.3	21.3	47.0258	56.5542	110.427	4.61592	105.811
10	1.0767	124.365	Red Clay-Addisu Gebeya 2	15.3	21.3	45.4574	54.668	106.053	5.07905	100.974
11	1.0767	123.179	Red Clay-Addisu Gebeya 2	15.3	21.3	44.4871	53.5011	103.199	5.21899	97.9803
12	1.0767	131.644	Red Clay-Addisu Gebeya 2	15.3	21.3	46.3057	55.6882	108.504	4.9138	103.591
13	1.0767	139.637	Red Clay-Addisu Gebeya 2	15.3	21.3	48.0584	57.796	113.144	4.14768	108.996
14	1.0767	146.541	Red Clay-Addisu Gebeya 2	15.3	21.3	49.5801	59.626	116.591	2.90119	113.69
15	1.0767	152.302	Red Clay-Addisu Gebeya 2	15.3	21.3	50.8635	61.1695	118.8	1.15059	117.649
16	1.0767	156.854	Red Clay-Addisu Gebeya 2	15.3	21.3	51.5829	62.0346	119.868	0	119.868
17	1.0767	160.116	Red Clay-Addisu Gebeya 2	15.3	21.3	51.5802	62.0314	119.86	0	119.86
18	1.0767	161.218	Red Clay-Addisu Gebeya 2	15.3	21.3	50.9694	61.2968	117.976	0	117.976
19	1.0767	149.877	Red Clay-Addisu Gebeya 2	15.3	21.3	47.2395	56.8112	106.47	0	106.47
20	1.0767	133.33	Red Clay-Addisu Gebeya 2	15.3	21.3	51.4957	61.9298	119.599	0	119.599
21	1.0767	114.923	Red Clay-Addisu Gebeya 2	15.3	21.3	63.913	76.8631	157.901	0	157.901
22	1.0767	94.3977	Red Clay-Addisu Gebeya 2	15.3	21.3	57.6135	69.2871	138.47	0	138.47

23	1.0767	71.4064	Red Clay-Addisu Gebeya 2	15.3	21.3	50.8476	61.1503	117.6	0	117.6
24	1.0767	45.4613	Red Clay-Addisu Gebeya 2	15.3	21.3	43.5548	52.3799	95.1052	0	95.1052
25	1.0767	15.8392	Red Clay-Addisu Gebeya 2	15.3	21.3	35.6549	42.8793	70.7374	0	70.7374

- **Global Minimum Query (janbu simplified) - Safety Factor: 1.05011**

Slice Number	Width [m]	Weight [kN]	Base Material	Base Cohesion [kPa]	Base Friction Angle [degrees]	Shear Stress [kPa]	Shear Strength [kPa]	Base Normal Stress [kPa]	Pore Pressure [kPa]	Effective Normal Stress [kPa]
1	1.1377	5.64312	Red Clay-Addisu Gebeya 2	15.3	21.3	19.6778	20.6639	13.7576	0	13.7576
2	1.1377	17.759	Red Clay-Addisu Gebeya 2	15.3	21.3	23.6856	24.8725	24.5522	0	24.5522
3	1.1377	40.8975	Red Clay-Addisu Gebeya 2	15.3	21.3	31.5809	33.1634	45.8173	0	45.8173
4	1.1377	65.0324	Red Clay-Addisu Gebeya 2	15.3	21.3	38.4099	40.3346	66.7991	2.58869	64.2104
5	1.1377	87.6447	Red Clay-Addisu Gebeya 2	15.3	21.3	43.5368	45.7184	85.3914	7.37243	78.019
6	1.1377	108.791	Red Clay-Addisu Gebeya 2	15.3	21.3	48.1997	50.615	102.119	11.5403	90.5787
7	1.1377	128.51	Red Clay-Addisu Gebeya 2	15.3	21.3	52.4341	55.0616	117.092	15.109	101.983
8	1.1377	146.828	Red Clay-Addisu Gebeya 2	15.3	21.3	56.2657	59.0852	130.392	18.0891	112.303
9	1.1377	163.757	Red Clay-Addisu Gebeya 2	15.3	21.3	59.713	62.7052	142.074	20.4857	121.588
10	1.1377	176.456	Red Clay-Addisu Gebeya 2	15.3	21.3	61.8901	64.9914	149.75	22.2982	127.452
11	1.1377	175.086	Red Clay-Addisu Gebeya 2	15.3	21.3	59.8398	62.8384	145.371	23.4413	121.929
12	1.1377	176.485	Red Clay-Addisu Gebeya 2	15.3	21.3	58.8129	61.76	143.373	24.2093	119.164
13	1.1377	187.439	Red Clay-Addisu Gebeya 2	15.3	21.3	60.8404	63.8891	148.987	24.3627	124.624
14	1.1377	197.14	Red Clay-Addisu Gebeya 2	15.3	21.3	62.5783	65.7141	153.182	23.8768	129.306
15	1.1377	205.229	Red Clay-Addisu Gebeya 2	15.3	21.3	63.9304	67.134	155.667	22.7189	132.948
16	1.1377	211.605	Red Clay-Addisu Gebeya 2	15.3	21.3	64.8786	68.1297	156.347	20.8455	135.501
17	1.1377	216.13	Red Clay-Addisu Gebeya 2	15.3	21.3	65.3965	68.6735	155.096	18.2002	136.896
18	1.1377	218.627	Red Clay-Addisu Gebeya 2	15.3	21.3	65.4476	68.7272	151.742	14.7083	137.033
19	1.1377	213.279	Red Clay-Addisu Gebeya 2	15.3	21.3	63.5415	66.7256	142.17	10.2706	131.9
20	1.1377	194.203	Red Clay-Addisu Gebeya 2	15.3	21.3	58.2247	61.1423	122.783	5.20379	117.58

21	1.1377	171.769	Red Clay-Addisu Gebeya 2	15.3	21.3	79.2139	83.1833	174.112	0	174.112
22	1.1377	145.605	Red Clay-Addisu Gebeya 2	15.3	21.3	71.6677	75.259	153.787	0	153.787
23	1.1377	114.624	Red Clay-Addisu Gebeya 2	15.3	21.3	61.0387	64.0974	125.159	0	125.159
24	1.1377	76.8721	Red Clay-Addisu Gebeya 2	15.3	21.3	48.933	51.385	92.5533	0	92.5533
25	1.1377	27.9924	Red Clay-Addisu Gebeya 2	15.3	21.3	34.5762	36.3088	53.8848	0	53.8848

- **Global Minimum Query (janbu corrected) - Safety Factor: 1.13014**

Slice Number	Width [m]	Weight [kN]	Base Material	Base Cohesion [kPa]	Base Friction Angle [degrees]	Shear Stress [kPa]	Shear Strength [kPa]	Base Normal Stress [kPa]	Pore Pressure [kPa]	Effective Normal Stress [kPa]
1	1.12886	5.4895	Red Clay-Addisu Gebeya 2	15.3	21.3	18.2009	20.5696	13.5157	0	13.5157
2	1.12886	18.953	Red Clay-Addisu Gebeya 2	15.3	21.3	22.4355	25.3553	25.7904	0	25.7904
3	1.12886	43.0369	Red Clay-Addisu Gebeya 2	15.3	21.3	30.1394	34.0617	48.1213	0	48.1213
4	1.12886	66.6956	Red Clay-Addisu Gebeya 2	15.3	21.3	36.3124	41.0381	68.734	2.71922	66.0148
5	1.12886	88.8637	Red Clay-Addisu Gebeya 2	15.3	21.3	40.9993	46.335	87.0267	7.4259	79.6008
6	1.12886	109.595	Red Clay-Addisu Gebeya 2	15.3	21.3	45.2631	51.1536	103.484	11.5245	91.9596
7	1.12886	128.928	Red Clay-Addisu Gebeya 2	15.3	21.3	49.1351	55.5295	118.214	15.031	103.183
8	1.12886	146.886	Red Clay-Addisu Gebeya 2	15.3	21.3	52.6384	59.4888	131.294	17.9556	113.338
9	1.12886	163.48	Red Clay-Addisu Gebeya 2	15.3	21.3	55.7895	63.0499	142.775	20.3028	122.472
10	1.12886	174.608	Red Clay-Addisu Gebeya 2	15.3	21.3	57.386	64.8542	149.172	22.0721	127.1
11	1.12886	172.455	Red Clay-Addisu Gebeya 2	15.3	21.3	55.2631	62.455	144.143	23.1964	120.946
12	1.12886	175.353	Red Clay-Addisu Gebeya 2	15.3	21.3	54.7579	61.8841	143.414	23.9317	119.482
13	1.12886	186.306	Red Clay-Addisu Gebeya 2	15.3	21.3	56.671	64.0462	149.086	24.058	125.028
14	1.12886	195.796	Red Clay-Addisu Gebeya 2	15.3	21.3	58.2525	65.8335	153.163	23.5507	129.612
15	1.12886	203.701	Red Clay-Addisu Gebeya 2	15.3	21.3	59.4789	67.2195	155.544	22.377	133.167
16	1.12886	209.92	Red Clay-Addisu Gebeya 2	15.3	21.3	60.3329	68.1846	156.135	20.4937	135.642
17	1.12886	214.317	Red Clay-Addisu Gebeya 2	15.3	21.3	60.7901	68.7013	154.812	17.8446	136.968
18	1.12886	216.718	Red Clay-Addisu Gebeya 2	15.3	21.3	60.8166	68.7313	151.399	14.3555	137.044

19	1.12886	210.646	Red Clay-Addisu Gebeya 2	15.3	21.3	58.8585	66.5184	141.296	9.92754	131.369
20	1.12886	191.659	Red Clay-Addisu Gebeya 2	15.3	21.3	53.8911	60.9045	121.91	4.94057	116.969
21	1.12886	169.509	Red Clay-Addisu Gebeya 2	15.3	21.3	74.3855	84.066	176.376	0	176.376
22	1.12886	143.683	Red Clay-Addisu Gebeya 2	15.3	21.3	66.3737	75.0116	153.152	0	153.152
23	1.12886	113.109	Red Clay-Addisu Gebeya 2	15.3	21.3	56.5453	63.9041	124.663	0	124.663
24	1.12886	75.8566	Red Clay-Addisu Gebeya 2	15.3	21.3	45.35	51.2519	92.212	0	92.212
25	1.12886	27.6232	Red Clay-Addisu Gebeya 2	15.3	21.3	32.0687	36.2421	53.7135	0	53.7135

- **Global Minimum Query (spencer) - Safety Factor: 1.19503**

Slice Number	Width [m]	Weight [kN]	Base Material	Base Cohesion [kPa]	Base Friction Angle [degrees]	Shear Stress [kPa]	Shear Strength [kPa]	Base Normal Stress [kPa]	Pore Pressure [kPa]	Effective Normal Stress [kPa]
1	1.10146	6.00992	Red Clay-Addisu Gebeya 2	15.3	21.3	18.4663	22.0678	17.3584	0	17.3584
2	1.10146	24.9297	Red Clay-Addisu Gebeya 2	15.3	21.3	25.2991	30.2332	38.3016	0	38.3016
3	1.10146	43.5646	Red Clay-Addisu Gebeya 2	15.3	21.3	31.526	37.6745	57.3877	0	57.3877
4	1.10146	61.215	Red Clay-Addisu Gebeya 2	15.3	21.3	36.9612	44.1698	74.0473	0	74.0473
5	1.10146	77.8895	Red Clay-Addisu Gebeya 2	15.3	21.3	41.6855	49.8154	88.5276	0	88.5276
6	1.10146	93.5919	Red Clay-Addisu Gebeya 2	15.3	21.3	45.2721	54.1015	100.845	1.32462	99.5208
7	1.10146	108.321	Red Clay-Addisu Gebeya 2	15.3	21.3	48.1	57.481	111.339	3.15098	108.188
8	1.10146	122.07	Red Clay-Addisu Gebeya 2	15.3	21.3	50.5546	60.4143	120.264	4.55231	115.712
9	1.10146	132.221	Red Clay-Addisu Gebeya 2	15.3	21.3	51.8782	61.996	125.293	5.52367	119.769
10	1.10146	129.479	Red Clay-Addisu Gebeya 2	15.3	21.3	49.4468	59.0904	118.4	6.08332	112.317
11	1.10146	128.801	Red Clay-Addisu Gebeya 2	15.3	21.3	47.8189	57.145	113.642	6.3151	107.327
12	1.10146	137.987	Red Clay-Addisu Gebeya 2	15.3	21.3	49.1082	58.6858	117.369	6.08994	111.279
13	1.10146	146.551	Red Clay-Addisu Gebeya 2	15.3	21.3	50.2612	60.0637	120.205	5.39201	114.813
14	1.10146	153.973	Red Clay-Addisu Gebeya 2	15.3	21.3	51.1567	61.1338	121.759	4.20175	117.557
15	1.10146	160.197	Red Clay-Addisu Gebeya 2	15.3	21.3	51.8057	61.9094	122.042	2.49524	119.547
16	1.10146	165.156	Red Clay-Addisu Gebeya 2	15.3	21.3	52.2174	62.4014	121.052	0.243239	120.809

17	1.10146	168.766	Red Clay-Addisu Gebeya 2	15.3	21.3	51.585	61.6456	118.87	0	118.87
18	1.10146	168.808	Red Clay-Addisu Gebeya 2	15.3	21.3	50.0093	59.7626	114.04	0	114.04
19	1.10146	155.309	Red Clay-Addisu Gebeya 2	15.3	21.3	45.4907	54.3628	100.191	0	100.191
20	1.10146	138.198	Red Clay-Addisu Gebeya 2	15.3	21.3	54.3655	64.9684	127.393	0	127.393
21	1.10146	119.145	Red Clay-Addisu Gebeya 2	15.3	21.3	58.433	69.8292	139.86	0	139.86
22	1.10146	97.8848	Red Clay-Addisu Gebeya 2	15.3	21.3	52.0522	62.2039	120.303	0	120.303
23	1.10146	74.0562	Red Clay-Addisu Gebeya 2	15.3	21.3	45.4882	54.3598	100.183	0	100.183
24	1.10146	47.154	Red Clay-Addisu Gebeya 2	15.3	21.3	38.7218	46.2737	79.4435	0	79.4435
25	1.10146	16.4301	Red Clay-Addisu Gebeya 2	15.3	21.3	31.7423	37.933	58.0505	0	58.0505

- **Global Minimum Query (gle/morgenstern-price) - Safety Factor: 1.19605**

Slice Number	Width [m]	Weight [kN]	Base Material	Base Cohesion [kPa]	Base Friction Angle [degrees]	Shear Stress [kPa]	Shear Strength [kPa]	Base Normal Stress [kPa]	Pore Pressure [kPa]	Effective Normal Stress [kPa]
1	1.0767	8.02413	Red Clay-Addisu Gebeya 2	15.3	21.3	16.5197	19.7583	11.4351	0	11.4351
2	1.0767	26.4375	Red Clay-Addisu Gebeya 2	15.3	21.3	23.3523	27.9305	32.3956	0	32.3956
3	1.0767	43.9872	Red Clay-Addisu Gebeya 2	15.3	21.3	30.1516	36.0628	53.2539	0	53.2539
4	1.0767	60.6078	Red Clay-Addisu Gebeya 2	15.3	21.3	36.6471	43.8318	73.1802	0	73.1802
5	1.0767	76.3061	Red Clay-Addisu Gebeya 2	15.3	21.3	42.5985	50.9499	91.4371	0	91.4371
6	1.0767	91.0843	Red Clay-Addisu Gebeya 2	15.3	21.3	47.5102	56.8246	107.298	0.793523	106.505
7	1.0767	104.94	Red Clay-Addisu Gebeya 2	15.3	21.3	51.1908	61.2268	120.278	2.48185	117.796
8	1.0767	117.867	Red Clay-Addisu Gebeya 2	15.3	21.3	54.0369	64.6308	130.284	3.75773	126.527
9	1.0767	127.259	Red Clay-Addisu Gebeya 2	15.3	21.3	55.2418	66.0719	134.839	4.61592	130.224
10	1.0767	124.365	Red Clay-Addisu Gebeya 2	15.3	21.3	52.299	62.5522	126.275	5.07905	121.196
11	1.0767	123.179	Red Clay-Addisu Gebeya 2	15.3	21.3	49.7188	59.4662	118.5	5.21899	113.281
12	1.0767	131.644	Red Clay-Addisu Gebeya 2	15.3	21.3	49.8462	59.6185	118.585	4.9138	113.672
13	1.0767	139.637	Red Clay-Addisu Gebeya 2	15.3	21.3	49.7697	59.5271	117.584	4.14768	113.437

14	1.0767	146.541	Red Clay-Addisu Gebeya 2	15.3	21.3	49.4531	59.1484	115.367	2.90119	112.466
15	1.0767	152.302	Red Clay-Addisu Gebeya 2	15.3	21.3	49.0114	58.6201	112.261	1.15059	111.11
16	1.0767	156.854	Red Clay-Addisu Gebeya 2	15.3	21.3	48.1665	57.6095	108.518	0	108.518
17	1.0767	160.116	Red Clay-Addisu Gebeya 2	15.3	21.3	46.8222	56.0017	104.394	0	104.394
18	1.0767	161.218	Red Clay-Addisu Gebeya 2	15.3	21.3	45.226	54.0925	99.4973	0	99.4973
19	1.0767	149.877	Red Clay-Addisu Gebeya 2	15.3	21.3	41.1465	49.2133	86.983	0	86.983
20	1.0767	133.33	Red Clay-Addisu Gebeya 2	15.3	21.3	44.5812	53.3213	97.5198	0	97.5198
21	1.0767	114.923	Red Clay-Addisu Gebeya 2	15.3	21.3	55.8559	66.8064	132.107	0	132.107
22	1.0767	94.3977	Red Clay-Addisu Gebeya 2	15.3	21.3	50.9706	60.9634	117.121	0	117.121
23	1.0767	71.4064	Red Clay-Addisu Gebeya 2	15.3	21.3	46.0008	55.0192	101.874	0	101.874
24	1.0767	45.4613	Red Clay-Addisu Gebeya 2	15.3	21.3	40.7414	48.7287	85.7398	0	85.7398
25	1.0767	15.8392	Red Clay-Addisu Gebeya 2	15.3	21.3	34.8698	41.706	67.7281	0	67.7281

Interslice Data

- **Global Minimum Query (bishop simplified) - Safety Factor: 1.20262**

Slice Number	X coordinate [m]	Y coordinate - Bottom [m]	Interslice Normal Force [kN]	Interslice Shear Force [kN]	Interslice Force Angle [degrees]
1	-0.108437	0	0	0	0
2	0.968268	-0.177082	18.9915	0	0
3	2.04497	-0.309011	45.7544	0	0
4	3.12168	-0.396465	78.2132	0	0
5	4.19838	-0.439882	114.48	0	0
6	5.27509	-0.439481	152.86	0	0
7	6.35179	-0.395259	191.55	0	0
8	7.4285	-0.306996	228.867	0	0
9	8.5052	-0.174246	263.699	0	0
10	9.58191	0.00367082	294.655	0	0
11	10.6586	0.227689	319.811	0	0
12	11.7353	0.49902	339.68	0	0
13	12.812	0.819193	354.768	0	0
14	13.8887	1.1901	364.515	0	0
15	14.9654	1.61404	368.438	0	0
16	16.0421	2.09384	366.17	0	0
17	17.1188	2.63293	357.055	0	0
18	18.1955	3.23552	340.332	0	0
19	19.2722	3.90679	315.984	0	0
20	20.349	4.65321	287.344	0	0
21	21.4257	5.48297	243.518	0	0
22	22.5024	6.40662	166.445	0	0
23	23.5791	7.43816	85.603	0	0
24	24.6558	8.59672	4.07186	0	0
25	25.7325	9.90963	-73.9257	0	0
26	26.8092	11.4184	0	0	0

- **Global Minimum Query (janbu simplified) - Safety Factor: 1.05011**

Slice Number	X coordinate [m]	Y coordinate - Bottom [m]	Interslice Normal Force [kN]	Interslice Shear Force [kN]	Interslice Force Angle [degrees]
1	-1.76587	0	0	0	0
2	-0.628176	-0.50873	29.3824	0	0
3	0.509523	-0.938349	66.8728	0	0
4	1.64722	-1.29397	119.089	0	0
5	2.78492	-1.57949	181.853	0	0
6	3.92262	-1.79785	250.022	0	0
7	5.06032	-1.95118	320.507	0	0
8	6.19801	-2.04094	390.66	0	0
9	7.33571	-2.06793	458.183	0	0
10	8.47341	-2.03242	521.061	0	0
11	9.61111	-1.93408	576.734	0	0
12	10.7488	-1.772	621.239	0	0
13	11.8865	-1.54464	655.542	0	0
14	13.0242	-1.24977	680.816	0	0
15	14.1619	-0.884333	696.02	0	0
16	15.2996	-0.444279	700.239	0	0
17	16.4373	0.0756937	692.742	0	0
18	17.575	0.68252	673.014	0	0
19	18.7127	1.38535	640.811	0	0
20	19.8504	2.19649	597.77	0	0
21	20.9881	3.1329	549.025	0	0
22	22.1258	4.21894	450.038	0	0
23	23.2635	5.4916	335.843	0	0
24	24.4012	7.0119	214.994	0	0
25	25.5389	8.89491	96.3768	0	0
26	26.6766	11.4184	0	0	0

- **Global Minimum Query (janbu corrected) - Safety Factor: 1.13014**

Slice Number	X coordinate [m]	Y coordinate - Bottom [m]	Interslice Normal Force [kN]	Interslice Shear Force [kN]	Interslice Force Angle [degrees]
1	-1.54488	0	0	0	0
2	-0.416024	-0.498757	28.8491	0	0
3	0.712835	-0.919653	66.9559	0	0
4	1.84169	-1.26764	120.311	0	0
5	2.97055	-1.54649	183.585	0	0
6	4.09941	-1.75904	251.883	0	0
7	5.22827	-1.90736	322.212	0	0
8	6.35713	-1.99284	391.999	0	0
9	7.48599	-2.01626	459.011	0	0
10	8.61485	-1.97782	521.289	0	0

11	9.7437	-1.87718	575.982	0	0
12	10.8726	-1.71342	619.503	0	0
13	12.0014	-1.48499	653.256	0	0
14	13.1303	-1.18966	678.062	0	0
15	14.2591	-0.824366	692.87	0	0
16	15.388	-0.385079	696.789	0	0
17	16.5169	0.133483	689.107	0	0
18	17.6457	0.73822	669.326	0	0
19	18.7746	1.43824	637.216	0	0
20	19.9034	2.24577	594.609	0	0
21	21.0323	3.17768	546.459	0	0
22	22.1612	4.2582	446.235	0	0
23	23.29	5.52411	332.98	0	0
24	24.4189	7.03612	213.172	0	0
25	25.5477	8.90869	95.5843	0	0
26	26.6766	11.4184	0	0	0

- **Global Minimum Query (spencer) - Safety Factor: 1.19503**

Slice Number	X coordinate [m]	Y coordinate - Bottom [m]	Interslice Normal Force [kN]	Interslice Shear Force [kN]	Interslice Force Angle [degrees]
1	-0.329428	0	0	0	0
2	0.772027	-0.194664	23.6372	9.77223	22.4615
3	1.87348	-0.342453	57.0517	23.5866	22.4614
4	2.97494	-0.444141	97.4725	40.2976	22.4614
5	4.07639	-0.500253	142.175	58.7789	22.4615
6	5.17785	-0.511076	188.864	78.0811	22.4614
7	6.27931	-0.476664	235.059	97.1792	22.4614
8	7.38076	-0.396842	278.939	115.32	22.4614
9	8.48222	-0.271201	319.289	132.002	22.4614
10	9.58367	-0.0990887	354.636	146.616	22.4615
11	10.6851	0.120412	382.892	158.297	22.4614
12	11.7866	0.388503	404.885	167.39	22.4615
13	12.888	0.706711	421.411	174.222	22.4614
14	13.9895	1.07693	432.047	178.619	22.4614
15	15.091	1.50149	436.474	180.449	22.4614
16	16.1924	1.98323	434.514	179.639	22.4614
17	17.2939	2.52562	426.14	176.177	22.4614
18	18.3953	3.13293	410.54	169.728	22.4615
19	19.4968	3.8104	388.143	160.468	22.4614
20	20.5982	4.56458	362.486	149.861	22.4615
21	21.6997	5.40377	315.22	130.32	22.4615
22	22.8011	6.33868	248.567	102.764	22.4615
23	23.9026	7.38347	179.979	74.4077	22.4614
24	25.0041	8.55752	112.26	46.4113	22.4615

25	26.1055	9.88852	49.0007	20.2582	22.4615
26	27.207	11.4184	0	0	0

- **Global Minimum Query (gle/morgenstern-price) - Safety Factor: 1.19605**

Slice Number	X coordinate [m]	Y coordinate - Bottom [m]	Interslice Normal Force [kN]	Interslice Shear Force [kN]	Interslice Force Angle [degrees]
1	-0.108437	0	0	0	0
2	0.968268	-0.177082	19.7909	1.36371	3.94179
3	2.04497	-0.309011	49.179	6.72399	7.78548
4	3.12168	-0.396465	86.2626	17.4585	11.4414
5	4.19838	-0.439882	128.852	34.1276	14.8347
6	5.27509	-0.439481	174.627	56.4314	17.9084
7	6.35179	-0.395259	220.977	83.165	20.6239
8	7.4285	-0.306996	265.414	112.433	22.9582
9	8.5052	-0.174246	306.232	142.152	24.9006
10	9.58191	0.00367082	341.652	169.957	26.4483
11	10.6586	0.227689	369.608	193.258	27.6038
12	11.7353	0.49902	390.926	211.117	28.371
13	12.812	0.819193	406.565	223.081	28.7534
14	13.8887	1.1901	416.477	228.519	28.7534
15	14.9654	1.61404	420.752	227.224	28.3709
16	16.0421	2.09384	419.599	219.397	27.6039
17	17.1188	2.63293	412.898	205.399	26.4484
18	18.1955	3.23552	400.346	185.839	24.9005
19	19.2722	3.90679	382.194	161.903	22.9582
20	20.349	4.65321	361.519	136.058	20.6239
21	21.4257	5.48297	328.546	106.171	17.9085
22	22.5024	6.40662	266.594	70.6098	14.8347
23	23.5791	7.43816	200.596	40.5981	11.4414
24	24.6558	8.59672	132.04	18.0532	7.7855
25	25.7325	9.90963	63.2856	4.36075	3.94179
26	26.8092	11.4184	0	0	0

Probabilistic Analysis Results (Global Minimum)

- Method: bishop simplified
- Factor of Safety, mean: 1.205084
- Factor of Safety, standard deviation: 0.087113
- Factor of Safety, minimum: 0.914353
- Factor of Safety, maximum: 1.526260
- Probability of Failure: 0.600% (= 6 failed surfaces / 1000 valid surfaces)
- Reliability index: 2.35422 (assuming normal distribution)
- Reliability index: 2.54790 (assuming lognormal distribution)
- Method: janbu simplified

- Factor of Safety, mean: 1.051945
- Factor of Safety, standard deviation: 0.073569
- Factor of Safety, minimum: 0.813378
- Factor of Safety, maximum: 1.304660
- Probability of Failure: 22.400% (= 224 failed surfaces / 1000 valid surfaces)
- Reliability index: 0.70607 (assuming normal distribution)
- Reliability index: 0.69005 (assuming lognormal distribution)
- Method: janbu corrected
- Factor of Safety, mean: 1.132124
- Factor of Safety, standard deviation: 0.079076
- Factor of Safety, minimum: 0.875657
- Factor of Safety, maximum: 1.403420
- Probability of Failure: 4.600% (= 46 failed surfaces / 1000 valid surfaces)
- Reliability index: 1.67084 (assuming normal distribution)
- Reliability index: 1.74393 (assuming lognormal distribution)
- Method: spencer
- Factor of Safety, mean: 1.201432
- Factor of Safety, standard deviation: 0.086172
- Factor of Safety, minimum: 0.915356
- Factor of Safety, maximum: 1.514600
- Probability of Failure: 0.600% (= 6 failed surfaces / 1000 valid surfaces)
- Reliability index: 2.33756 (assuming normal distribution)
- Reliability index: 2.52607 (assuming lognormal distribution)
- Method: gle/morgenstern-price
- Factor of Safety, mean: 1.201133
- Factor of Safety, standard deviation: 0.086621
- Factor of Safety, minimum: 0.912622
- Factor of Safety, maximum: 1.517440
- Probability of Failure: 0.600% (= 6 failed surfaces / 1000 valid surfaces)
- Reliability index: 2.32197 (assuming normal distribution)
- Reliability index: 2.50852 (assuming lognormal distribution)

List Of Coordinates

Water Table

X	Y
-11.6	-2.31005
-2.8	-2.31164
9.648	0.549
19.637	2.987
28.098	5.935
33.715	8.807
36.904	10.2152

Line Load

X	Y
28.0232	11.4184
21.0583	11.4184

Line Load

X	Y
27.9815	11.4184
21.1417	11.4184

Line Load

X	Y
-2.08851	0
-9.17853	0

Line Load

X	Y
-2.0468	0
-9.26194	0

External Boundary

X	Y
-11.6	-5.998
36.904	-5.998
36.904	14.171
33.11	14.171
30	11.4184
18.9293	11.4184
10.954	6.039
8.954	6.039
0	0
-11.6	0

APPENDIX B

Addisu gebeya 2.fez

RS2 Analysis Information

Project Summary

File Name:	Addisu gebeya 2.fez
Last saved with RS2 version:	11.015
Analysis:	Converted from Slide v6.02 with RS2 11.015

General Settings

Single stage model	
Analysis Type:	Plane Strain
Solver Type:	Conjugate Gradient
Units:	Metric, stress as kPa
Permeability Units:	meters/second
Time Units:	days

Analysis Options

Maximum Number of Iterations:	500
Tolerance:	0.01
Number of Load Steps:	Automatic
Convergence Type:	Comprehensive
Tensile Failure:	Reduces Shear Strength

Joint tension reduces joint stiffness by a factor of 0.01

Strength Reduction Settings

Inital Estimate of SRF:	1
Step Size:	Automatic
Tolerance (SRF):	0.01
Limit SSR Search Area:	No
Accelerate SSR Analysis:	No
Reduce SSR Iterations after failure:	Yes
Apply SSR to Mohr-Coulomb Tensile Strength:	Yes
Convergence Parameters:	Automatic

Groundwater Analysis

Method:	Static
Pore Fluid Unit Weight:	9.81 kN/m3
Grid Interpolation:	Modified Chugh
Probability:	None

Field Stress

Field stress:	Gravity
Using actual ground surface	
Effective stress ratio (horizontal/vertical in-plane):	1
Effective stress ratio (horizontal/vertical out-of-plane):	1
Locked-in horizontal stress (in-plane):	0
Locked-in horizontal stress (out-of-plane):	0

Mesh

Mesh type:	Uniform
Element type:	6 Noded triangles

Stage Name	# of Elements	# of Nodes
1	4929	10044
SRF: 1	4929	10044
SRF: 1.09	4929	10044
SRF: 1.14	4929	10044
SRF: 1.16	4929	10044
SRF: 1.17	4929	10044
SRF: 1.18	4929	10044
SRF: 1.2	4929	10044
SRF: 1.4	4929	10044

Mesh Quality

All elements are of good quality

<u>Poor quality elements defined as:</u>

Side length ratio (maximum / minimum) > 30.00
Minimum interior angle < 2.0 degrees
Maximum interior angle > 175.0 degrees

Excavation Areas

Original Un-deformed Areas

External Boundary Area: 619.622 m2
External Boundary Perimeter: 127.709 m

1

Values not available until this stage is viewed in a window

SRF: 1

Values not available until this stage is viewed in a window

SRF: 1.09

External Boundary Area: 619.660 m2 (0.0375843 m2 change from original area)
External Boundary Perimeter: 127.695 m (-0.0140382 m change from original perimeter)

SRF: 1.14

External Boundary Area: 619.661 m2 (0.0391197 m2 change from original area)
External Boundary Perimeter: 127.698 m (-0.010532 m change from original perimeter)

SRF: 1.16

External Boundary Area: 619.662 m2 (0.039709 m2 change from original area)
External Boundary Perimeter: 127.699 m (-0.00950395 m change from original perimeter)

SRF: 1.17

External Boundary Area: 619.662 m2 (0.0400673 m2 change from original area)
External Boundary Perimeter: 127.700 m (-0.00884447 m change from original perimeter)

SRF: 1.18

External Boundary Area: 619.664 m2 (0.0416655 m2 change from original area)
External Boundary Perimeter: 127.705 m (-0.00367586 m change from original perimeter)

SRF: 1.2

External Boundary Area: 619.668 m2 (0.0457874 m2 change from original area)
External Boundary Perimeter: 127.719 m (0.0100214 m change from original perimeter)

SRF: 1.4

External Boundary Area: 619.756 m2 (0.134321 m2 change from original area)
External Boundary Perimeter: 128.070 m (0.361119 m change from original perimeter)

Material Properties

Red Clay-Addisu Gebeya 2

Material Color	
Initial Element Loading	Field Stress and Body Force
Unit Weight	19.5 kN/m3
Elastic Type	Isotropic
Poisson's Ratio	0.4
Young's Modulus	50000 kPa
Use Residual Young's Modulus	No
Failure Criterion	Mohr-Coulomb
Material Type	Plastic
Peak Tensile Strength	39.24 kPa
Peak Friction Angle	21.3 degrees
Peak Cohesion	15.3 kPa
Residual Tensile Strength	39.24 kPa
Residual Friction Angle	21.3 degrees
Residual Cohesion	15.3 kPa
Dilation Angle	0 degrees
Apply SSR (Shear Strength Reduction)	Yes
Use Unsaturated Parameters	Yes
Unsaturated Shear Strength Angle	0 degrees
Air Entry Value	0
Material Behaviour	Drained
Porosity Value	0.5
Static Water Mode	Piezometric Lines
Piezo to Use	1

Shear Strength Reduction - Material Properties

Strength Reduction Factor: 1

Maximum Total Displacement: 0.0221691 m
Converged: yes

Material	Red Clay-Addisu Gebeya 2
Peak friction angle	21.3 degrees
Peak cohesion	15.3 kPa
Residual Friction Angle	21.3 degrees
Residual Cohesion	15.3 kPa

Strength Reduction Factor: 1.09

Maximum Total Displacement: 0.0227163 m
Converged: yes

Material	Red Clay-Addisu Gebeya 2
Peak friction angle	19.6817 degrees
Peak cohesion	14.0367 kPa
Residual Friction Angle	19.6817 degrees
Residual Cohesion	14.0367 kPa

Strength Reduction Factor: 1.14

Maximum Total Displacement: 0.0230783 m
Converged: yes

Material	Red Clay-Addisu Gebeya 2
Peak friction angle	18.8809 degrees
Peak cohesion	13.4211 kPa
Residual Friction Angle	18.8809 degrees
Residual Cohesion	13.4211 kPa

Strength Reduction Factor: 1.16

Maximum Total Displacement: 0.0232529 m
Converged: yes

Material	Red Clay-Addisu Gebeya 2
Peak friction angle	18.5778 degrees
Peak cohesion	13.1897 kPa
Residual Friction Angle	18.5778 degrees
Residual Cohesion	13.1897 kPa

Critical Strength Reduction Factor: 1.17

Maximum Total Displacement: 0.0233477 m
Converged: yes

Material	Red Clay-Addisu Gebeya 2
Peak friction angle	18.4298 degrees
Peak cohesion	13.0769 kPa
Residual Friction Angle	18.4298 degrees
Residual Cohesion	13.0769 kPa

Strength Reduction Factor: 1.18

Maximum Total Displacement: 0.0234439 m
Converged: no

Material	Red Clay-Addisu Gebeya 2
Peak friction angle	18.2841 degrees
Peak cohesion	12.9661 kPa
Residual Friction Angle	18.2841 degrees
Residual Cohesion	12.9661 kPa

Strength Reduction Factor: 1.2

Maximum Total Displacement: 0.0369142 m
Converged: no

Material	Red Clay-Addisu Gebeya 2
Peak friction angle	17.9991 degrees
Peak cohesion	12.75 kPa
Residual Friction Angle	17.9991 degrees
Residual Cohesion	12.75 kPa

Strength Reduction Factor: 1.4

Maximum Total Displacement: 0.326274 m
Converged: no

Material	Red Clay-Addisu Gebeya 2
Peak friction angle	15.5619 degrees
Peak cohesion	10.9286 kPa
Residual Friction Angle	15.5619 degrees
Residual Cohesion	10.9286 kPa

Displacements

Displacement data is not available until total displacement is viewed in a window

Yielded Elements

Yielded Mesh Elements

Number of yielded mesh elements is not available for 1 until the stage is viewed in a window

Number of yielded mesh elements is not available for SRF: 1 until the stage is viewed in a window

Number of yielded mesh elements on SRF: 1.09:	642
Number of yielded mesh elements on SRF: 1.14:	713
Number of yielded mesh elements on SRF: 1.16:	751
Number of yielded mesh elements on SRF: 1.17:	774
Number of yielded mesh elements on SRF: 1.18:	795
Number of yielded mesh elements on SRF: 1.2:	839
Number of yielded mesh elements on SRF: 1.4:	1602

List of All Coordinates

External boundary

X	Y
-11.6	-5.998
36.904	-5.998
36.904	14.171
33.11	14.171
30	11.4184
28.0462	11.4184
28.0212	11.4184
21.0048	11.4184
18.9293	11.4184
10.954	6.039
8.954	6.039
0	0
-0.997124	0
-7.9	0
-11.6	0

Piezometric line

X	Y
-11.6	-2.31005
-2.8	-2.31164
9.648	0.549
19.637	2.987
28.098	5.935
33.715	8.807
36.904	10.2152

APPENDIX C

PSSA Addisu gebeya 2.fez

RS2 Analysis Information

Project Summary

File Name:	PSSA Addisu gebeya 2.fez
Last saved with RS2 version:	11.015
Analysis:	Converted from Slide v6.02 with RS2 11.015

General Settings

Single stage model

Analysis Type:	Plane Strain
Solver Type:	Conjugate Gradient
Units:	Metric, stress as kPa
Permeability Units:	meters/second
Time Units:	days

Options

Maximum Number of Iterations:	500
Tolerance:	0.01
Number of Load Steps:	Automatic
Convergence Type:	Comprehensive
Tensile Failure:	Reduces Shear Strength

Joint tension reduces joint stiffness by a factor of 0.01

Strength Reduction Settings

Inital Estimate of SRF:	1
Step Size:	Automatic
Tolerance (SRF):	0.01
Limit SSR Search Area:	No
Accelerate SSR Analysis:	No
Reduce SSR Iterations after failure:	Yes
Apply SSR to Mohr-Coulomb Tensile Strength:	Yes
Convergence Parameters:	Automatic

Groundwater Analysis

Method:	Static
Pore Fluid Unit Weight:	9.81 kN/m3
Grid Interpolation:	Modified Chugh

Probability Analysis

Analysis Type:	Latin-Hypercube
Number of Samples:	100

Statistical Variables

Number of Statistical Variables Used: 2

Variable Type	Material/Joint Name	Property Type	Distribution	Mean	Standard Deviation	Min	Max
Material Property	Red Clay-Addisu Gebeya 2	Friction Angle (peak)	Normal	21.3	1.704	16.188	26.412
Material Property	Red Clay-Addisu Gebeya 2	Cohesion (peak)	Normal	15.3	3.825	3.825	26.775

Field Stress

Field stress:	Gravity
Using actual ground surface	
Effective stress ratio (horizontal/vertical in-plane):	1
Effective stress ratio (horizontal/vertical out-of-plane):	1
Locked-in horizontal stress (in-plane):	0
Locked-in horizontal stress (out-of-plane):	0

Mesh

Mesh type:	Uniform
Element type:	6 Noded triangles

Stage Name	# of Elements	# of Nodes
1	4929	10044
SRF: 0.49	4929	10044
SRF: 0.74	4929	10044
SRF: 0.86	4929	10044
SRF: 0.92	4929	10044
SRF: 0.95	4929	10044
SRF: 0.97	4929	10044
SRF: 0.98	4929	10044
SRF: 0.99	4929	10044
SRF: 1	4929	10044

Mesh Quality

All elements are of good quality

Poor quality elements defined as:

Side length ratio (maximum / minimum) > 30.00
Minimum interior angle < 2.0 degrees
Maximum interior angle > 175.0 degrees

Excavation Areas

Original Un-deformed Areas

External Boundary Area: 619.622 m2
External Boundary Perimeter: 127.709 m

1

External Boundary Area: 619.620 m2 (-0.00210763 m2 change from original area)
External Boundary Perimeter: 127.680 m (-0.0292687 m change from original perimeter)

SRF: 0.49

Values not available until this stage is viewed in a window

SRF: 0.74

Values not available until this stage is viewed in a window

SRF: 0.86

Values not available until this stage is viewed in a window

SRF: 0.92

Values not available until this stage is viewed in a window

SRF: 0.95

Values not available until this stage is viewed in a window

SRF: 0.97

External Boundary Area: 619.620 m2 (-0.00164973 m2 change from original area)
External Boundary Perimeter: 127.680 m (-0.0290156 m change from original perimeter)

SRF: 0.98

Values not available until this stage is viewed in a window

SRF: 0.99

Values not available until this stage is viewed in a window

SRF: 1

Values not available until this stage is viewed in a window

Material Properties

Red Clay-Addisu Gebeya 2

Material Color	
Initial Element Loading	Field Stress and Body Force
Unit Weight	19.5 kN/m3
Elastic Type	Isotropic
Poisson's Ratio	0.4
Young's Modulus	50000 kPa
Use Residual Young's Modulus	No
Failure Criterion	Mohr-Coulomb
Material Type	Plastic
Peak Tensile Strength	39.24 kPa
Peak Friction Angle	21.3 degrees
Peak Cohesion	15.3 kPa
Residual Tensile Strength	39.24 kPa
Residual Friction Angle	21.3 degrees
Residual Cohesion	15.3 kPa
Dilation Angle	0 degrees
Apply SSR (Shear Strength Reduction)	Yes
Use Unsaturated Parameters	Yes
Unsaturated Shear Strength Angle	0 degrees

Air Entry Value	0
Material Behaviour	Undrained
Fluid Bulk Modulus	2.2e+06 kPa
Porosity Value	0.3
Static Water Mode	Piezometric Lines
Piezo to Use	1

Strength Reduction Factor Statistics

Probability of Failure:	100 %
Critical SRF mean value:	0.97
Critical SRF std. dev. value:	0.0024
NOTE:	Critical SRF is present only in 69 out of 100 files

File #	Critical SRF
1	0.97
2	0.97
3	0.97
4	0.97
5	0.96
6	0.97
7	0.97
8	0.97
9	0.98
10	0.97
11	0.97
12	0.97
13	0.96
14	0.97
15	0.97
16	0.97
17	0.97
18	0.97
19	0.97
20	0.97
21	0.97
22	0.97
23	0.97
24	0.97
25	0.97
26	0.97
27	0.97
28	0.97
29	0.97
30	0.97
31	0.97
32	0.97
33	0.97
34	0.97
35	0.97
36	0.97

37	0.97
38	0.97
39	0.97
40	0.97
41	0.97
42	0.97
43	0.97
44	0.97
45	0.97
46	0.97
47	0.97
48	0.97
49	0.97
50	0.97
51	0.97
52	0.97
53	0.97
54	0.97
55	0.97
56	0.97
57	0.97
58	0.97
59	0.97
60	0.97
61	0.97
62	0.97
63	0.97
64	0.98
65	0.97
66	0.97
67	0.97
68	0.97
69	0.97
70	None Converged
71	None Converged
72	None Converged
73	None Converged
74	None Converged
75	None Converged
76	None Converged
77	None Converged
78	None Converged
79	None Converged
80	None Converged
81	None Converged
82	None Converged
83	None Converged
84	None Converged
85	None Converged
86	None Converged
87	None Converged
88	None Converged
89	None Converged
90	None Converged
91	None Converged
92	None Converged

93	None Converged
94	None Converged
95	None Converged
96	None Converged
97	None Converged
98	None Converged
99	None Converged
100	None Converged

Probability of Failure:	100 %
Critical SRF mean value:	0.97
Critical SRF std. dev. value:	0.0024
NOTE:	Critical SRF is present only in 69 out of 100 files

File #	Critical SRF
1	0.97
2	0.97
3	0.97
4	0.97
5	0.96
6	0.97
7	0.97
8	0.97
9	0.98
10	0.97
11	0.97
12	0.97
13	0.96
14	0.97
15	0.97
16	0.97
17	0.97
18	0.97
19	0.97
20	0.97
21	0.97
22	0.97
23	0.97
24	0.97
25	0.97
26	0.97
27	0.97
28	0.97
29	0.97
30	0.97
31	0.97
32	0.97
33	0.97
34	0.97
35	0.97
36	0.97

37	0.97
38	0.97
39	0.97
40	0.97
41	0.97
42	0.97
43	0.97
44	0.97
45	0.97
46	0.97
47	0.97
48	0.97
49	0.97
50	0.97
51	0.97
52	0.97
53	0.97
54	0.97
55	0.97
56	0.97
57	0.97
58	0.97
59	0.97
60	0.97
61	0.97
62	0.97
63	0.97
64	0.98
65	0.97
66	0.97
67	0.97
68	0.97
69	0.97
70	None Converged
71	None Converged
72	None Converged
73	None Converged
74	None Converged
75	None Converged
76	None Converged
77	None Converged
78	None Converged
79	None Converged
80	None Converged
81	None Converged
82	None Converged
83	None Converged
84	None Converged
85	None Converged
86	None Converged
87	None Converged
88	None Converged
89	None Converged
90	None Converged
91	None Converged
92	None Converged

93	None Converged
94	None Converged
95	None Converged
96	None Converged
97	None Converged
98	None Converged
99	None Converged
100	None Converged

Probability of Failure:	100 %
Critical SRF mean value:	0.97
Critical SRF std. dev. value:	0.0024
NOTE:	Critical SRF is present only in 69 out of 100 files

File #	Critical SRF
1	0.97
2	0.97
3	0.97
4	0.97
5	0.96
6	0.97
7	0.97
8	0.97
9	0.98
10	0.97
11	0.97
12	0.97
13	0.96
14	0.97
15	0.97
16	0.97
17	0.97
18	0.97
19	0.97
20	0.97
21	0.97
22	0.97
23	0.97
24	0.97
25	0.97
26	0.97
27	0.97
28	0.97
29	0.97
30	0.97
31	0.97
32	0.97
33	0.97

34	0.97
35	0.97
36	0.97
37	0.97
38	0.97
39	0.97
40	0.97
41	0.97
42	0.97
43	0.97
44	0.97
45	0.97
46	0.97
47	0.97
48	0.97
49	0.97
50	0.97
51	0.97
52	0.97
53	0.97
54	0.97
55	0.97
56	0.97
57	0.97
58	0.97
59	0.97
60	0.97
61	0.97
62	0.97
63	0.97
64	0.98
65	0.97
66	0.97
67	0.97
68	0.97
69	0.97
70	None Converged
71	None Converged
72	None Converged
73	None Converged
74	None Converged
75	None Converged
76	None Converged
77	None Converged
78	None Converged
79	None Converged
80	None Converged
81	None Converged
82	None Converged
83	None Converged
84	None Converged
85	None Converged
86	None Converged
87	None Converged
88	None Converged
89	None Converged

90	None Converged
91	None Converged
92	None Converged
93	None Converged
94	None Converged
95	None Converged
96	None Converged
97	None Converged
98	None Converged
99	None Converged
100	None Converged

Shear Strength Reduction - Material Properties

Strength Reduction Factor: 0.49

Maximum Total Displacement: 0.0184936 m
Converged: yes

Material	Red Clay-Addisu Gebeya 2
Peak friction angle	38.5086 degrees
Peak cohesion	31.2245 kPa
Residual Friction Angle	38.5086 degrees
Residual Cohesion	31.2245 kPa

Strength Reduction Factor: 0.74

Maximum Total Displacement: 0.0192849 m
Converged: yes

Material	Red Clay-Addisu Gebeya 2
Peak friction angle	27.7834 degrees
Peak cohesion	20.6757 kPa
Residual Friction Angle	27.7834 degrees
Residual Cohesion	20.6757 kPa

Strength Reduction Factor: 0.86

Maximum Total Displacement: 0.019812 m
Converged: yes

Material	Red Clay-Addisu Gebeya 2
Peak friction angle	24.3873 degrees
Peak cohesion	17.7907 kPa
Residual Friction Angle	24.3873 degrees
Residual Cohesion	17.7907 kPa

Strength Reduction Factor: 0.92

Maximum Total Displacement: 0.0201119 m
Converged: yes

Material	Red Clay-Addisu Gebeya 2
Peak friction angle	22.9666 degrees

Peak cohesion	16.6304 kPa
Residual Friction Angle	22.9666 degrees
Residual Cohesion	16.6304 kPa

Strength Reduction Factor: 0.95

Maximum Total Displacement:	0.0202708 m
Converged:	yes
Material	**Red Clay-Addisu Gebeya 2**
Peak friction angle	22.3134 degrees
Peak cohesion	16.1053 kPa
Residual Friction Angle	22.3134 degrees
Residual Cohesion	16.1053 kPa

Critical Strength Reduction Factor: 0.97

Maximum Total Displacement:	0.0203829 m
Converged:	yes
Material	**Red Clay-Addisu Gebeya 2**
Peak friction angle	21.8973 degrees
Peak cohesion	15.7732 kPa
Residual Friction Angle	21.8973 degrees
Residual Cohesion	15.7732 kPa

Strength Reduction Factor: 0.98

Maximum Total Displacement:	0.0204394 m
Converged:	no
Material	**Red Clay-Addisu Gebeya 2**
Peak friction angle	21.6947 degrees
Peak cohesion	15.6122 kPa
Residual Friction Angle	21.6947 degrees
Residual Cohesion	15.6122 kPa

Strength Reduction Factor: 0.99

Maximum Total Displacement:	0.020494 m
Converged:	no
Material	**Red Clay-Addisu Gebeya 2**
Peak friction angle	21.4956 degrees
Peak cohesion	15.4545 kPa
Residual Friction Angle	21.4956 degrees
Residual Cohesion	15.4545 kPa

Strength Reduction Factor: 1

Maximum Total Displacement:	0.0206172 m
Converged:	no
Material	**Red Clay-Addisu Gebeya 2**
Peak friction angle	21.3 degrees
Peak cohesion	15.3 kPa
Residual Friction Angle	21.3 degrees
Residual Cohesion	15.3 kPa

Displacements

Displacement data is not available until total displacement is viewed in a window

Yielded Elements

Yielded Mesh Elements

Number of yielded mesh elements on 1: 542
Number of yielded mesh elements is not available for SRF: 0.49 until the stage is viewed in a window
Number of yielded mesh elements is not available for SRF: 0.74 until the stage is viewed in a window
Number of yielded mesh elements is not available for SRF: 0.86 until the stage is viewed in a window
Number of yielded mesh elements is not available for SRF: 0.92 until the stage is viewed in a window
Number of yielded mesh elements is not available for SRF: 0.95 until the stage is viewed in a window
Number of yielded mesh elements on SRF: 0.97: 503
Number of yielded mesh elements is not available for SRF: 0.98 until the stage is viewed in a window
Number of yielded mesh elements is not available for SRF: 0.99 until the stage is viewed in a window
Number of yielded mesh elements is not available for SRF: 1 until the stage is viewed in a window

List of All Coordinates

External boundary

X	Y
-11.6	-5.998
36.904	-5.998
36.904	14.171
33.11	14.171
30	11.4184
28.0462	11.4184
28.0212	11.4184
21.0048	11.4184
18.9293	11.4184
10.954	6.039
8.954	6.039
0	0
-0.997124	0
-7.9	0
-11.6	0

Piezometric line

X	Y
-11.6	-2.31005
-2.8	-2.31164
9.648	0.549
19.637	2.987
28.098	5.935
33.715	8.807
36.904	10.2152

APPENDIX D

Minimum Slip Surfaces

SLIDE V6.0

Kolfe 1

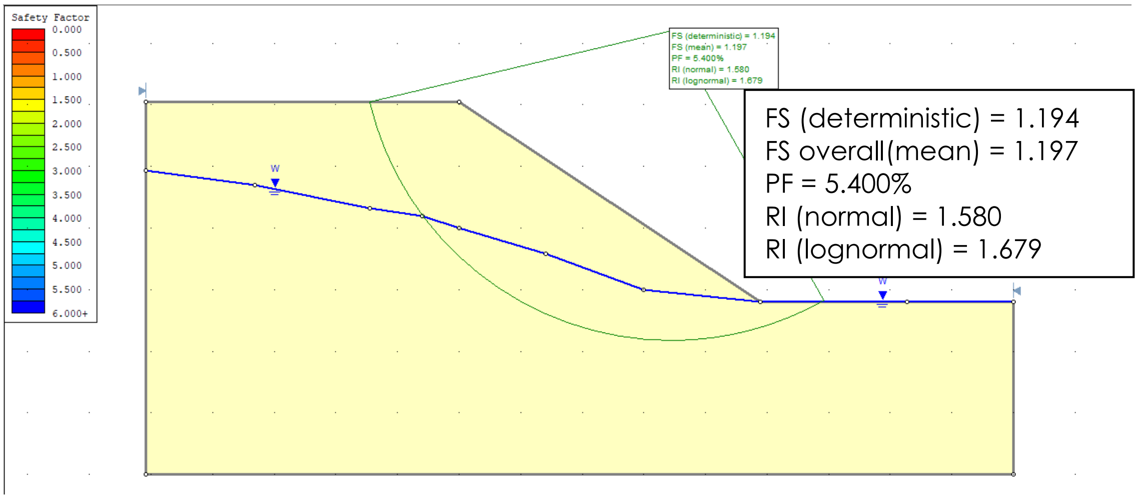

Kolfe 2

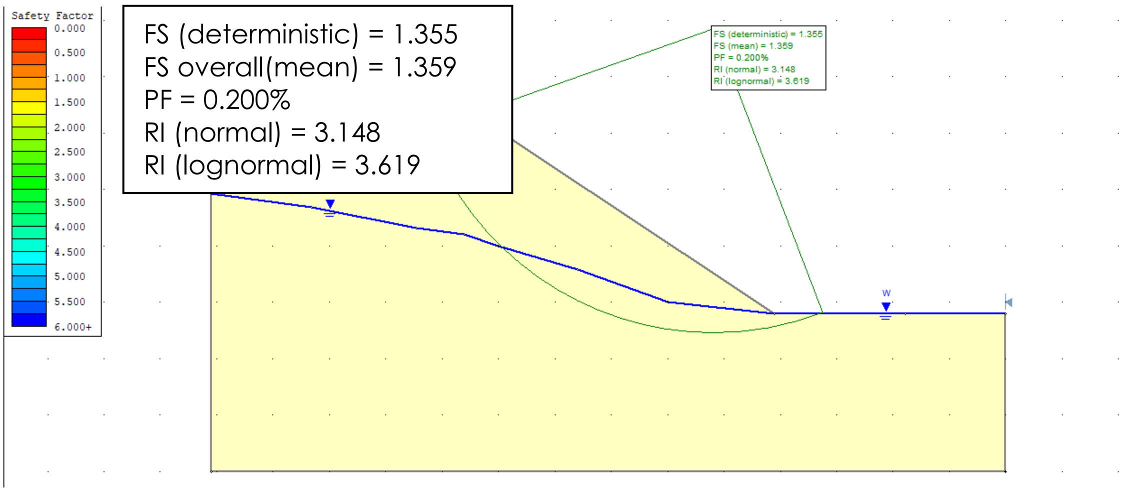

Kolfe 3

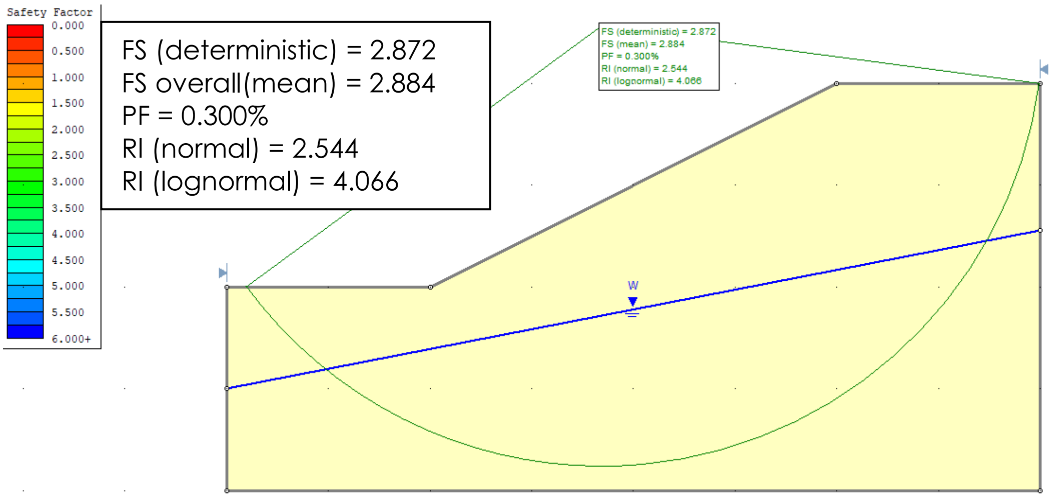

Addisu gebeya 1

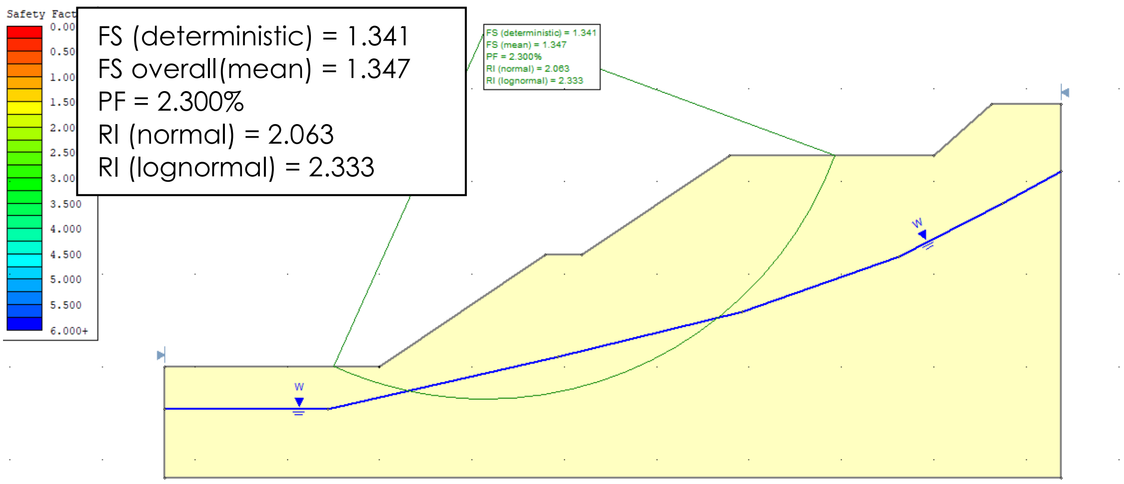

Addisu gebeya 2

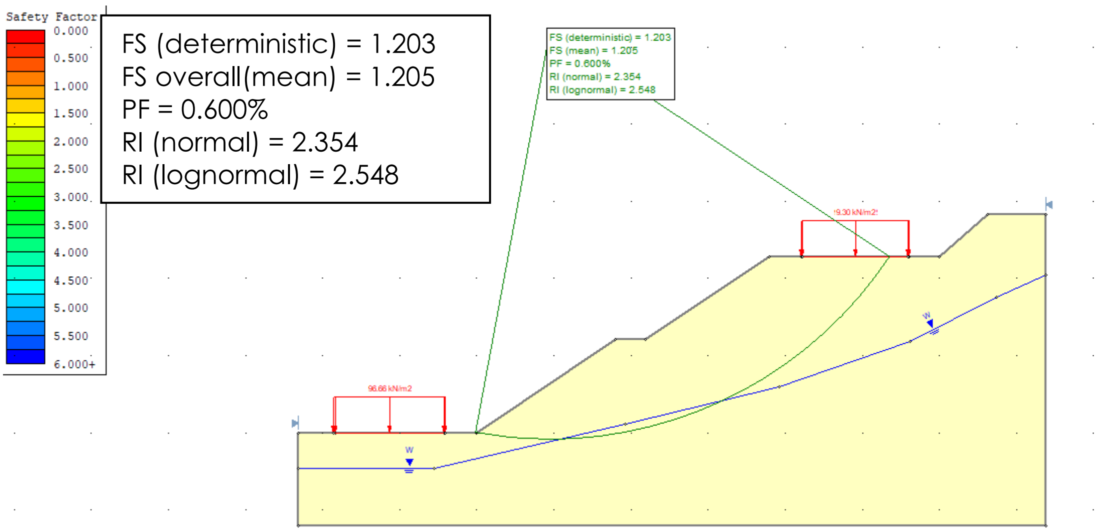

Arada

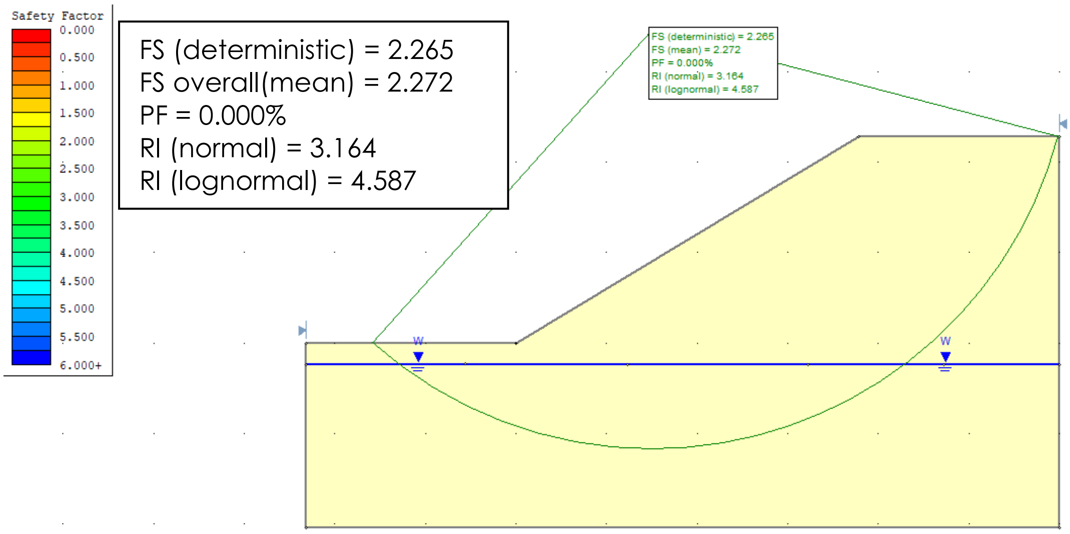

Asko

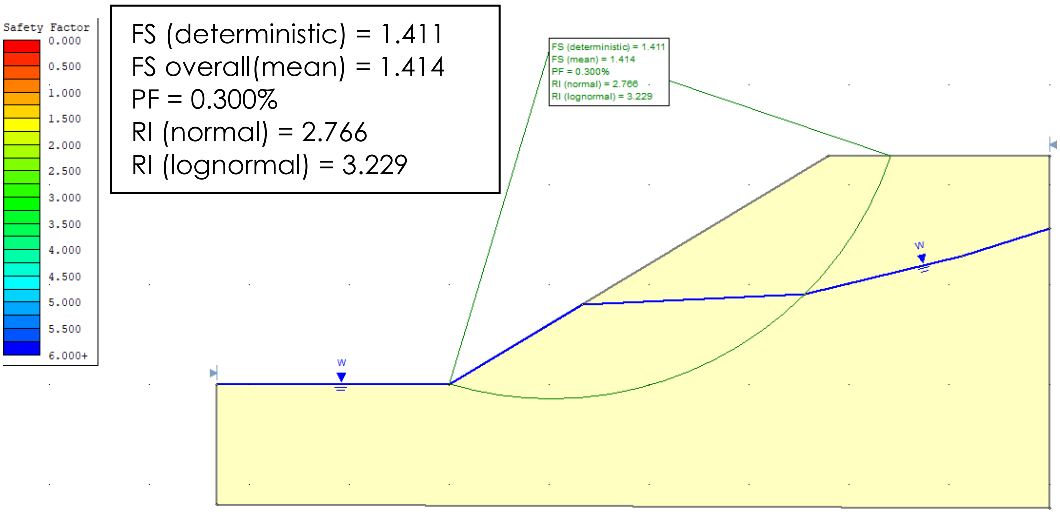

RS2 V11

Kolfe 1

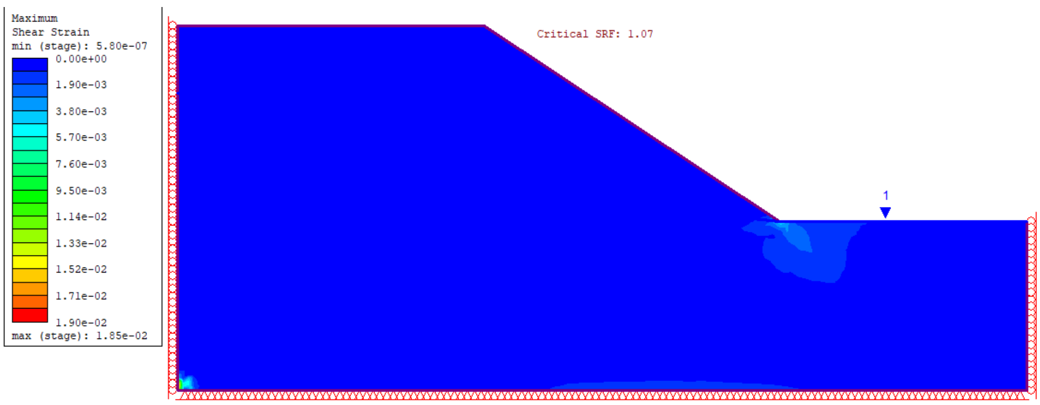

Kolfe 2

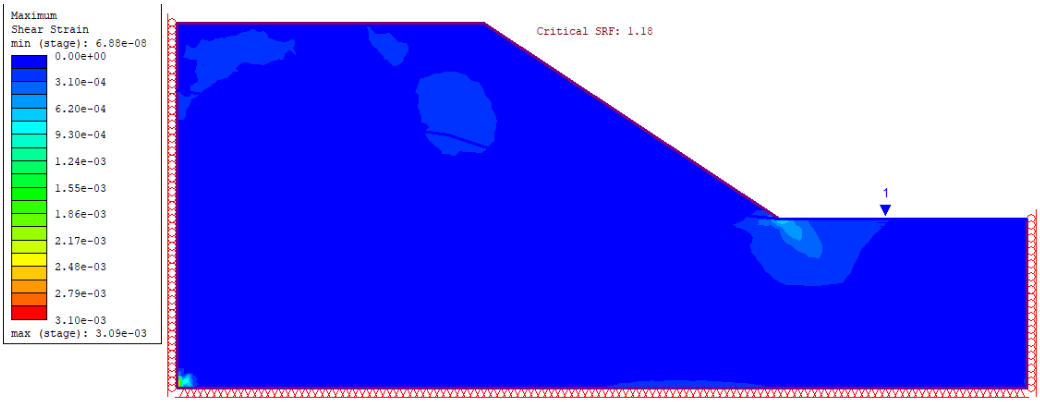

Kolfe 3

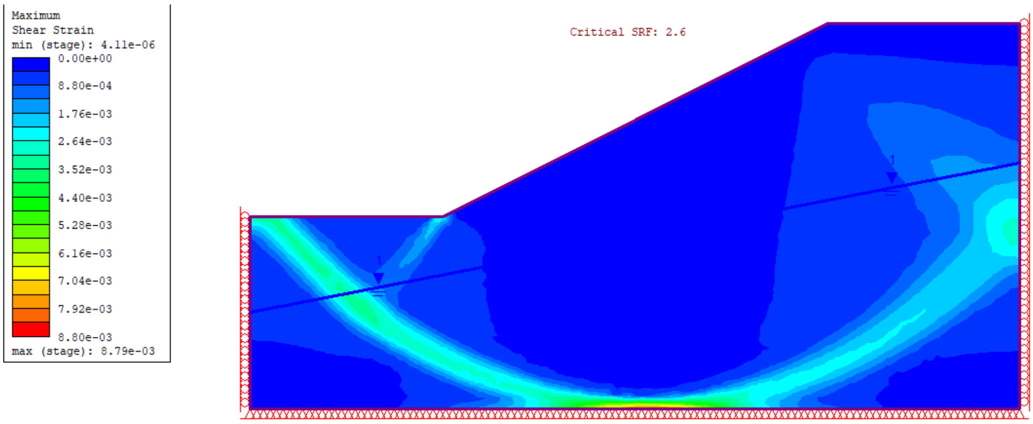

Addisu gebeya 1

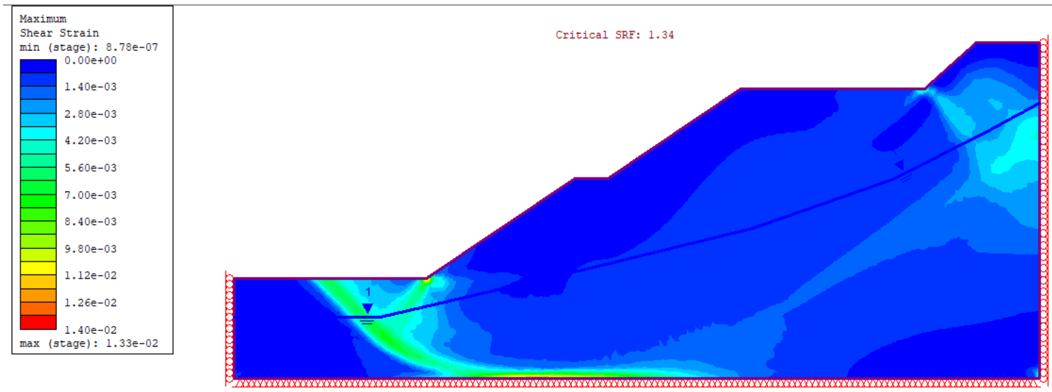

Addisu gebeya 2

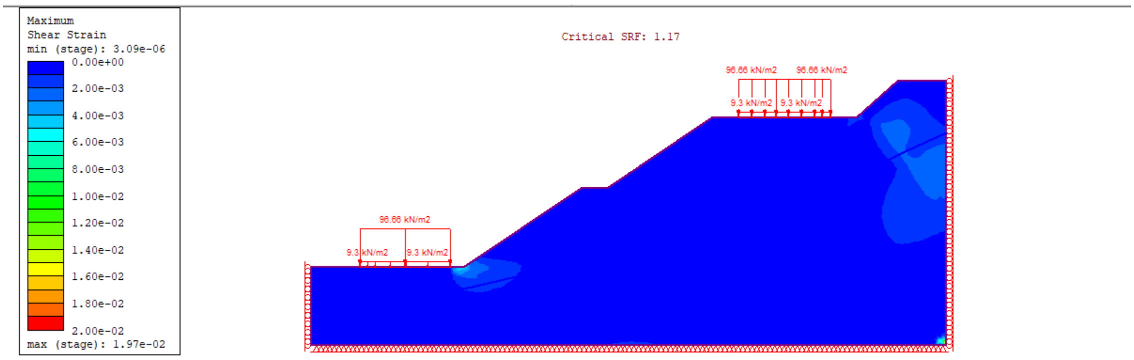
Maximum
Shear Strain
min (stage): 3.09e-06
0.00e+00
2.00e-03
4.00e-03
6.00e-03
8.00e-03
1.00e-02
1.20e-02
1.40e-02
1.60e-02
1.80e-02
2.00e-02
max (stage): 1.97e-02
Critical SRF: 1.17
96.66 kN/m2
96.66 kN/m2
9.3 kN/m2
9.3 kN/m2
96.66 kN/m2
9.3 kN/m2
9.3 kN/m2

Arada

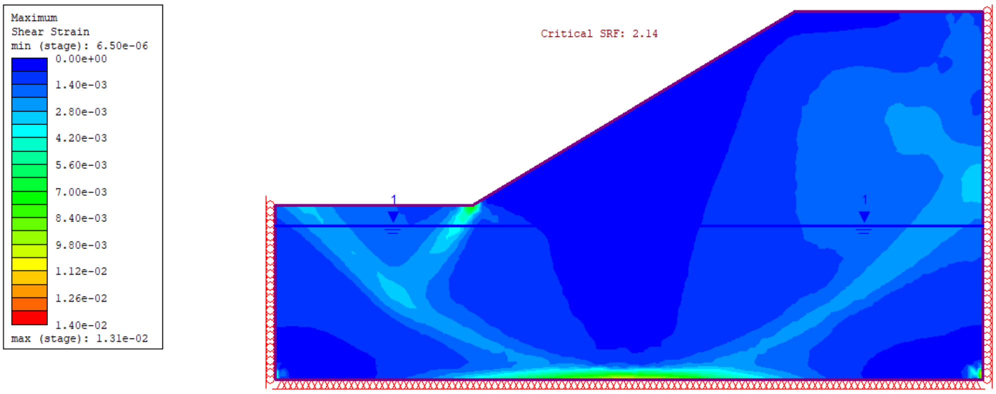
Maximum
Shear Strain
min (stage): 6.50e-06
0.00e+00
1.40e-03
2.80e-03
4.20e-03
5.60e-03
7.00e-03
8.40e-03
9.80e-03
1.12e-02
1.26e-02
1.40e-02
max (stage): 1.31e-02
Critical SRF: 2.14

Asko

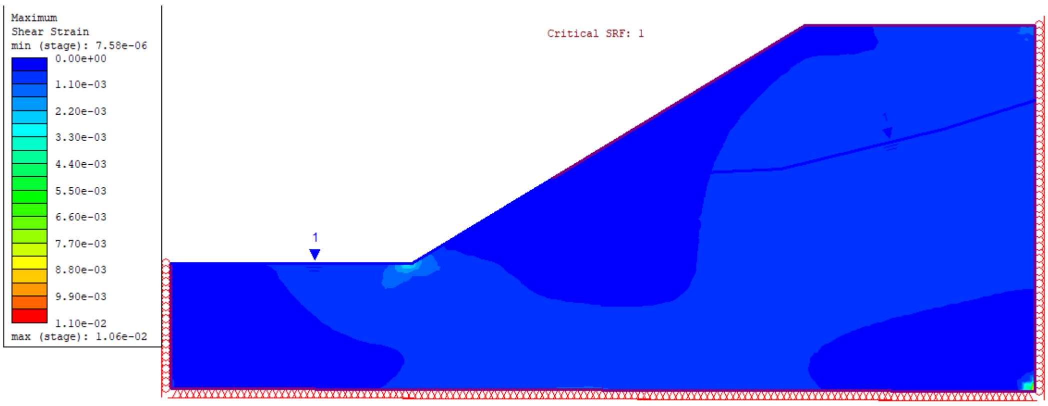
Maximum
Shear Strain
min (stage): 7.58e-06
0.00e+00
1.10e-03
2.20e-03
3.30e-03
4.40e-03
5.50e-03
6.60e-03
7.70e-03
8.80e-03
9.90e-03
1.10e-02
max (stage): 1.06e-02
Critical SRF: 1